

***Copolymerization of Ethylene and Polar  
Monomers by Metallocene Catalyst***

**Dissertation**

submitted to

Department of Chemistry

University of Hamburg

in partial fulfillment of the requirements

for the German academic degree

Dr. rer. nat.

**Mércia Barbosa Cavalcante Fernandes**

Hamburg 2007



Gutachter / Reviewers:

Prof. Dr. W. Kaminsky

Prof. Dr.-Ing. W.-M. Kulicke

Disputation: January, 25<sup>th</sup>, 2008.



To Guilherme and Beatriz



## Acknowledgments

The present work was carried out in the research group of Prof.Dr.Walter Kaminsky at the Institute of Technical and Macromolecules Chemistry, University of Hamburg between October/2003 and June/2006.

My sincerely thanks to Prof.Dr.Walter Kaminsky for giving me the opportunity to work in his laboratory, his kindness, the financial support and the interesting subject of this work.

I would also like to thanks Prof.Dr.Ulf Friedrich Schuchardt to show me the direction in Germany.

I am grateful to many people who have gone out of their way to help me in this work. Special thanks to:

- Matthias Hoff and Katrin Scharlach for their friendship and the funny days that we spent together in the laboratory as well as during DSC measurements.
- Andreas, Sacha Rulhoff and Stephan for the GPC measurements.
- Inge Schult, Björn, Jens, Steffi and Burcak for the NMR measurements.
- Mr. Horbaschk for his technical support and conversation in different topics.
- Holger, Kathleen, Jens P. and Peter for the electronics, glass work and chemicals ordering.
- Ms Graeska for all elemental analysis
- Felix Scheliga for the synthesis of the monomers HBE and DBE and fruitful technical discussions.
- Henning S. for the work during his practical training.

My very special thanks for my husband Guilherme. This work would never have been completed without his love, constant support, technical discussions and the review of this thesis. I would also like to thanks my lovely baby Beatriz without whom, everything in my life would not have been the same.





# 1 Table of Contents

<b>1</b>	<b>Table of Contents.....</b>	<b>I</b>
<b>2</b>	<b>Abbreviation.....</b>	<b>IV</b>
<b>3</b>	<b>Summary.....</b>	<b>1</b>
<b>4</b>	<b>Zusammenfassung.....</b>	<b>3</b>
<b>5</b>	<b>General Aspects.....</b>	<b>5</b>
5.1	Polyolefin Development.....	5
5.2	Polymerization Mechanism.....	6
5.3	The Role of Cocatalyst.....	7
<b>5.4</b>	<b>Functionalization of Polyolefins.....</b>	<b>9</b>
5.4.1	Functionalization Process.....	10
5.4.2	Classification of Functional Polymer by Structure.....	12
5.4.2.1	Side Group functionalized polyolefins.....	12
5.4.2.2	Functional Polyolefin Graft Copolymer.....	13
5.4.2.3	Chain End Functionalized Polyolefin.....	13
5.4.2.4	Functional Polyolefin Block Copolymer.....	14
<b>5.5</b>	<b>Metallocene as a Catalyst for Copolymerization with Functional Monomers.....</b>	<b>14</b>
<b>6</b>	<b>The Aim of This Work.....</b>	<b>17</b>
<b>7</b>	<b>Results and Discussions.....</b>	<b>18</b>
7.1	Introduction.....	18
<b>7.2</b>	<b>Copolymerization of Ethylene with Methyl Methacrylate (MMA).....</b>	<b>20</b>
7.2.1	Effect of TIBA Concentration.....	22
7.2.1.1	GPC and DSC Results.....	23
7.2.2	Effect of MAO and Catalyst Concentration.....	23
7.2.3	Effect of Comonomer Concentration.....	26
7.2.3.1	GPC and DSC Results.....	27
7.2.3.2	<sup>1</sup> HNMR and <sup>13</sup> CNMR Spectroscopy Results.....	28
7.2.4	Partial Conclusions.....	30
<b>7.3</b>	<b>Copolymerization of Ethylene with Vinyl Acetate (VA).....</b>	<b>31</b>
7.3.1	Effect of MAO Concentration and Pressure.....	32
7.3.1.1	GPC and DSC Results.....	34
7.3.1.2	<sup>1</sup> HNMR and FTIR Spectroscopy Results.....	35
7.3.2	Effect of Comonomer Concentration.....	36
7.3.2.1	GPC and DSC Results.....	37
7.3.3	Catalyst System Effect.....	37
7.3.3.1	GPC and DSC Results.....	38
7.3.3.2	FTIR Spectroscopy Results.....	39
7.3.4	Polymerization Tests with Cocatalyst other than MAO.....	40

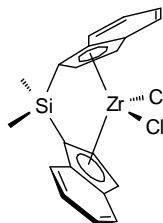
7.3.5	Partial Conclusions.....	41
<b>7.4</b>	<b>Copolymerization of Ethylene with Allyl Ethers.....</b>	<b>43</b>
<b>7.4.1</b>	<b>Copolymerization of Ethylene with Allyl Ethyl Ether (AEE).....</b>	<b>43</b>
7.4.1.1	Effect of the Catalyst System.....	44
7.4.1.1.1	GPC and DSC Results.....	46
7.4.1.1.2	Scanning Electron Microscopy (SEM) Results.....	48
7.4.1.1.3	<sup>1</sup> H NMR Results.....	49
7.4.1.2	The Temperature Effect.....	51
7.4.1.3	The MAO Effect.....	54
7.4.1.4	The Pressure Effect.....	56
7.4.1.5	Partial Conclusions.....	57
<b>7.4.2</b>	<b>Comparison between the Results of the Copolymerization of Ethylene with Allyl Propyl Ether and The Copolymerization of Ethylene with Allyl Ethyl Ether.....</b>	<b>59</b>
7.4.2.1	Effect of Comonomer Concentration.....	59
7.4.2.1.1	DSC and GPC Results.....	60
7.4.2.1.2	<sup>1</sup> H NMR Spectroscopy Results.....	61
7.4.2.2	Effect of Polymerization Temperature.....	62
7.4.2.2.1	DSC and GPC Results.....	62
7.4.2.3	Effect of Catalyst Concentration.....	63
7.4.2.3.1	DSC and GPC Results.....	64
7.4.2.4	Partial Conclusions.....	65
<b>7.4.3</b>	<b>Comparison of the Results obtained in the Copolymerization of Ethylene with AEE, APE and ABE respectively.....</b>	<b>67</b>
7.4.3.1	Determination of TIBA:Allyl Ether Ratio and TIBA:Allyl Ether Precontact Time.....	67
7.4.3.2	Effect of Comonomer Structure.....	70
7.4.3.2.1	<sup>1</sup> H NMR, <sup>13</sup> C NMR, FTIR and Elemental Analyses Results.....	74
7.4.3.2.2	GPC and DSC Results.....	80
7.4.3.3	Partial Conclusions.....	86
<b>7.5</b>	<b>Copolymerization of Ethylene and MODE.....</b>	<b>88</b>
7.5.1	Results with the Catalyst System (3)/MAO .....	88
7.5.1.1	Determination of the MODE:TIBA Ratio.....	88
7.5.1.2	Effect of the Reaction Temperature and MODE Concentration.....	89
7.5.1.2.1	GPC and DSC Results.....	90
7.5.1.2.2	<sup>1</sup> H NMR, <sup>13</sup> C NMR and Elemental Analyses (EA) Results.....	91
7.5.1.2.3	Fourier Transform Infrared Spectroscopy (FTIR) Results.....	93
7.5.2	Results with the Catalyst System Ph <sub>2</sub> Si(OctHFlu)(Ind)ZrCl <sub>2</sub> /MAO.....	94
7.5.2.1	<sup>13</sup> C NMR and <sup>13</sup> C(DEPT-135)NMR Spectroscopy Results.....	96
7.5.2.2	GPC and DSC Results.....	98

7.5.2.3	Fourier Transform Infrared (FTIR) Spectroscopy Results.....	99
7.5.3	Catalyst System Ni diimine/MAO Results.....	100
7.5.3.1	Effect of Comonomer Concentration.....	100
7.5.3.2	GPC and DSC Results.....	101
7.5.3.3	<sup>1</sup> H NMR and <sup>13</sup> C NMR Spectroscopy Results.....	102
7.5.3.4	Fourier Transform Infrared (FTIR) Spectroscopy Results.....	103
7.5.4	Comparison among the Used Catalysts Systems.....	103
7.5.5	Partial Conclusions.....	105
<b>7.6</b>	<b>Copolymerization of Ethylene with HBE and DBE.....</b>	<b>106</b>
7.6.1	Copolymerization Results of Ethylene with HBE.....	107
7.6.1.1	<sup>1</sup> H NMR and FTIR Spectroscopy Results.....	107
7.6.1.2	Elemental Analyses, GPC and DSC Results.....	109
7.6.2	Copolymerization Results of Ethylene with DBE.....	110
7.6.2.1	<sup>1</sup> H NMR, GPC and DSC Results.....	111
7.6.3	Partial Conclusions.....	112
<b>8</b>	<b>Conclusions.....</b>	<b>113</b>
<b>9</b>	<b>Experimental Section.....</b>	<b>115</b>
9.1	General Procedures.....	115
9.2	Chemicals.....	116
9.3	Gases.....	116
9.4	Comonomers.....	116
9.5	Methylaluminoxane (MAO).....	117
9.6	Triisobutylaluminium (TIBA).....	117
9.7	Solvents.....	117
9.8	Catalysts.....	117
9.9	Safety.....	118
9.10	Analytical Techniques.....	119
9.10.1	<sup>1</sup> H NMR Spectroscopy.....	119
9.10.2	Differential Scanning Calorimetry – DSC.....	119
9.10.3	Gel Permeation Chromatography – GPC.....	119
9.10.4	Elemental Analysis.....	120
9.10.5	Elemental analysis: Determination of Oxygen.....	120
9.10.6	Electron Microscopy.....	120
<b>10.0</b>	<b>References.....</b>	<b>121</b>

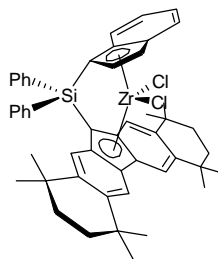
## 2 Abbreviations

ABS	Acrylonitrile-Butadiene-Styrene Terpolymer
AEE	Allyl Ethyl Ether
APE	Allyl Propyl Ether
ABE	Allyl Butyl Ether
ASA	Acrylonitrile Styrene Acrylate Copolymer
<sup>13</sup> C NMR	Carbon 13 Nuclear Magnetic Resonance
C	Concentration
DBE	9-Decenyl Butyl Ether
DEPT	Distorsionless Enhancement by Polarization Transfer
DSC	Differential Scanning Calorimetry
EA	Elemental Analysis
EPS	Expandable Polystyrene
EVA	Ethylene Vinyl Acetate Copolymer
FG	Functional Group
FT-IR	Fourier Transform Infrared Spectroscopy
GPC	Gel Permeation Chromatography
h	Hour
<sup>1</sup> H NMR	Hydrogen 1 Nuclear Magnetic Resonance
HBE	5 Hexenyl Butyl Ether
HDPE	High Density Polyethylene
IR	Incorporation Rate
LDPE	Low Density Polyethylene
LR	Latent Reactivity
M	Metal
MAO	Methylaluminoxane
MMA	Methylmethacrylate
M <sub>n</sub>	Number-Average Molecular Weight
M <sub>w</sub>	Weight-Average Molecular Weight
PA	Polyamide
PC	Polycarbonate
Pd	Polydispersity Index
PE	Polyethylene
PET	Polyester
P <sub>ETH</sub>	Ethylene Pressure

Ph	Phenyl
PMMA	Polymethylmethacrylate
ppm	Parts per Million
PUR	Polyurethane
PVC	Polyvinyl Chloride
PS	Polystyrene
R	Alkyl
<i>rac</i>	racemic
SAN	Styrene Acrylonitrile Copolymer
SEM	Scanning Electron Microscopy
T (%)	Transmittance
T <sub>m</sub>	Melting temperature
T <sub>g</sub>	Glass transition temperature
TIBA	Triisobutylaluminium
TCE-d2	bis-Deutero-Tetrachlorethane
VA	Vinyl Acetate
X	Molar Fraction
δ	Chemical Shift (NMR)

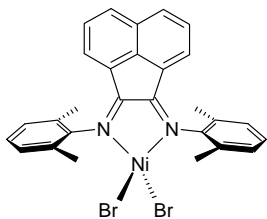


[Dimethylsilyl-bis-(1-η<sup>5</sup>-indenyl)]zirconiumdichloride



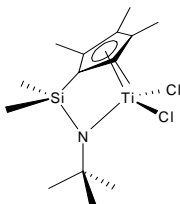
[Diphenylsilyl-(1- η<sup>5</sup>-indenyl)(1,1,4,4,7,7,10,10-octamethyl-1,2,3,4,7,8,9,10-octahydrodibenzol[b,h]-9-η<sup>5</sup>-fluorenyl)]-zirconiumdichloride

[Ar-N=C(An)-C(An)=N-Ar]NiBr<sub>2</sub> (Ar = 2,6-Me<sub>2</sub>C<sub>6</sub>H<sub>3</sub>)



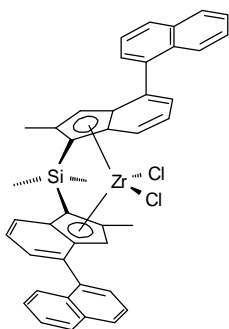
[Bis(2,6-dimethylphenylimino)acenaphthen]nickeldibromide

[Me<sub>2</sub>Si(Me<sub>4</sub>Cp)(N<sub>tert</sub>Bu)]TiCl<sub>2</sub>



[Dimethylsilylen-(tertbutylamido)-(2,3,4,5-tetramethyl-1-η<sup>5</sup>-cyclopentadienyl)]titaniumdichloride

rac-[Me<sub>2</sub>Si(2-Me-4-(1-Naph)Ind)<sub>2</sub>]ZrCl<sub>2</sub>



rac-[Dimethylsilyl-bis(2-methyl-4-(1-naphthyl)-1-η<sup>5</sup>-indenyl)] zirconiumdichloride

### 3 Summary

Nowadays, the modification of polyolefins such as polyethylene in a controlled and mild manner is one of the most important challenges in the polymer engineering. The modification of polyethylene by introduction of even low amount of functional groups into the main chain, can improve its properties. New applications are possible in areas such as good adhesion/coating, barrier properties, solvent resistance and printability are required.

In this work copolymerizations of ethylene with oxygen containing monomers such as esters and ethers were achieved using metallocene/MAO catalyst systems. Most of copolymerizations required the protection/deprotection strategy to be used and Triisobutylaluminium (TIBA) was chosen as a protecting agent. Additionally, the right design of the monomer structure was used as a second approach to prevent catalyst deactivation.

Methylmethacrylate (MMA) and Vinyl Acetate (VA) have been copolymerized with ethylene using a sequential polymerization approach. The polymers obtained in these polymerizations show different physical properties when compared with the properties of the original polyethylene. They are mainly insoluble and therefore difficult to be characterized. However, a set of experimental evidence by DSC, GPC, FT-IR and NMR show that a truly copolymers have been synthesized.

Additionally, Allyl Ethyl Ether (AEE), Allyl Propyl Ether (APE) and Allyl Butyl Ether (ABE) have been successfully copolymerized with ethylene in the presence of the catalyst system  $\text{Me}_2\text{SiInd}_2\text{ZrCl}_2/\text{MAO}$  using TIBA as protecting agent. The direct copolymerization approach leads to incorporation up to 16 mol % of polar groups into the polyethylene backbone. The structures of the ether as well as the reaction parameters greatly influence the catalytic activity. The studies have shown that the polymerization is favored by an increase of the methylene spacers after the oxygen atom in the ether structure.

Further in this study was investigated the copolymerization of ethylene with 2,7-Octadienylmethylether. Based on the experimental data, the copolymerization was achieved in the presence of three catalyst systems:  $\text{Me}_2\text{SiInd}_2\text{ZrCl}_2/\text{MAO}$ ,  $\text{Ph}_2\text{Si}(\text{OctHFlu})(\text{Ind})\text{ZrCl}_2/\text{MAO}$  and  $[\text{Ar}-\text{N}=\text{C}(\text{An})-\text{C}(\text{An})=\text{N}-\text{Ar}]\text{NiBr}_2$  (Ar = 2,6-

$e_2C_6H_3$ ]/MAO. These catalyst systems allowed the synthesis of copolymers with considerable incorporation rates of the functional group into the polyethylene main chain (maximum of 0.47 mol% (7.3 wt %), for the catalyst  $Ph_2Si(OctHFlu)(Ind)ZrCl_2/MAO$ ). In general, the molecular weights, melting points and catalytic activities are systematically reduced by an increase the polar monomer feed ratio.

To sum up, the employment of 5-Hexenyl Butyl Ether (HBE) and 9-Decenyl Butyl Ether (DBE) in the experiments demonstrated that the placement of the oxygen atom far from the double bond greatly enhance the catalytic activity. However, long methylene spacers can also be detrimental to the catalyst system. The optimum activity, as well as incorporation rate (0.60 mol %) was achieved with 4 methylene spacers between the functional group and the double bond.



## 4 Zusammenfassung

Heutzutage ist die Modifizierung von Polyolefinen wie Polyethylen durch eine kontrollierte copolymerization eine der wichtigsten Herausforderungen in der Polymer-Technik. Die Modifizierung von Polyethylen durch die Einführung von wenigen funktionellen Gruppen in die Hauptkette verbessert die Eigenschaften der Polymere und ihre Anwendung in Gebieten in denen zum Beispiel gutes Festkleben/Überzug, Barriere-Eigenschaften, lösender Widerstand oder Druckfähigkeit erforderlich sind.

In dieser Arbeit wurde eine direkte Copolymerization von Ethylen mit einem sauerstoffhaltigen Ester oder Ether durchgeführt. Als Katalysator wurde ein Metallocen/MAO-System verwendet. Ein Großteil der Copolymerizationen erforderte eine Komplexierung des Sauerstoffs (Protection-Strategie) durch TIBA (Triisobutylaluminum) als schützendes Agens. Zusätzlich wurde das Design der Monomerstruktur als eine zweite Methode verwendet, um die Katalysator-Deaktivierung zu verhindern.

Methylmethacrylat (MMA) und Vinylacetat (VA) konnten mit Ethylen copolymerisiert werden. Die dabei erhaltenen Copolymere zeigen veränderte physikalische Eigenschaften im Vergleich zum Homo-Polyethylen. Wegen ihrer weitgehenden Unlöslichkeit lassen sie sich schlecht charakterisieren. Jedoch zeigen die Untersuchungen der Produkte durch DSC, GPC, FT-IR und NMR, dass echte Copolymere synthetisiert worden sind.

Die Allylether, Allylethylether (AEE), Allylpropylether (APE) und Allylbutylether (ABE) wurden erfolgreich mit Ethylen in Gegenwart vom Katalysator-System  $\text{Me}_2\text{SiInd}_2\text{ZrCl}_2/\text{MAO}$  copolymerisiert wobei TIBA verwendet wurde, um den Sauerstoff zu komplexieren. Die direkte Copolymerizations-Methode führt zum Einbau bis zu 16 mol % an polaren Gruppen in die Polyethylen-Hauptkette. Die Strukturen der Ether sowie die Reaktionsparameter beeinflussen die katalytische Aktivität stark. Die Studien haben gezeigt, dass die Polymerization durch die Erhöhung der Zahl der Methylengruppen zwischen dem Sauerstoffatom und der Doppelbindung bevorzugt wird.

Des Weiteren wurden in dieser Arbeit Copolymerizationen von Ethylen mit 2,7-Octadienylmethylether durchgeführt. Wobei drei Katalysator-Systeme:  $\text{Me}_2\text{SiInd}_2\text{ZrCl}_2/\text{MAO}$ ,

$\text{Ph}_2\text{Si}(\text{OctHFlu})(\text{Ind})\text{ZrCl}_2/\text{MAO}$  and  $[\text{Ar}-\text{N}=\text{C}(\text{An})-\text{C}(\text{An})=\text{N}-\text{Ar}]\text{NiBr}_2$  (Ar = 2,6- $\text{e}_2\text{C}_6\text{H}_3$ )]/MAO verwendet wurden. Diese Katalysator-Systeme erlaubten die Synthese von Copolymeren mit beträchtlichen Einbauraten der funktionellen Gruppen in die Polyethylen Hauptkette (Maximum 0.47 mol % (7.3 wt %), für den Katalysator  $\text{Ph}_2\text{Si}(\text{OctHFlu})(\text{Ind})\text{ZrCl}_2/\text{MAO}$ ). Im Allgemeinen werden die Molekulargewichte, Schmelzpunkte und katalytischen Aktivitäten durch größere Mengen des polaren Monomers in der Ausgangslösung stark reduziert.

Ferner, demonstrierte die Copolymerisation von 5-Hexenylbutylether (HBE) und 9-Decenylbutylether (DBE) mit Ethylen, in den Experimenten, dass die eine Stellung des Sauerstoff-Atoms weit entfernt von der Doppelbindung außerordentlich die katalytische Tätigkeit erhöht. Jedoch können lange Methylen-Distanzen auch wieder zu einer Erniedrigung der Aktivität führen. Eine Optimale Anzahl an Methylengruppen sowie ein Einbau vom 0.60 mol % wurde mit 4 Methylengruppen zwischen der funktionellen Gruppe und der Doppelbindung erreicht.

## 5 General Aspects

### 5.1 Polyolefin Development

The development of polyolefin dates back to the early 1930s with the production of low density polyethylene (LDPE) by free radical initiators<sup>1</sup>. The reaction required elevated temperature (200-400°C) and high pressure (500-1200 atm) to produce LDPE containing both long and short chain branches.

With the discovery of catalytic polymerization of ethylene by Karl Ziegler in the early 1953s, using the catalyst system  $\text{TiCl}_4/\text{Et}_3\text{Al}$ , synthetic polymers became one of the most growing commercial markets<sup>1</sup>.

The subsequent breakthrough was in 1954, with the discovery that the Ziegler catalyst was able to promote the stereoselective polymerization of propylene and other long chain  $\alpha$ -olefins by Giulio Natta. This discovery has allowed increasing the numbers of applications in this field<sup>2</sup>. The most important stereospecific structures of polymers are shown in Figure 01.

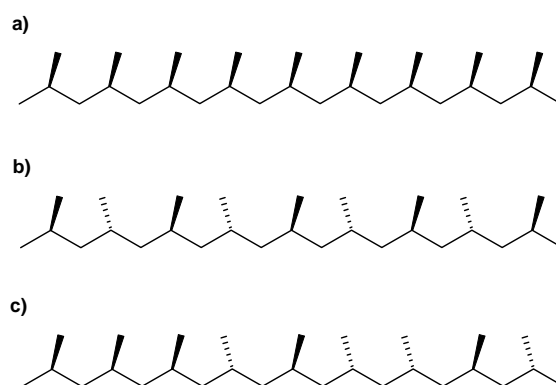


Figure 01: Stereospecific polymer structure: a) isotactic, b) syndiotactic and c) atactic.

In the late 1970s, in Germany, Kaminsky and Sinn<sup>3</sup> discovered a new class of Ziegler-Natta catalyst, based on metallocene/methylaluminoxane. This new generation of catalyst showed higher activity and produced polymers with higher molecular weight than the commercially used Ziegler-Natta catalyst.

A further step was the discovery of chiral ansa-metallocenes with well defined active centers by Brintzinger in 1982<sup>4</sup>. This catalyst was used for the synthesis of highly isotactic propylene by Kaminsky, Brintzinger and coauthors in 1985<sup>5</sup>. Since then, the structure of the metallocenes has been modified worldwide in industrial and academic areas to provide a range of different catalyst-structures that can be used to synthesize highly isotactic, syndiotactic, atactic or hemi-isotactic polyolefins with different molecular weights and different degrees of tacticity<sup>6-10</sup>.

## 5.2 Polymerization Mechanisms

Despite the tremendous amount of research that has been conducted in this area<sup>11-16</sup>, the real mechanism of Ziegler Natta Polymerization had been controversial for long time. However, it is generally agreed that a polyolefin is produced by multiple insertions of olefins into a metal-carbon bond. Of the various mechanisms that have been proposed, one that is widely accepted is the Cossée and Arlmann mechanism<sup>14,15,17,18</sup>. Basically, the authors considered that the monomer is incorporated into the polymer by an insertion reaction between a metal atom of the catalyst and a terminal carbon of a coordinated polymer chain.

The key features of the insertion mechanism are that the active metal center bearing the growing alkyl chain must have an available coordination site for the incoming monomer, and that insertion occurs via chain migration to the closest carbon of the double bond, which undergoes *cis* opening with formation of the new metal-carbon and carbon-carbon bonds. The new C-C bond is then on the site previously occupied by the coordinated monomer molecule.

This mechanism was originally proposed for the olefin insertion into a metal-alkyl group bond in the heterogeneous polymerization of olefins, but it can also be used to describe the basic steps in olefin polymerization with metallocene/MAO catalysts. The proposed mechanism for the insertion of olefins is shown in Figure 02.

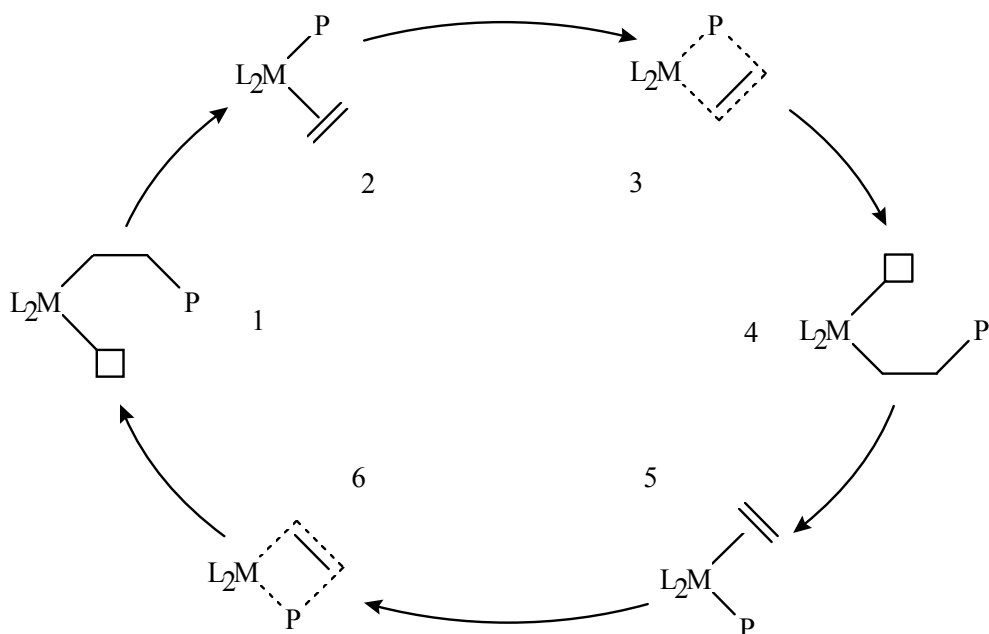


Figure 02: Possible path for the insertion of olefins into the metal-polymer bond.: vacant coordination site, P polymer chain.

In the proposed mechanism first olefin coordinates to a vacant site of the metallocene (1) and forms a  $\pi$ -complex (2). Then, the olefin-unit is inserted into the growing chain (4) via a four-membered transition state (3). The next insertion can either follow immediately by coordination and insertion of the next olefin molecule (5,6). An inversion of configuration at the stereocenter (1 to 4) is followed by the coordination and insertion of the next olefin molecule for the retention mechanism (4 to 1). This process, which involves shifting of the growing polymer chain to the position previously occupied by a coordinated monomer, continues until termination of the polymer chain. Termination of the polymer chain takes place via  $\beta$ -hydride transfer to the metal or to the monomer or  $\beta$ -methyl transfer to the metal or chain-transfer to the aluminium.

### 5.3 The Role of the Cocatalyst

In the late 80, ethylene was for the first time polymerized using metallocene/aluminoxane catalyst<sup>19</sup>. During the reaction was observed an increase in the activity of dicyclopentadienyl and tricyclopentadienyl catalysts after addition of a small amount of water in the polymerization media. The water reacts with the alkylaluminium yield alumininoxanes that is responsible for the increase in catalyst activity.

The more effective and commonly used cocatalyst among other alumininoxanes is MAO

(methylaluminoxane). Studies suggest that MAO exists as mixture of cyclic or linear oligomers and also three dimensional open cage structure. The most commonly used MAO may have the structure present in Figure 03.

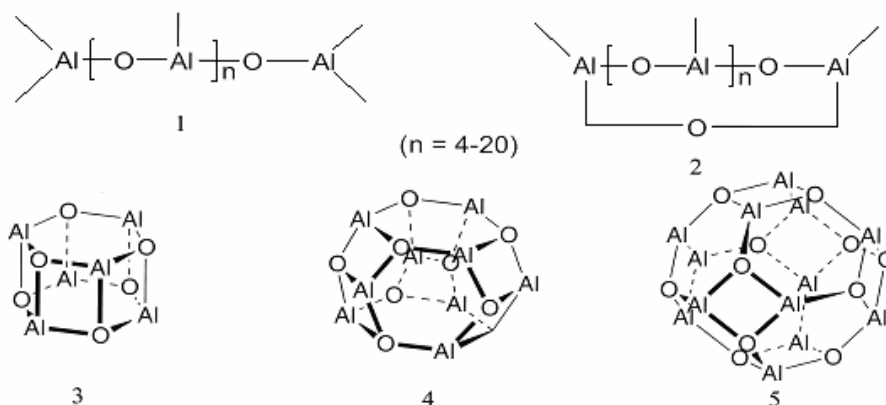


Figure 03: MAO structure 1)Linear; 2)Cyclic 3,4,5) three dimensional open cage structure.

The activation process of the catalyst with MAO has been described in two steps: the first one is alkylation of the halogenated metallocene complex. As a second reaction, monomethylation takes place, and an excess of MAO leads to dialkylated species, Figure 04.

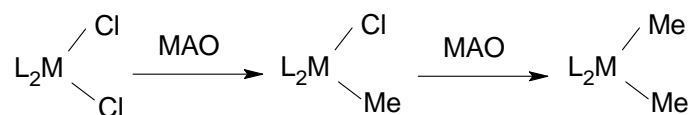


Figure 04: Alkylation of metallocene complex.

Subsequently, the MAO complex can seize a methyl anion, a Cl<sup>-</sup> anion or an OR<sup>-</sup> anion from the metallocene, forming an AlL<sub>4</sub><sup>-</sup> anion which can distribute the electron over the whole cage, thus stabilizing the charged system. The formed cationic L<sub>2</sub>M(CH<sub>3</sub>)<sup>+</sup> is generally regarded as the active site in olefin polymerization, Figure 05.

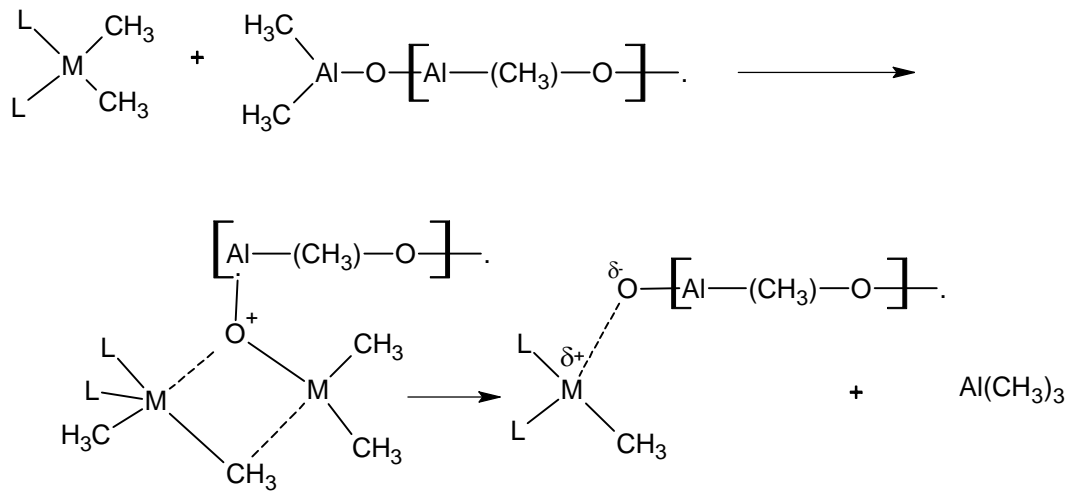


Figure 05: Formation of active center.

### 5.4 Functionalization of Polyolefins

The global production of plastics is over than 225 Million tons in 2004 with an estimated demand of 304 Million tons in 2010<sup>20</sup>. Among these plastics, polyethylene is the highest volume macromolecules produced in the world (31% of the global production)<sup>20</sup>, Figure 06.

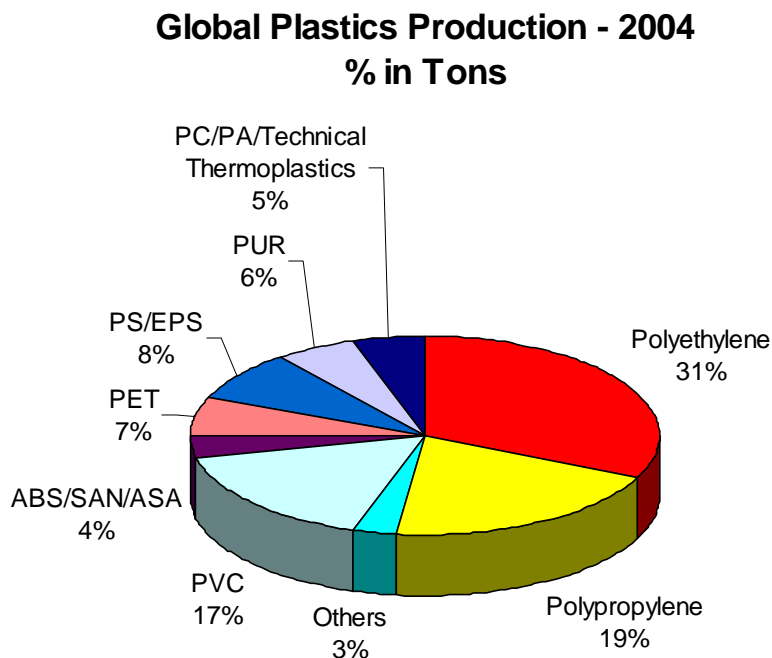


Figure 06: Global plastics production. Source: Plastics Europe Deutschland, WG Statistics and Market Research.

Generally speaking, light weight, easy processing, good chemical resistance and impact strength, recyclable, low cost and excellent electrical properties can be cited as polyethylene properties that justify his broad use in industrial applications. However, the low surface tension, poor barrier properties (except to water), poor temperature resistance, poor adhesion, dyeability, printability and compatibility with others monomers are properties that still need to be improved.

The need of polyethylene properties improvement has driven a considerable part of the industrial and academic research efforts in last decades. Since the onset of commercialization of PE and PP in the early 1950, the functionalization of polyolefins has lured researchers around the world mainly focused in the necessity to improve their compatibility with others materials.

One way to modify the properties of a polymer is the introduction of a functional group into an originally nonpolar material<sup>21</sup>. These functional groups control important polymer properties such as adhesion, barrier properties, surface properties, solvent resistance, miscibility with other polymer and reological properties. The functionalization of polyolefins offers an opportunity to broad application spectrum in areas that has not been explored before. Nowadays, few functionalization processes are available, and most commercial functionalized polymers have ill-defined molecular structure<sup>22</sup>.

#### **5.4.1 Functionalization Processes**

The introduction of even low concentrations of functional groups into polyolefins can be enough to change the properties of these materials for specific applications without compromising the desired features characteristic of the start materials (e.g., processability, chemical robustness, and mechanical strength)<sup>23</sup>. There are at least four approaches<sup>24</sup> to incorporate the functional group into polyolefins backbone: (a) Direct copolymerization with olefins bearing the desired functional group. (b) Direct copolymerization with olefins containing a protected functional group. (c) Direct copolymerization with a monomer bearing substituents with latent reactivity and (d) Direct post-polymerization functionalization of a polyolefin<sup>23</sup>, Figure 07.



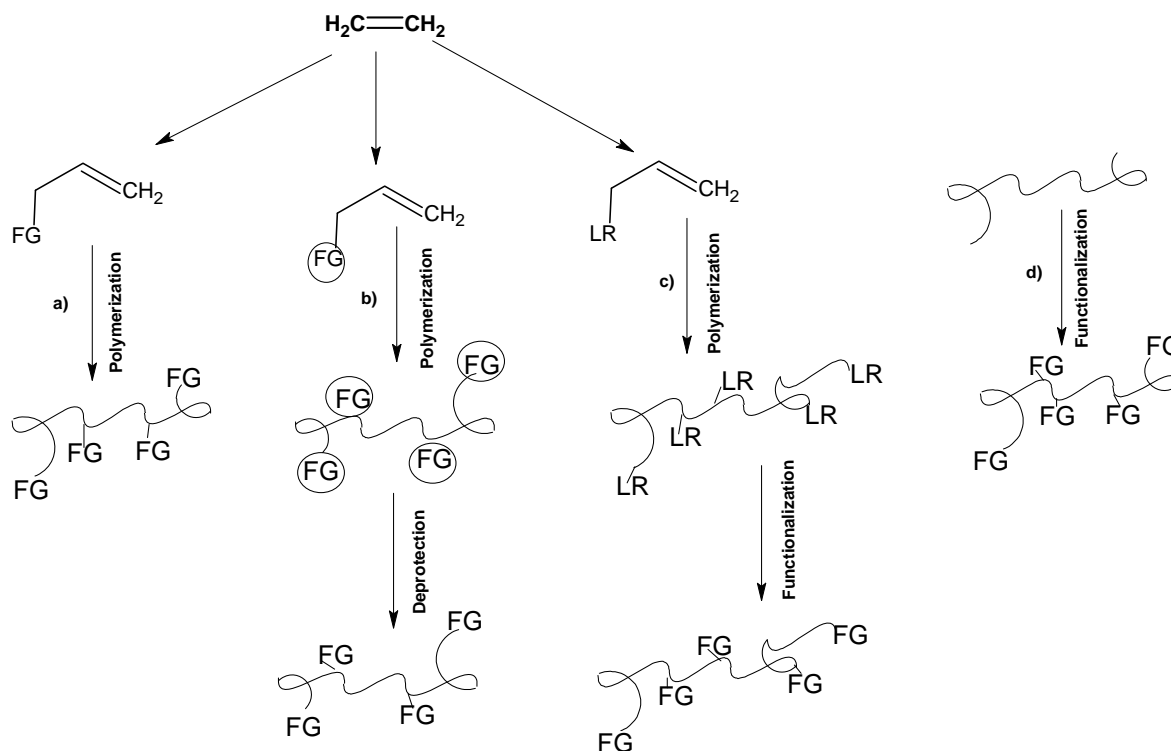


Figure 07: Functionalization processes. (a) Direct copolymerization with olefins bearing the desired functional group (FG). (b) Direct copolymerization with olefins containing a protected functional group. (c) Direct copolymerization with a monomer bearing substituents with latent reactivity (LR) and (d) Direct post-polymerization functionalization of a polyolefin<sup>23</sup>.

Theoretically, the direct copolymerization with olefins bearing the desired functional group, route a), is the most straightforward way to access side group functionalized polyolefins. This approach has the advantages of ensuring a random distribution of the incorporated functional groups along the polyolefin chain and control the insertion during the copolymerization<sup>24</sup>. Unfortunately, this reaction is very difficult because the formation of stable complex between the Lewis acid component of the catalyst and the nonbonding electron pairs on the functional group, this complexation leads to catalyst deactivation.

There are some approaches that can reduce the deactivation of metallocene catalyst in the copolymerization with functional comonomers: The introduction of steric and electronic protection on the functional group<sup>25-27</sup> (route b), enhancing the steric hindrance of the catalyst active sites, or use the heteroatom resistant late transition metal catalyst<sup>28-30</sup>. As illustrated in Figure 07, the synthesis of functionalized polyolefins employing the functional group protection method involves not only the copolymerization of olefins with functional monomers, but also the protection and deprotection reactions.

The third approach is the copolymerization involving one reactive monomer. The key factor in this route is the design of a comonomer containing reactive group that can simultaneously fulfill some requirements: the reactive group must be stable to metallocene catalyst, soluble in the polymerization media and must be easy to be interconvert to form polar groups under mild reaction conditions<sup>22</sup>.

The last approach described here, (route d) is the chemical modification of the preformed polymer. The idea is activate the polymer in order to break some stable C-H bonds and generate free radicals along the polymer chain. The radicals undertake chemical reactions with some reagents coexisting in the system<sup>22</sup>.

### 5.4.2 Classification of Functional Polymer by Structure

Regarding to their structure, functional polyolefins can be classified into four categories<sup>24</sup>: Side group functionalized polyolefins, functional polyolefin graft copolymer, chain end functionalized polyolefin and functional polyolefin block copolymer.

#### 5.4.2.1 Side group functionalized polyolefins

This is a polyolefin containing functional groups either directly substituted from polyolefin backbone or being separated from the backbone by an alkyl spacer, Figure 08.

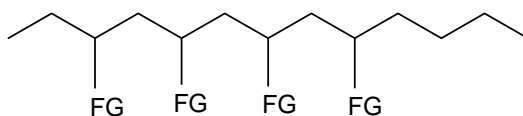


Figure 08: Side group functionalized polyolefins.

The side group functionalized polyolefin can be obtained by the direct copolymerization of an olefin with a functional group, using the routes a) or b) described before in the Figure 07. Additionally is also possible to exert protection on the catalyst active site designing the structure of the catalyst as well as the co catalyst<sup>24</sup>. Besides protection strategies, a satisfactory separation of the functional group from the double bond of the monomer leads to a successful olefin/functional monomer copolymerization<sup>31-34</sup>.

### 5.4.2.2 Functional Polyolefin Graft Copolymer

This polymer is structurally similar to side group functionalized polyolefins, the main difference is that the side group is not a group but rather a polymer chain composed of many functional repeated units, Figure 09.

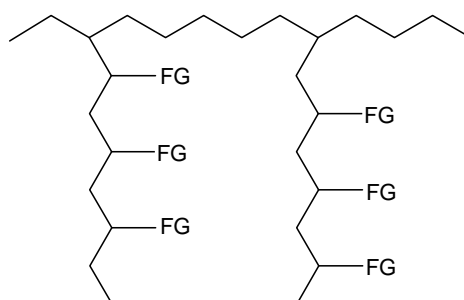


Figure 09: Functional polyolefin graft copolymer.

This approach is divided in two categories: graft copolymerization approach and the macromonomer approach. In the first one, to obtain control over the graft lengths and graft density is necessary to generate in the polyolefin chain grafting sites prior to graft reaction which is required to follow the living polymerization mechanism. The grafting sites can be an initiator (or its precursor) moiety for living anionic or controlled/"living" radical polymerization. In the second approach, the grafting chain is first designed to be a macromonomer and subsequently its copolymerization results in the graft copolymer<sup>24</sup>.

### 5.4.2.3 Chain End Functionalized Polyolefin

These polymers containing only a functional group at the chain end, Figure 10.

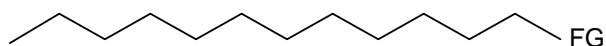


Figure 10: Chain end functionalized polyolefin.

In general three approaches are employed to obtain chain end functionalized polyolefins: chemical modification of chain end-unsaturated polyolefins; living olefin coordination polyolefin and in situ chain transfer reaction by chain transfer agent containing a polar group or its precursor using metallocene or Ziegler Natta olefin polymerization.

#### 5.4.2.4 Functional Polyolefin Block Copolymers

This polymer consists basically of polyolefin block and a functional block, however, it also has functional groups at the chain end<sup>24</sup>, Figure 11.

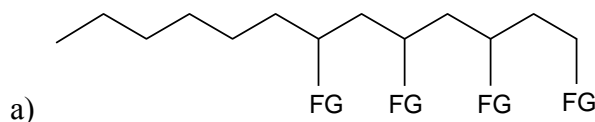


Figure 11: Functional polyolefin block copolymer.

A numbers of approaches have been developed to obtain functional polyolefin block copolymers<sup>35-36</sup>. Among them the most studied ones are: living olefin coordination polymerization, transformation from olefin coordination to controlled/"living" radical polymerization and transformation from olefin coordination to living anionic polymerization.

### 5.5 Metallocene as a Catalyst for Copolymerization with Functional Monomers

Since the discovery of the chiral zirconocene polymerization catalyst by Brintzinger and Kaminsky<sup>5</sup>, the use of metallocene has strongly influenced the industrial and academic research and leads to a wide range of new polymeric materials that result in a large number of new applications.

The reactivity of most functional groups toward the metal catalysts requires protection-deprotection strategies<sup>37</sup>. A selection of protection agent is very important because it should not only prevent the catalyst deactivation but also provide an easy protection and deprotection process. The most commonly employed protecting groups for compatibility with metallocene are based on aluminum, boron and silicon. Aluminum offers an advantage because of its existence in polymerization media<sup>38</sup>. Additionally, recent research showed that the longer the space between the double bond and the functionality is, the better the tolerance of functionality by metallocene catalyst<sup>31-34</sup> is.

It is important to remember that research on this subject carried out in laboratories as well as in industries has rendered a large number of journal publications but also an even large number of patents. The recent progress in direct functionalization of olefin using metallocene/MAO catalyst and involving monomers containing protected functional group is

present in this section.

Ethylene and propylene copolymerization with 5-hexen-1-ol pre-treated with alkylaluminum was performed using [dimethylsilylbis(9-fluorenyl)]zirconium dichloride/methylaluminoxane as the catalyst<sup>39</sup>. The results showed that the system protected with trimethylaluminium (TMA) was less effective than that protect with triisobuthylaluminium (TIBA). The alkyl(5-hexen-1-ol)aluminium were prepared under nitrogen flow. The obtained pre-treated monomers are giving in Figure 12. The monomers MH1 and MH2 were obtained when 5-hexen-1-ol was pre-treated with TMA and the monomer BH1 was obtained when 5-hexen-1-ol was pre-treated with TIBA.

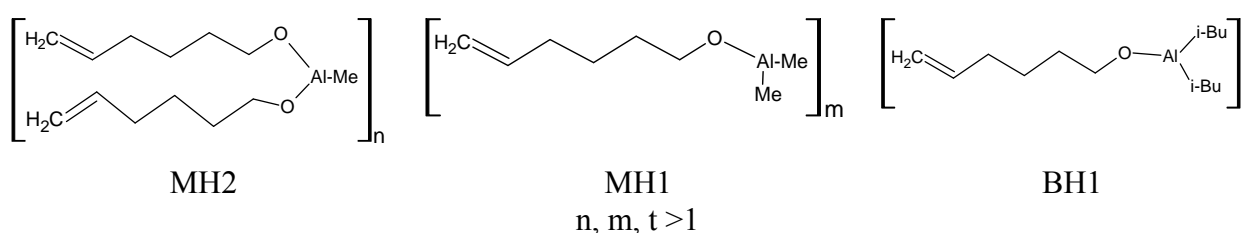


Figure 12: Al masked comonomers.

It was observed that the molecular weights of the alternating copolymers can be controlled by the type of the alkylaluminium added during the polymerization. Additionally, it also depends on the alkylaluminium used (masking agent, additive and cocatalyst). The TIBA system produced higher molecular weight copolymers ( $M_n = 9400$ ) than TMA system.  $^{13}\text{C}$ NMR analysis proved that the obtained copolymer is an alternating copolymer containing 50% of 5-hexen-1-ol, whereas the poly(propylene-co-5-hexen-ol) acted as random copolymer. The surface property was evaluated by means of water drop contact angle measurements. The copolymers containing large amount of 5-hexen-1-ol units showed good hydrophilic properties.

Hagihara et al<sup>40</sup> studied the copolymerization of propylene with 3-buten-1-ol protected with alkyl-aluminium (TMA or TIBA). The polymerization was conducted with an isospecific zirconocene catalyst (rac-dimethylsilylbis(1-indienyl)zirconium dichloride), combined with MAO as cocatalyst and if it was necessary, addition of TMA or  $\text{H}_2$  as the chain transfer reagent was used. The results indicated that the activity and molecular weights of the polymer obtained were greatly influenced by the protected group. The TIBA protected system produced a copolymer containing 3-buten-1-ol in the main chain. While the TMA protected system produced end-hydroxylated polypropylen using additional TMA. The copolymerisation using hydrogen as a chain transfer agent indicated formation of end

functionalised copolymer.

Oberhauser and co-workers<sup>41</sup> have shown that cationic metallocene catalysts are able to copolymerising olefins containing tertiary amines to a range of polymer microstructures. Five different aminoolefins were synthesized and used as monomers. These monomers included substituted 5-amino-1-pentenes and one 4-amino-1-butene with dimethyl, diethyl, diisopropyl, or diphenyl substitution patterns on nitrogen. It was observed that the bigger the substitution (diisopropyl > diethyl > dimethyl), the higher was the activity. Diphenyl substitution and shortening of the methylen spacer, by one carbon, cause a decrease in catalytic activity. The authors investigated three different catalyst systems to compare their effectiveness for the polymerisation of a diisopropyl-substituted aminopentene. In agreement with previous studies of Giannini<sup>42</sup> and co-workers, the author found that polymerisation with  $\text{TiCl}_3/\text{Al}(\text{i-Bu})_3$  produced very high molecular weight polymers but with extremely low activity. It was observed up to 40 times higher activities for a MAO based homogeneous catalyst system. A higher catalyst activity was found when the protonolysis reaction of dimethylzirconocenes with aluminium free initiator was used.

In 1997, Hakala et al<sup>43</sup>, copolymerized propylene with several different oxygen-functionalized olefins using a homogeneous  $\text{Et}(\text{Ind})_2\text{ZrCl}_2$  catalyst activated with MAO (methylaluminoxane). The comonomers differ from each other by the functional group (alcohol, acid, ester and ketone), in the length of spacer between the functional group and the double bond and in steric hindrance of oxygen containing group. The catalytic activity has strong dependence of the concentration of the monomer in feed. The higher the concentration of monomer in feed, the lower the catalytic activity. It was also observed that the longer the spacer group between the double bond and the functionality, the better the incorporation. In this work the highest comonomer incorporation was 2,7 mol % and it was achieved with the copolymerization of propylene with 10-undecen-1-ol. The deactivation of the catalyst was higher with compounds containing keto or methyl ester groups.

## 6 The Aim of This Work

Functionalization of polyolefins has long been an area of intensive research in polymer chemistry. The functionalization process can significantly broaden the end use of polyolefins. It is well known that even low incorporation rates of polar monomers into polyethylene main chain is sufficient to modify and boost its original properties. Toughness, adhesion, barrier and surface properties, solvent resistance are among the properties that could be controlled by the presence of polar groups.

The aim of this work was to copolymerize ethylene with oxygen containing monomers (ethers and esters) in the presence of metallocene catalyst systems. In order to circumvent the deactivation of the catalyst inherent to the direct polymerization approach used in this work, TIBA was chosen as a protecting agent.

The polar monomers were chosen as oxygen containing groups to be copolymerized with ethylene mainly because these groups can impart very desirable properties to polyolefins (adhesion and compatibility for example). Ether monomers undergo only weak complexation with aluminum for protection purpose and have not been extensively studied<sup>21</sup>.

Considering this fact a set of different catalysts were tested in order to find out a suitable active catalyst for this novel polymerization route. As part of this investigation the influence of the reaction parameters such as pressure, reaction temperature, protecting agent: polar monomer ratio, catalyst system, cocatalyst as well as catalyst and cocatalyst quantity were deeply investigated.

The effectiveness of the catalyst was discussed in terms of its activity, comonomer incorporation and the physical and chemical properties of the obtained polymers that were characterized using GPC, DSC, SEM and NMR spectroscopy.

## 7 Results and Discussion

### 7.1 Introduction

An ideal approach to copolymerize ethylene with functional monomers would be by a direct functionalization mechanism. However, as it has been described before, the reactivity of the functional groups toward the metal catalyst requires protection and deprotection strategies.

Among all functional groups, oxygen containing groups are the most studied for copolymerization with ethylene and  $\alpha$ -olefins. These groups are of interest because of their potential to be a precursor for polyolefin elastomers, since both ionic and chemical cross links may be introduced<sup>21</sup>. Additionally, these types of copolymers have excellent dyeing properties, good permeability of gaseous materials and novel weather-proof functions with high chemical reactivity<sup>44</sup>.

Aaltonen and coworkers has carried out the most comprehensive study of copolymerization of olefin with oxygenated functional groups using zirconocene catalyst in the presence of an excess of MAO as a monomer protecting agent<sup>34,43</sup>. These studies showed that alcohols and to some extent carboxylic acids are less deactivating than esters and ketones. Steric protection was also important to prevent catalytic deactivation, as noted by methyl and tert butyl ester and primary, secondary and tertiary alkenols. Additionally, monomers of sufficient spacer length showed similar deactivation effect independent of the functional group.

This work presents results of copolymerization of ethylene with the following oxygenated comonomers: methyl methacrylate (MMA), vinyl acetate (VA), allyl ethyl ether (AEE), allyl propyl ether (APE), allyl butyl ether (ABE), 2,7-Octadienylmethylether (MODE), 5 hexenyl butyl ether (HBE) and 9 decenyl butyl ether (DBE).

Polymerization results of ethylene with MMA and VA have been already published in the open technical literature. Even after a detailed screening carried out by the author, no published results of copolymerization of ethylene with AEE, APE, ABE, MODE, HBE and DBE in the presence of metallocene catalyst system were found. This work seems to be the first attempt to copolymerize ethylene with the six above mentioned monomers.



Keeping in mind that any new result could shed lights on the novel polymerization route, the effect of different monomers into the ethylene-polar monomer copolymerization and also the influence of different polymerization conditions were investigated in this work.

Five catalyst systems activated with methylaluminoxane (MAO) were investigated using triisobutylaluminium (TIBA) as a protect agent to prevent the deactivation of metallocene catalyst during the polymerization reaction. The structure of catalyst systems and the protect agent used in this work are giving in the Figure 13.

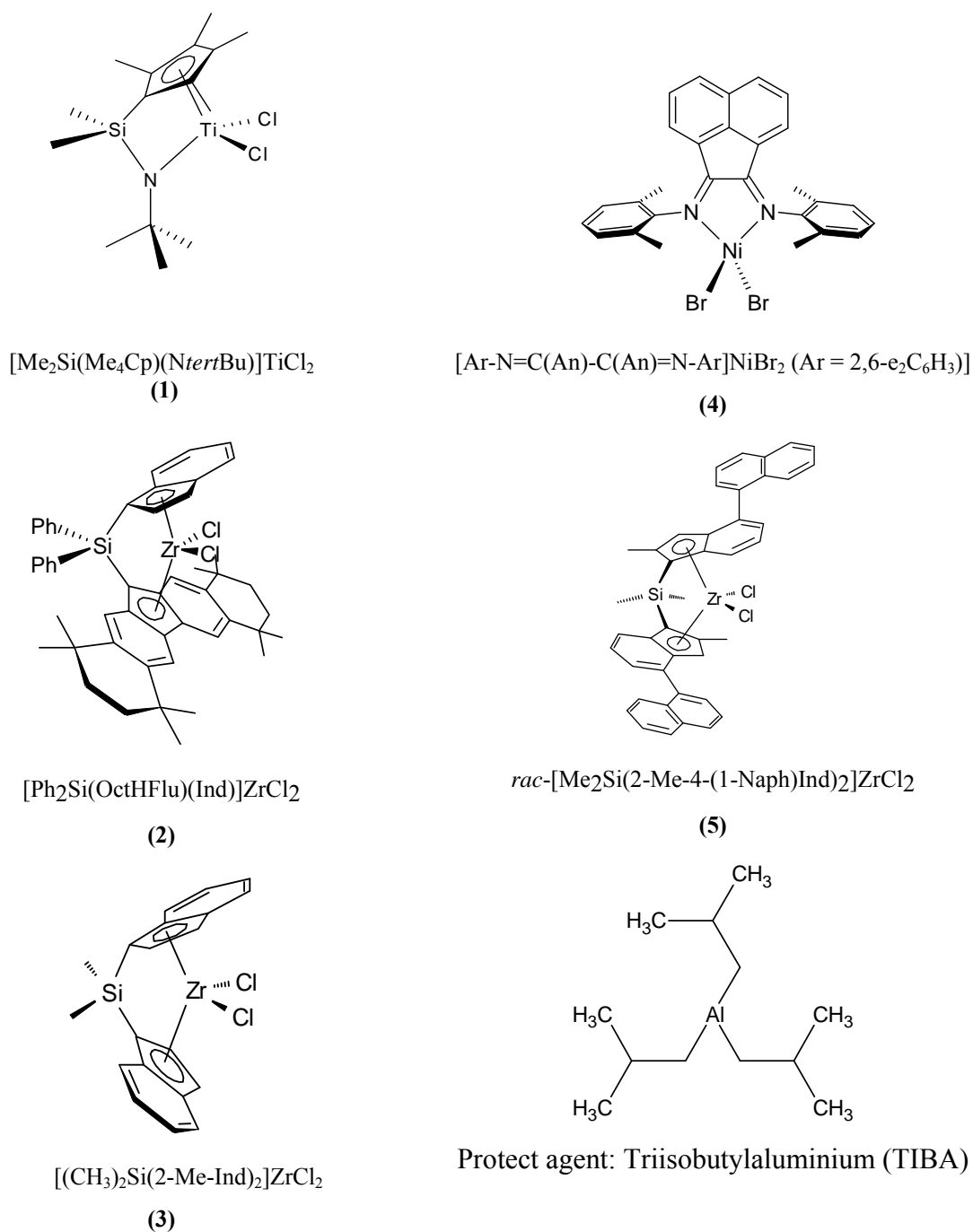


Figure 13: Structures of the Catalysts and the protect agent used in this work.

## 7.2 Copolymerization of Ethylene with Methyl Methacrylate (MMA)

Among the monomers containing oxygen as functional groups, methyl methacrylate plays a very important role because the range of different structures that can be obtained by modifying the ester group, as well as the numerous of practical application of these polymers.

In the following reports were investigated the synthesis of block copolymers of methyl methacrylate with ethylene and propylene using the living nature of the metallocene mediated methacrylate polymerization.

In 2001, Höcker and co workers<sup>109</sup> reported for the first time the block copolymerization of ethylene and MMA using zirconocene based catalyst. The catalyst was generated in situ from  $\text{Me}_2\text{C}(\text{Cp})(\text{Ind})\text{ZrMe}_2$  and  $\text{B}(\text{C}_6\text{F}_5)_3$  in toluene. Block copolymerization was achieved via the sequential addition of the monomers, starting with ethylene. Moreover, neither the GPC results nor the  $^1\text{H}$ NMR spectra are a proof of whether the obtained polymers are really copolymers or rather a polymer blend. However, after investigation of the solubility of the products in organic solvents, it seems that the major part of PMMA containing polymer is really a block copolymer. In this way the authors proposed a polymerization mechanism via insertion polymerization with a cationic zirconocene complex as the active specie, Figure 14.

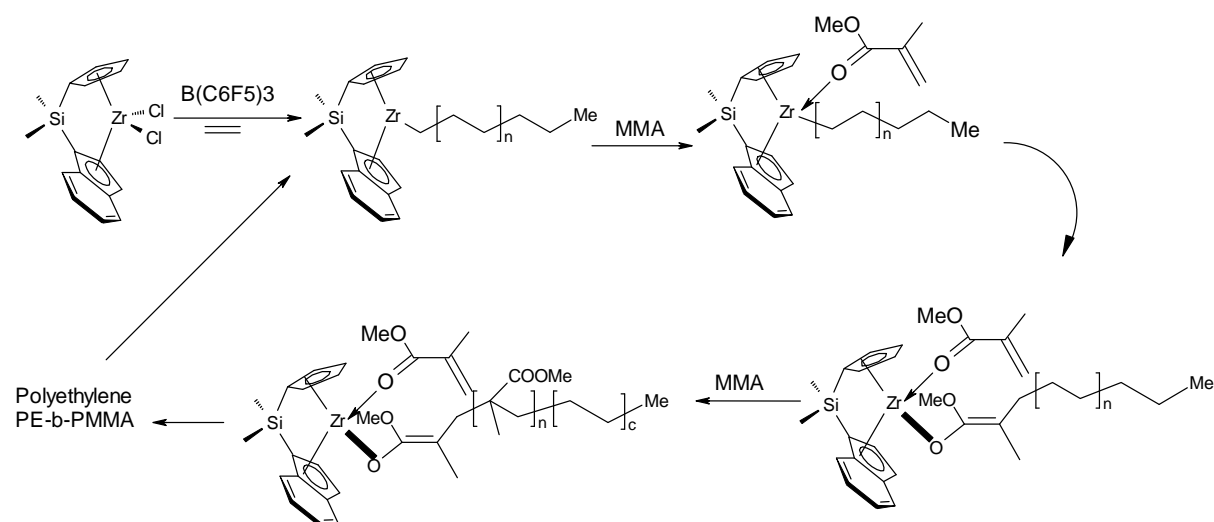


Figure 14: Proposed mechanism of block copolymerization.

Sequential stereoblock copolymerization of propylene and methyl methacrylate using group IV single site catalyst has been carried out<sup>46</sup>. When activated with  $\text{B}(\text{C}_6\text{F}_5)_3$ , catalyst (1):  $\text{C}_2$ -symmetric *rac*- $\text{Et}(\text{Ind})_2\text{ZrMe}_2$  yields isotactic PP-b-PMMA diblock copolymers, whereas

catalyst (2):  $C_s$ -symmetric  $Me_2Si(C_5Me_4)(tBuN)TiMe_2$  affords atactic PP-b-PMMA diblock copolymers. A small amount of PMMA homopolymer was formed during the copolymerization with catalyst (1) and it was extracted with boiling methylene chloride from the block copolymer product. However, the separation of the isotactic PP was not possible, due to the similarity in the solubility of both diblock copolymer and isotactic PP in the boiling solvent.

On the other hand, the copolymerization catalyzed by catalyst (2), both PMMA and PP homopolymers were easily removed from the block copolymer by solvent extraction using boiling heptane. The obtained block copolymers have high molecular weight and narrow polydispersity ( $M_n=21100$ ;  $P_d=1,08$ ), and moderated syndiotacticity for PMMA blocks ( $[rr] \approx 80\%$ ). These two catalyst systems activated with  $B(C_6F_5)_3$  show their ability to carry out mechanism crossover by switching active species from cationic metal alkyl in coordination insertion in PP polymerization step to cationic metallocene enolate in group transfer type of MMA polymerization step and produced stereodiblock copolymers.

The exact parameters of ethylene/MMA copolymerization that have been carried out in this work, using the catalyst system (1)/MAO and the respective results are present in the following section. The structure of the monomers and the probable obtained copolymer is giving in Figure 15.

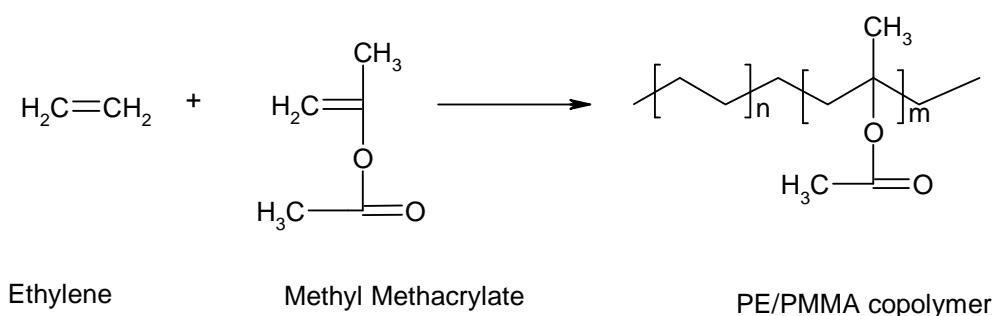


Figure 15: Structure of the monomers and probable obtained copolymer.

Obviously, it is very important to understand each reaction step and further optimize the reaction condition to achieve the control of the functionalized polymers. Consider this fact an initial study was made to establish the condition for optimum catalysts efficiency in terms of activity of copolymerization and characteristics of the obtained polymer.

### 7.2.1 Effect of TIBA Concentration

As described before, the direct copolymerization of functional monomers using the protection and deprotection methods was used as initial approach in this work.

The general procedure of the copolymerization of ethylene with MMA was achieved by a two-step procedure: homopolymerization of ethylene with the catalyst system (1)/MAO at 60°C in toluene at 2 bar, followed by sequential addition of MMA<sup>48</sup>. It is very important to note that the order of addition of MMA and ethylene causes a strong effect on the activity. The addition of protected MMA must follow ethylene in the reaction; otherwise it was not possible to obtain any results.

The catalytic activity varies with the changes in MMA/TIBA ratio in feed, as can be seen in Figure 16. The highest activity was found at the ratio MMA:TIBA = 0,6, after that the catalytic activity decreases systematically with increase in the MMA:TIBA ratio.

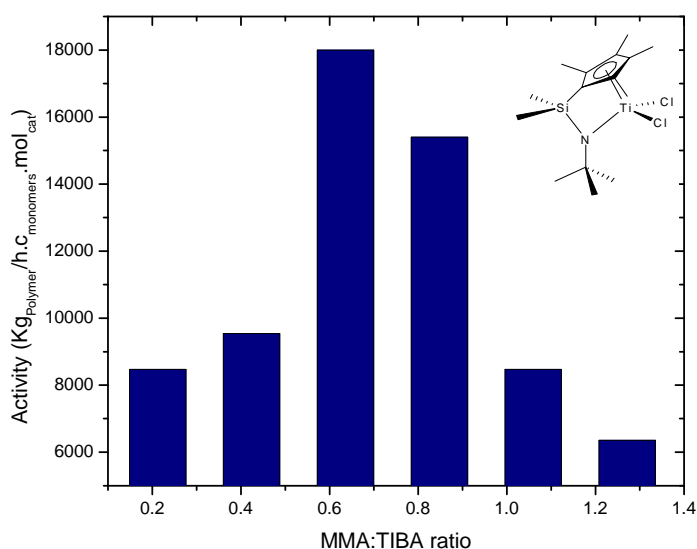


Figure 16: Copolymerization of ethylene with MMA. Activity as a function of MMA/TIBA ratio in feed. Polymerization conditions: 30°C, ethylene pressure: 2bar, toluene volume: 200mL, polymerization  $t_{MMA}$ : 1h30min, cocatalyst MAO;  $[MMA]=1\text{mol/L}$

### 7.2.1.1 GPC and DSC Results

The homogeneity of the obtained copolymer at this condition was also considered, and in some extent, the actual composition of the copolymer was not possible to be predicted. Polymerizations were carried out with different ratios of MMA/TIBA in order to assess the role of the protect agent.

Table 1: Investigation of the optimum ratio MMA/TIBA Ratio<sup>a</sup>

Run	MMA/TIBA Ratio	T <sub>m</sub> (°C)	Pd	Mn (Kg/mol)
1	0,2	140,7	2,0	83,1
2	0,4	138,6	2,0	53,6
3	0,6	142,4	2,0	58,3
4	0,8	142,5	2,0	54
5	1,0	140,8	1,9	55
6	1,2	141,0	1,9	53

<sup>a</sup>Polymerization conditions: 30°C, ethylene pressure 2bar, toluene volume 200mL, polymerization t<sub>MMA</sub> 1h30min, cocatalyst MAO; [MMA]=1mol/L

The variation of the ratio MMA:TIBA did not render significant changes in the melting points of the obtained polymers, as can be seen in Table 1. However, the molecular weight of the obtained polymers decrease with increase values of the MMA:TIBA ratio. Additionally, GPC measurements suggest that the polymerization was well defined with polydispersity index of 2.

Considering the previous results, the following experiments were carried out with the ratio MMA/TIBA=1. The relatively high catalytic activity and the effect of this ratio on the molecular weights of the obtained polymers were decisive in setting this reaction parameter.

The next step with the system ethylene/MMA was the investigation of the effect of the catalyst concentration and the ratio Al:Ti by varying the amount of MAO and catalyst concentration during the polymerization reaction.

### 7.2.2 Effect of MAO Concentration and Catalyst Concentration

A large excess of alkyl aluminoxane activators present in MMA polymerizations can complicate the polymerization result, especially with a long reaction time, because alkyl aluminoxanes have been found to slowly polymerize MMA to PMMA with large

polydispersity values<sup>47</sup>.

Considering this fact, the influence of the Al:Ti ratio on the catalytic activity as well as on the polymer properties was investigated by varying the amount of MAO in the polymerization medium between 200 and 600 mg. The obtained results are shown in Table 2.

Table 2: Results for ethylene and MMA copolymerization<sup>a</sup>

Run	MAO (mg)	Pd	$M_n \times 10^{-4}$ (g/mol)	$T_m$ (°C)	Activity $10^{-3}$ (Kg <sub>Polymer</sub> /mol <sub>Ti</sub> .h.C <sub>monomers</sub> )
14	200	1,8	12,4	140,9	285
23	400	2,1	13,1	138,0	189
24	600	1,9	13,1	137,0	77,7

<sup>a</sup>Polymerization conditions: 30°C, ethylene pressure 2 bar, toluene volume 200mL, polymerization  $t_{MMA}$ : 4h, cocatalyst MAO;  $[M]_{MMA}=0,05\text{mol/L}$ .

Despite the fact that the catalytic activity decrease with increase in MAO concentration in feed, the molecular weight of the obtained polymers did not change significantly. On the other hand, the melting points of the polymers slightly decrease with the increase in MAO concentration, see Figure 17.

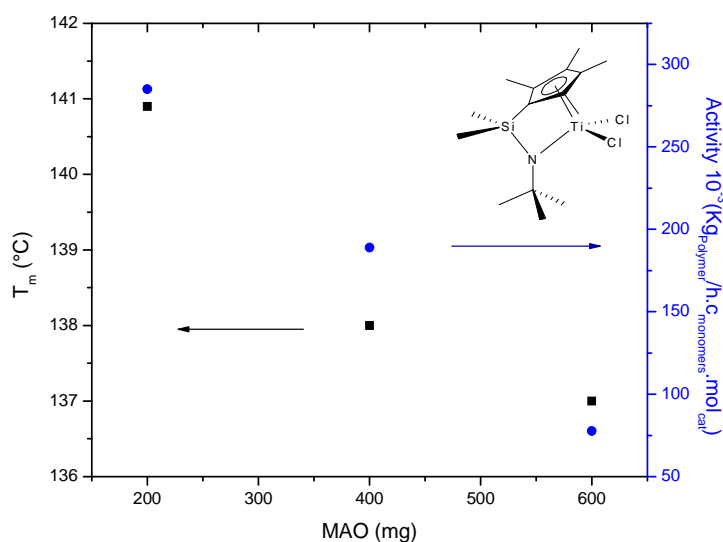


Figure 17: Melting point and Catalytic Activity as a function of MAO concentration in feed.

The following experiments were done using 600mg of MAO, due to the changes observed in the melting point of the obtained polymer. In addition to the investigation on the ratio Al:Ti, considering the variation of the MAO amount in feed, a systematic study on the catalyst concentration was carried out. The catalyst quantity varied from  $2 \times 10^{-6}$  to  $4 \times 10^{-6}$  mol in feed.

The results are present in Table 3.

Table 3: Results for ethylene and MMA copolymerization<sup>a</sup>

Run	Ccat (10 <sup>-6</sup> mol)	Pd	M <sub>n</sub> x10 <sup>-4</sup> (g/mol)	T <sub>m</sub> (°C)	Activity 10 <sup>-3</sup> (Kg <sub>Polymer</sub> /mol <sub>Ti</sub> .h.C <sub>monomers</sub> )
14	2	1,8	12,3	140,9	285
30	3	2,9	6,7	138,8	21,2
31	4	3,6	5,2	136,9	19

<sup>a</sup>Polymerization conditions: 30°C, ethylene pressure 2 bar, toluene volume 200mL, polymerization t<sub>MMA</sub>=4h, cocatalyst MAO; [MMA]=1mol/L.

The results obtained by varying the catalyst concentration agreed with the results obtained varying the amount of MAO in feed. The catalyst activity and the melting points of the obtained polymers decrease with increase in the catalyst concentration in feed, Figure 18. However, the molecular weights of the obtained polymers decrease significantly with the variation of the catalyst concentration and the polydispersity broadens sharply as can be seen in Table 3.

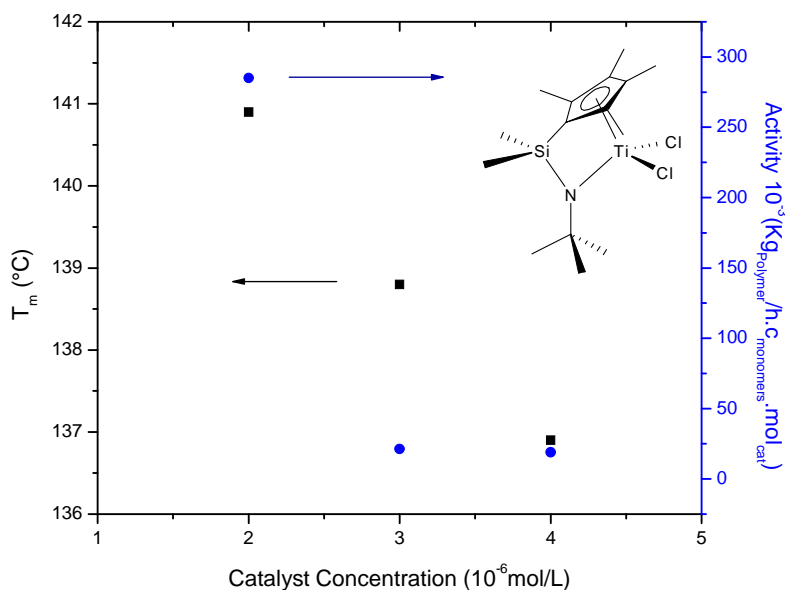


Figure 18: Melting point and catalytic activity as a function of catalyst concentration in feed.

Among the catalyst concentrations investigated in the previews section, the lower one (2 10<sup>-6</sup> mol) was chosen for the following experiments considering that even at this lower concentration, it was still possible to polymerize ethylene in the presence of the protected polar group at relatively high catalytic activity to yields polymers with considerable high molecular weight.

### 7.2.3 Effect of Comonomer Concentration

Ethylene and MMA were copolymerized using MMA/TIBA ratio 1:1 in the pretreatment step. At two specific temperatures, the comonomer concentration in the feed varies between 0 and 0.09 mol/L. Considering the previous results presented in the previous sections, the other reaction parameters such as MAO concentration, pressure and catalyst concentration were chosen and maintained constant during the polymerization.

The catalytic activity was investigated at 30 and 60°C by varying the comonomer concentration in feed, the results are given in the Figure 19. For comparison, results of ethylene homopolymerization at 30 and 60°C are also present in Figure 19.

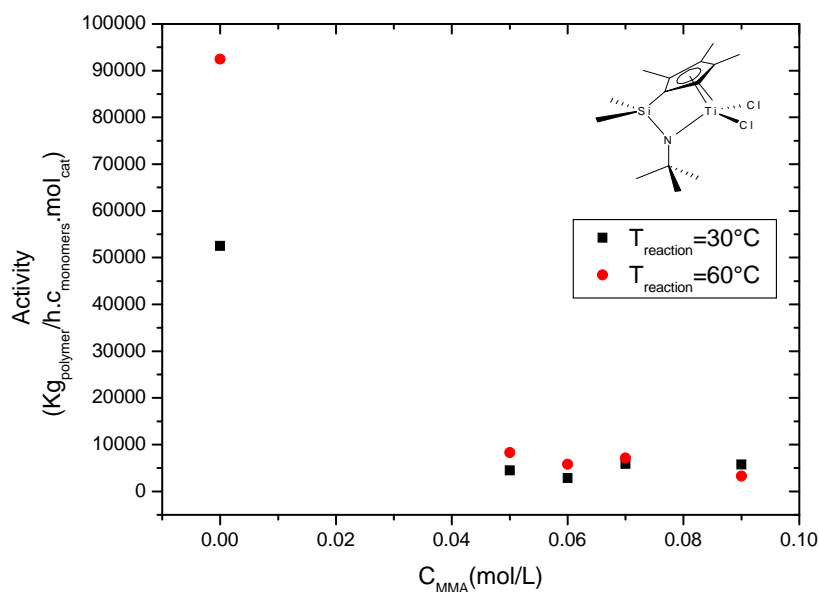


Figure 19: Activity as a function of comonomer concentration in feed. Polymerization conditions: Catalyst concentration:  $1(10^{-3}$  mol/L), MAO: 600mg,  $t_{MMA}=4$ h, pressure: 2bar;  $V_{reaction}=200$ mL, solvent: toluene.

The initial ethylene polymerization proceeds very rapidly and completes in 1 min. The subsequent copolymerization with MMA proceeds rather slowly<sup>48</sup> and reactions were carried out for 4 hours at 30°C and 60°C.



The polymerization decelerated dramatically after the addition of MMA. The presence of MMA protected monomer decrease the catalytic activity about one order of magnitude compared with homopolymerization of ethylene.

Resulting polymers are soluble in 1,2 dichlorobenzene and 1,2,4-trichlorobenzene at 100°C but insoluble in THF and CH<sub>2</sub>Cl<sub>2</sub>, suggesting quantitative conversion into the desired linear block copolymer. Repeated fractionation of the block copolymer in hot THF did not change the molar weight of the obtained polymers whereas the poly(MMA) in the blend of polyethylene is easily extracted with THF<sup>48</sup>.

### 7.2.3.1 GPC and DSC Results

The effect of the variation of MMA concentration in polymerization medium on the molecular weights of the polymers obtained was more evident at 60°C than at 30°C. GPC measurements revealed that the copolymers synthesized at 60°C have molecular weights slightly higher than the molecular weight of the PE homopolymer (Table 4 - run 16). Additionally, at 60°C the molecular weight of the polymers increase with increase in MMA concentration in feed, while the polydispersity index remains narrow. On the other hand, the polymers synthesized at 30°C did not follow any trend regarding to the molecular weight.

Table 4 : Results for ethylene and MMA copolymerization<sup>a,b</sup>

Run	C <sub>MMA</sub> (mol/L)	T <sub>m</sub> (°C)	Pd	Mn x10 <sup>-4</sup> (g/mol)
13 <sup>a</sup>	0	140,0	2,2	11,3
14 <sup>a</sup>	0,05	138,8	1,8	12,4
15 <sup>a</sup>	0,06	138,7	1,9	10,9
21 <sup>a</sup>	0,07	138,5	2,2	10,7
22 <sup>a</sup>	0,09	138,1	1,7	17,2
16 <sup>b</sup>	0	140,7	1,9	12,0
25 <sup>b</sup>	0,05	139,7	1,8	13,5
26 <sup>b</sup>	0,06	139,1	1,8	14,3
27 <sup>b</sup>	0,07	137,0	1,8	15,4
28 <sup>b</sup>	0,09	138,0	1,7	16,8

<sup>a</sup>Polymerization conditions: a)30°C and b)60°C, ethylene pressure: 2 bar, toluene volume: 200mL, polymerization t<sub>MMA</sub>=4hs, cocatalyst MAO; [MMA]=1mol/L.

A lowering in the melting points was observed in the obtained polymers when compared with the melting point of polyethylene obtained at the same polymerization conditions using the same catalyst system. In both temperatures, the melting points of the obtained polymers have

shown the same behavior, decrease with increase in the MMA concentration in feed. In addition, the melting points obtained at 60°C are relatively higher than that obtained at 30°C, see Figure 20.

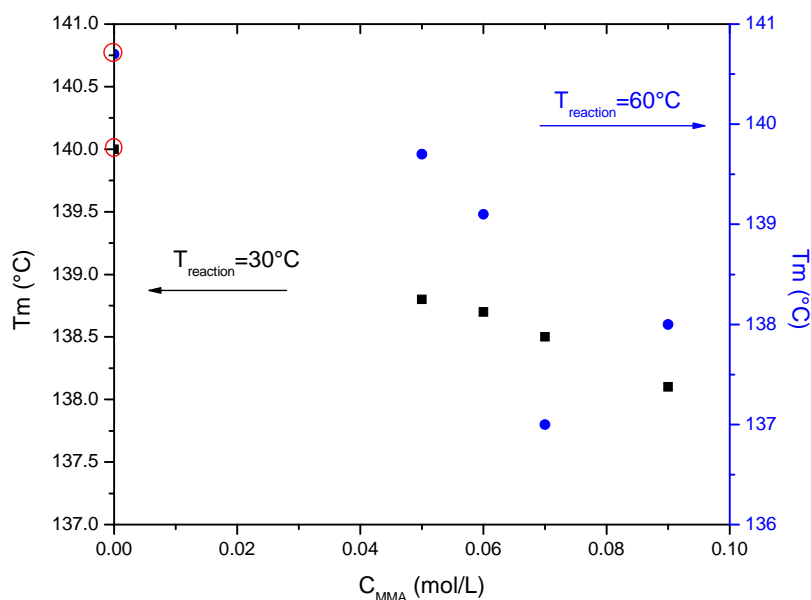


Figure 20: Melting points of the obtained copolymers as a function of MMA concentration at different temperatures. Polymerization conditions: ethylene pressure: 2bar, toluene volume: 200mL, polymerization  $t_{MMA}=4$ hs, cocatalyst: MAO;  $[MMA]=1$  mol/L.

### 7.2.3.2 $^1H$ NMR and $^{13}C$ NMR Spectroscopy Results

Analyses by  $^1H$ NMR and  $^{13}C$ NMR spectroscopy of the obtained polymers revealed that in all cases, in addition to the signal for polyethylene, signals assigned to the polar group of the MMA were present.

The  $^1H$ NMR spectrum of a typical obtained polymer illustrated in Figure 22, show that in addition to the resonances of polyethylene ( $\delta$  1,28, 0,93 ppm), resonances at  $\delta$  3,69 and 1,01 ppm can be assigned to methoxy and methyl protons in MMA units<sup>45,46</sup>(Figure 21).

Carbon	$^1H$ NMR assignment ( $\delta$ =ppm )
1	1,01
2	3,69
3	1,28

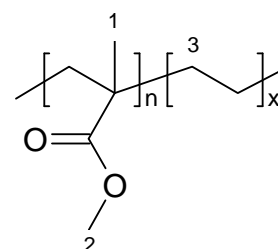


Figure 21:  $^1H$ NMR assignments in ppm for the obtained polymers.

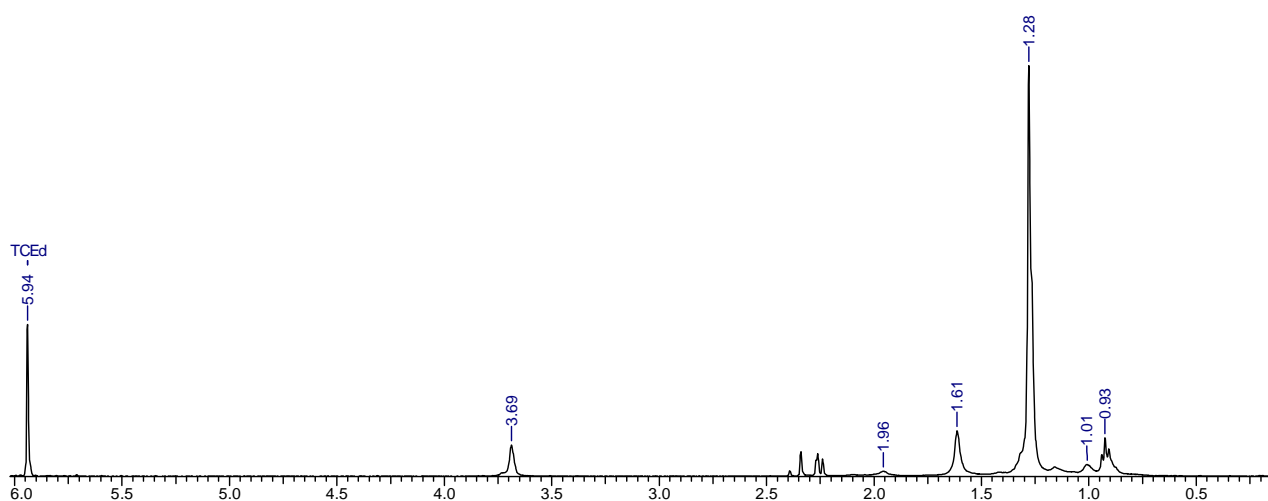


Figure 22:  $^1\text{H}$ NMR spectrum of the obtained polymer in run 21.

The  $^{13}\text{C}$ NMR spectrum of the same polymer shows the resonances for the methoxyl carbon, methylene carbon and methyl carbon in MMA units. In addition, the resonances at ( $\delta$  32.3, 30.16, 27.38 and 14.2) are attribute to a typical sequences of E co units while the resonances at  $\delta$  177.4, 54.7, 51.5, 45.6, 29.7 and 18.2 confirm the presence of MMA co-units, see Figure 23. It is worth to notice that the absence of splitting of the signal arising from C=O ( $\delta$  177.5 ppm) in the copolymer differing from those of the carbonyl carbons ( mainly at  $\delta$  176.6 ppm) in homo-PMMA indicates that MMA units are statistically incorporated into the polyethylene backbone<sup>45,46</sup>.

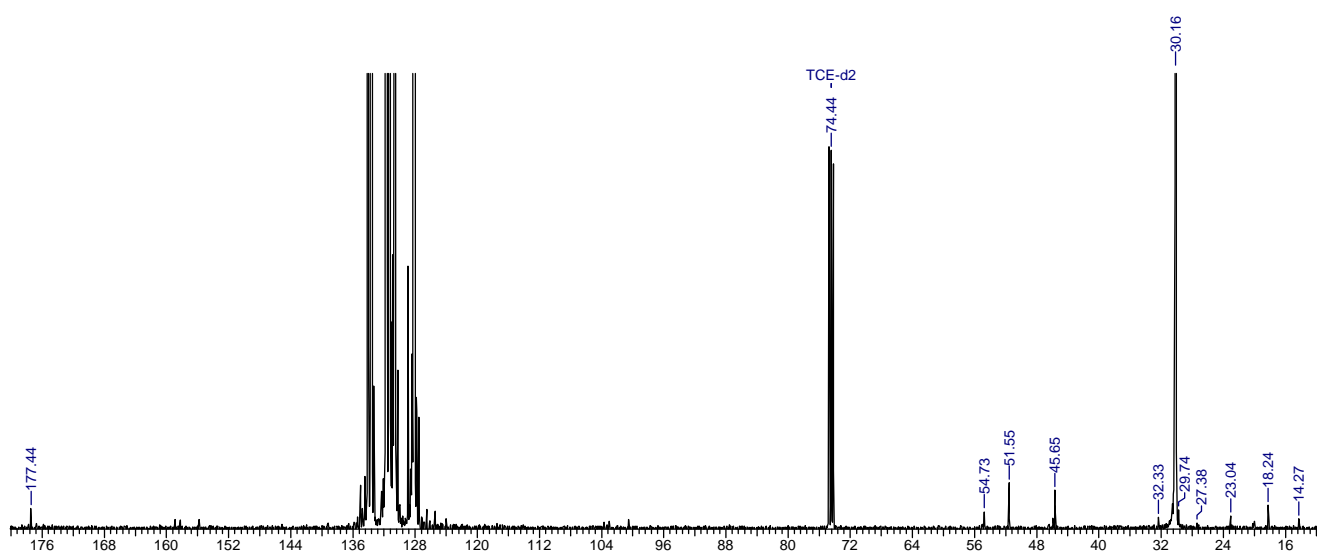


Figure 23:  $^{13}\text{C}$ NMR spectrum of the obtained polymer in run 21.

Considering the spectra showed above, it is easy to conclude that neither the GPC results nor NMR spectra are really a proof of whether the polymers obtained are block copolymers or rather a polymer blends<sup>109</sup>. Solvent fractionation failed to separate the copolymer from PE, due to heterogeneity in the polymerization step and the chain transfer and termination in PE polymerization reaction<sup>45</sup>. However, it was considered that after the extraction of PMMA with CH<sub>2</sub>Cl<sub>2</sub>, any remained signs of PMMA detected by NMR might be from PE-b-PMMA copolymer<sup>45</sup>.

#### **7.2.4 Partial conclusions**

Several findings of this study are significant for the production of a copolymer. The synthesis and characterization of a PE-co-MMA were described using triisobutylaluminum as protecting agent. Protecting the polar groups with TIBA leads to relatively higher catalytic activity toward the copolymerization of ethylene and MMA especially at 60°C.

Although the protection with TIBA is mandatory to yield polymer, it is clear that the presence of the polar groups slow down the catalyst activity. The ratio MMA:TIBA with different TIBA concentrations has no adverse effect on polymer properties. In fact, a small difference in the molecular weight is observed and the melting points of the obtained polymers remain almost constant.

Analysis by <sup>1</sup>HNMR and <sup>13</sup>CNMR spectroscopy of the obtained polymers revealed that in all cases, in addition to the signal for polyethylene, signals assigned to the polar group of the MMA were present. However, despite of the heterogeneous character of the polymerization procedure and after solvent extraction of the obtained polymer, the set of characterization results, especially <sup>1</sup>HNMR and <sup>13</sup>CNMR strongly suggest that a truly copolymer was synthesized.

### 7.3 Copolymerization of Ethylene with Vinyl Acetate (VA)

EVA is produced by copolymerization of ethylene and vinyl acetate (VA). Commercially, a copolymer of ethylene and vinyl acetate (PE-co-VA) is produced by free radical polymerization in a high pressure polyethylene process (HPPE)<sup>49</sup>. The copolymer poly(ethylene-co-vinyl acetate), EVA, is mainly recognized for its flexibility (even at low temperatures), adhesion characteristics and stress-cracking resistance. Due to acetate groups, EVA is more polar and less crystalline than LDPE. These copolymers are suitable for films, flexible tubes, catheters<sup>50</sup> and they are also largely used by footwear industry as material for shoes soles, due to their moderate price, easy processing and good combination of mechanical properties<sup>51-53</sup>.

There are many works devoted either to elucidate or to predict the final properties of the Ethylene-VA copolymers. On the other hand, only few works were focused in finding a suitable method to copolymerize ethylene and vinyl acetate in the presence of early transition metal catalysts.

Vinyl acetate was investigated for co- and terpolymerization with ethylene and ethylene propylene<sup>53</sup>. The catalyst used was [bis(N,N'-dimesityl-imino)acenaphthene]dibromonickel, activated by methylaluminoxane and trimethylaluminium (TMA). Triisobutylaluminium (TIBA) was employed to block the functional groups during the polymerization process. To block the polar groups, four methods have been employed. The best results regarding catalytic activity has been achieved when the monomer has been treated in situ with TMA at an VA/TMA ratio of 1/2, then the co-catalyst MAO was added to the reactor, followed by the introduction of the catalyst solution into the reactor. The presence of the polar monomer in the obtained copolymer was found by changes in the polymer physical properties, such as crystallinity, tensile strength and also by an improvement in the polarity of the polymer. Considering the lack of solubility of the obtained polymer, a further investigation on E-co-VA structure was not possible to be done.

The identification of the problems connected with the copolymerization of vinyl acetate and vinyl trifluoroacetate with ethylene, in the presence of cationic diimine Pd(II) and Ni(II) alkyl complex has also been studied<sup>54</sup>. This study provide information regarding insertion barrier of these monomers, their binding affinities relative to ethylene, the nature and stability of the

insertion products and the propensity of these inserted species to incorporated further monomer.

The needs for a better understanding of the behaviour of the copolymerization of VA and ethylene have driven our studies. Aiming to find optimal reactions conditions, we have run a set of experiments as described below. The structures of the monomers and the probable obtained copolymer are giving in Figure 24.

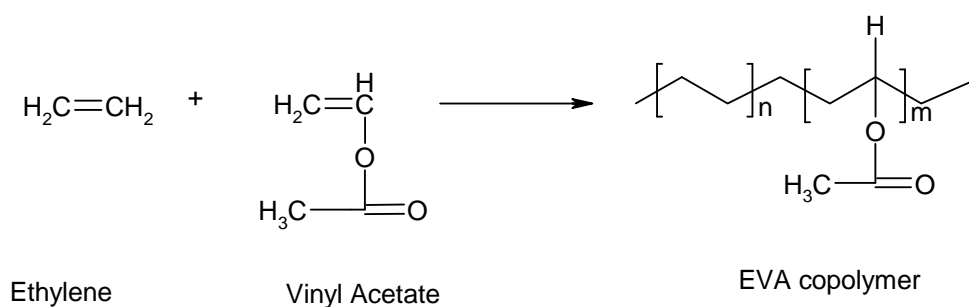
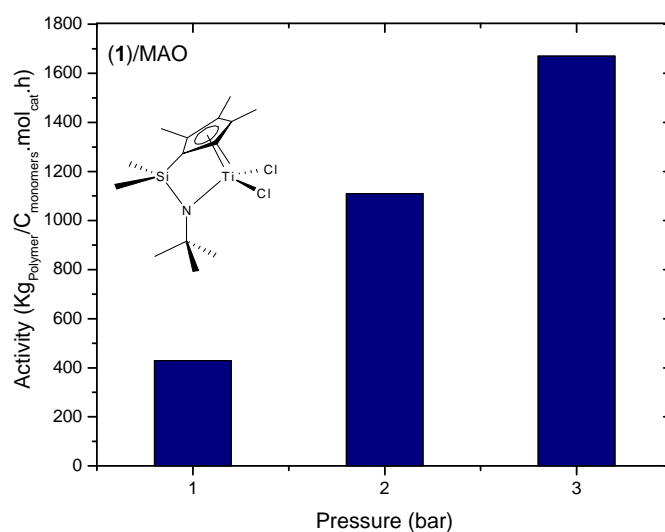


Figure 24: Structure of the monomers and probable obtained copolymer.

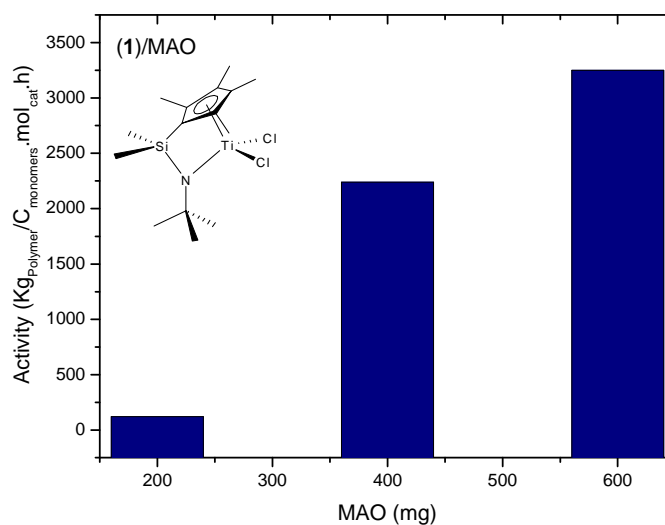
The polymerizations were carried out by varying some parameters, such as pressure, catalyst systems and their concentrations and co-catalyst systems and their concentrations. Considering the previews results in the copolymerization of MMA and ethylene, our starting point was the catalyst system (1)/MAO using the same approach that was applied for that system. This approach consists in a starting homopolymerization of ethylene with (1)/MAO at 60°C in toluene at 3 bar, followed by the sequential addition of VA<sup>48</sup>. Additionally, VA was pre treated with TIBA at room temperature just before the introduction into the reactor.

### 7.3.1 Effect of MAO Concentration and Pressure

Initially, the influence of the co-catalyst (MAO) concentration and the pressure of the reaction was investigated on the copolymerization of ethylene with protected vinyl acetate. The results of the catalyst activity as a function of MAO concentration and pressure are giving in the Figure 25.



a)



b)

Figure 25: a) Catalyst activity as function of pressure, b) Catalyst activity as function of MAO quantity. Polymerization conditions:  $[cat(1)] = 10^{-6} \text{ mol/mL}$ ,  $60^\circ\text{C}$ , toluene volume: 200mL, polymerization time: 1h, 400mg MAO;  $[VA] = 0,47 \text{ mol/L}$

At these particular reaction conditions, it was possible to obtain polymers in the presence of the protected functional monomer by varying MAO concentration in the polymerization medium. The results follow the expected behaviour for metallocene catalyst<sup>31</sup>. It was observed that the higher the concentration of MAO in the polymerization, the higher the catalytic activity. The same trend was observed by increase the pressure of the reaction: the higher the pressure, the higher the catalytic activity.

### 7.3.1.1 GPC and DSC results

The presence of VA seems to influence the final characteristics of the polymer. The highest activity leads to a polymer with high molecular weight, with a polydispersity index  $\approx 3,0$ , a characteristic of the single site catalyst. Additionally, the molecular weights and melting points of the obtained polymers decrease with a decrease in the concentration of MAO.

Table 5 : Results for ethylene and VA copolymerization<sup>a</sup>

Run	MAO (mg)	Pressure (bar)	T <sub>m</sub> (°C)	$\Delta H$ (J/g)	M <sub>n</sub> (Kg/mol)	Pd
62	600	3	137,5	67,6	590,5	3,0
63	400	3	135,2	135,2	249,6	3,0
72	200	3	132,3	74,0	227,6	2,5
75	200	1	120,5	0,19	180,0	3,0
74	200	2	77,1	2,27.E-3	246,6	2,3
76	200	3	72,3	5,01.E-3	159,7	3,6

<sup>a</sup>Polymerization conditions: [cat(1) = 10<sup>-6</sup> mol/mL, 60°C, toluene volume:200mL, polymerization time:1h, 400mg MAO; [VA]=0,47mol/L

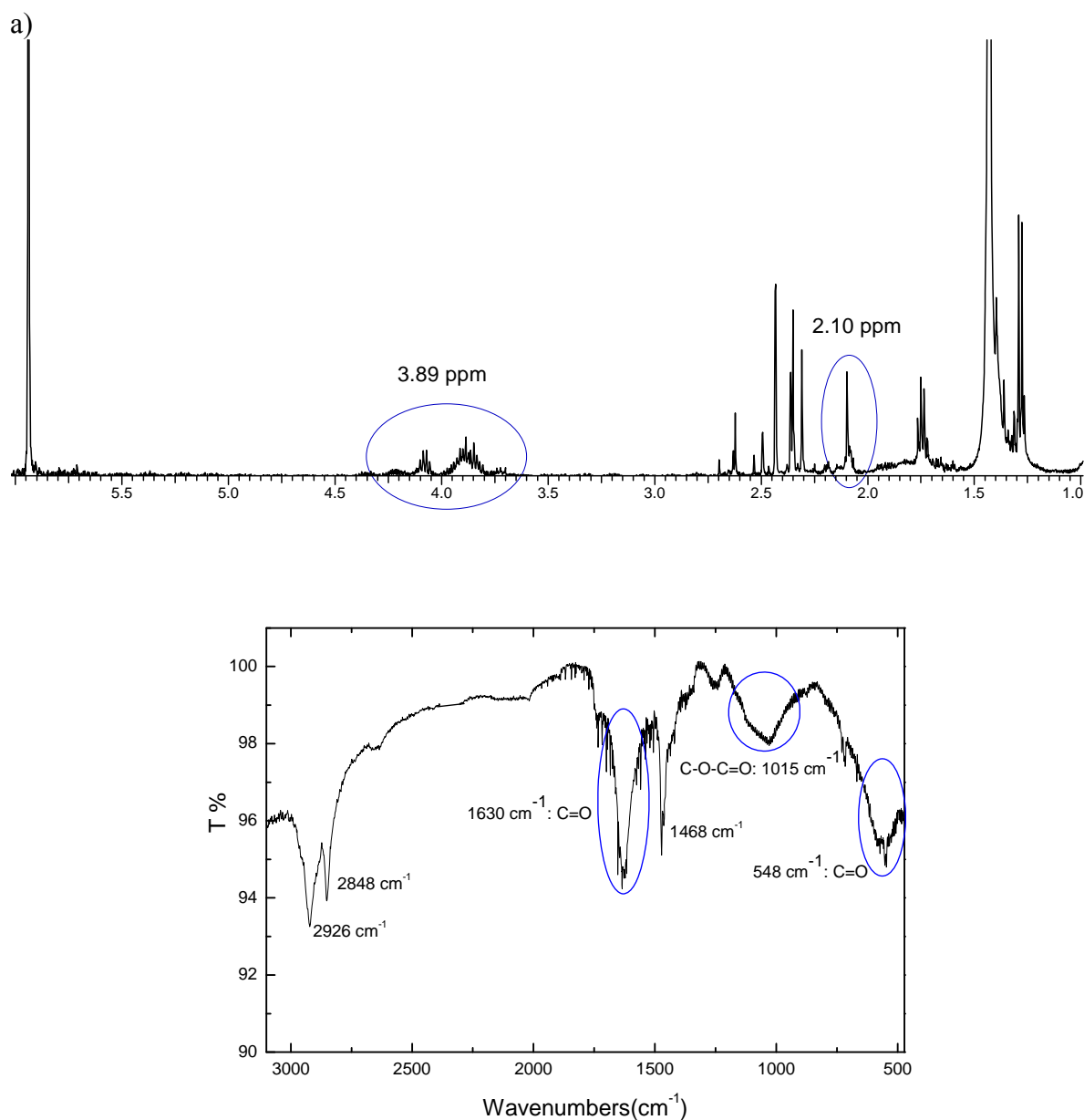
The results presented in Table 5, allow an approximate evaluation of the degree of crystallinity of the obtained polymer. The degree of crystallinity of PE is  $\approx 60\%$ , based on the melting heat value of  $\approx 175$ J/g and assumed specific melting heat value of 290J/g for the extrapolated 100% crystalline PE<sup>55</sup>. By varying the MAO concentration in feed, it is possible to observe some variation in the crystallinity of the obtained polymer. The system presents a maximum and a minimum value at the experimental conditions. The maximum value was 46.5% crystallinity observed at MAO amount of 400mg. The minimum value was 23% crystallinity at MAO amount of 600mg. The intermediate value was 25% of crystallinity found at 200mg of MAO in feed. These results lead to a conclusion that the PE lost part of its crystallinity in the presence of VA. On the other hand, the pressure effect on the crystallinity and melting point of the copolymer is very pronounceable. The increase in the pressure leads to a steep decrease in the crystallinity of the copolymers.

Considering the overall effect on polymer physical properties (melting point, molecular weight and polydispersity index) and the catalyst activity intensity, the concentration of 400 mg MAO and a pressure of 3 bar were chosen as standard for the subsequent reactions. Based on the experimental results obtained with the ethylene-MMA system, the same catalyst system and a reaction temperature of 60°C were used.



### 7.3.1.2 $^1\text{H}$ NMR and FTIR Spectroscopy Results

The solubility of the copolymers is strongly affected by the presence of VA. It was not possible to dissolve completely the obtained polymers in several organic solvents. Assuming the partial solubility of the sample, it was not possible to visualize a typical  $^{13}\text{C}$ NMR spectrum in solution of the sample. On the other hand, comparing the  $^1\text{H}$ NMR spectra of the PE with the  $^1\text{H}$ NMR spectra of the obtained polymer, it was possible to compare both materials, Figure 26 a).



b)

Figure 26: a) Typical  $^1\text{H}$ NMR spectrum of the obtained copolymer, b) FTIR spectrum of the obtained copolymer. Polymerization conditions:  $[\text{cat}(\mathbf{1})] = 10^{-6} \text{ mol/mL}$ ,  $60^\circ\text{C}$ , toluene volume: 200mL, polymerization time: 1h, 200mg MAO;  $[\text{VA}] = 0,47 \text{ mol/L}$ , catalyst system ( $\mathbf{1}$ )/MAO

Figure 26 a) shows that the  $^1\text{H}$ NMR spectrum of the obtained copolymer is composed of several peaks. Some of these peaks are not present in the  $^1\text{H}$ NMR of the polyethylene. Using the chemical shift of each peak, it is possible to associate the assignments with the presence of the polar group of the VA present in the copolymer. In particular, the methyl group at  $\delta$  2.10 ppm and the peaks at  $\delta$  3.89 ppm and 4.09 ppm assigned to the methyldene signals appear upfield of those for free VA ( $\delta$  4.60 ppm and 4.91 ppm) consistent with olefin complex rather than O-bound complex<sup>54</sup>.

Using the infrared (IR) spectrum of EVA as reference, we could confirm the presence of the VA in the polyethylene chain. The characteristic absorbance of some bands assigned to the VA units (1630: C=O, 1122: C-O-C=O, 1015 C-O-C=O, 548: C=O  $\text{cm}^{-1}$ )<sup>56</sup> and the absorbance of the ethylene groups (2926, 2848, 1468, 720  $\text{cm}^{-1}$ ) can be observed in Figure 26b. These results together with the results observed by  $^1\text{H}$ NMR spectrum of the obtained copolymers suggest that a copolymer has been synthesized.

### 7.3.2 Comonomer Concentration Effect

The copolymerization behavior of the system ethylene-VA was evaluated when the concentration of VA varied from 0,47 to 0,1 mol/L in feed, using the catalyst system (1)/MAO and TIBA as protect agent. At the studied experimental conditions, it was observed a strong decrease in the catalytic activity with increase in VA concentration in feed, Figure 27. This behavior was also observed for the previous system ethylene-MMA.

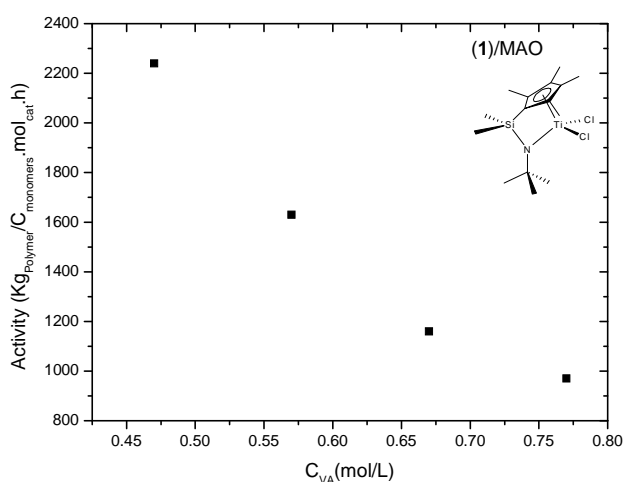


Figure 27: Catalytic activity as a function of VA concentration in feed. Polymerization conditions:  $[\text{cat}(1)] = 10^{-6} \text{ mol/mL}$ ,  $60^\circ\text{C}$ , ethylene pressure: 3bar, toluene volume: 200mL, polymerization time: 1h, 400mg MAO.

### 7.3.2.1 GPC and DSC Results

The melting temperatures ( $T_m$ ) and heats of fusion of the copolymers, as determined by DSC, are indicated in Table 6. It was observed a lowering of  $T_m$  and a decrease in crystallinity, when comparing with an ethylene homopolymer.

Table 6: Results for ethylene and VA copolymerization<sup>a</sup>

Run	$C_{VA}$ (mol/L)	$T_m$ (°C)	$\Delta H$ (J/g)	$M_n$ (Kg/mol)	Pd
63	0,47	135,2	135,2	249,7	3,05
69	0,57	133,3	89,6	320,7	2,47
70	0,67	132,7	77,1	n.d.	n.d.
71	1	131,1	75,1	161,4	2,36

<sup>a</sup>Polymerization conditions:  $[cat(5)] = 10^{-6}$  mol/mL, 60°C, ethylene pressure 3bar, toluene volume 200mL, polymerization time 1h, 400mg MAO;  $[ ]_{VA}=0,47$  mol/L, n.d.=not determined

Additionally, the polydispersity index of the obtained polymer decreases with an increase in the comonomer concentration, even though, the molecular weight did not follow any trend, starting to increase with the comonomer concentration and then decrease. Considering the poor solubility of the obtained polymer in all of the common organic solvents, it was not excluded the possibility that during the GPC analysis some fractionation has occurred<sup>57</sup>. This phenomenon could explain the unexpected behavior of the molecular weight of the sample 71.

### 7.3.3 Catalyst System Effect

Intending to find a new catalyst system that was able to polymerize ethylene and vinyl acetate, a systematic study was conducted to evaluate the effect of the catalyst systems (2)/MAO, (3)/MAO, (4)/MAO, (5)/MAO on the copolymerization of VA and ethylene. Attempts to copolymerize ethylene with vinyl acetate in the presence of the catalyst systems (2)/MAO, (3)/MAO and (4)/MAO were unsuccessful. The functionality was not incorporated into a polymer and has plunged the polymerization activity.

The results of the copolymerization of ethylene with VA using the catalyst (5)/MAO and (1)/MAO were compared in the Figure 28. Generally, the catalyst system (5)/MAO present high catalyst activity at lower catalyst concentration than that used with the catalyst system (1)/MAO. Additionally, at the same catalyst concentration, it is possible to see that the activity is 1 order of magnitude higher for the catalyst system (1)/MAO than for the catalyst

system (5)/MAO (Figure 28). Both catalyst systems are able to copolymerize ethylene in the presence of protected vinyl acetate with considerable catalytic activity.

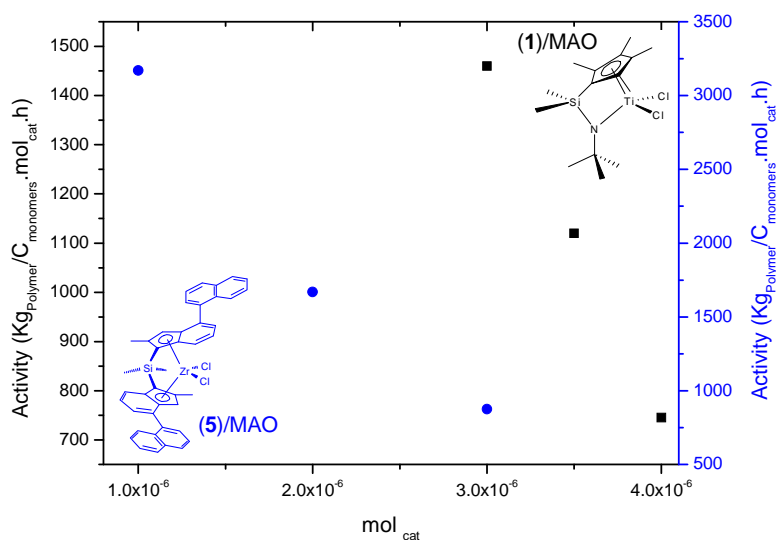


Figure 28: Catalytic activity as function of catalyst quantity for two different catalyst systems.

### 7.3.3.1 GPC and DSC Results

Above all, the different catalyst systems have influenced the physical properties of the polymers. The catalyst system (5)/MAO produced a polymer with high molecular weight and narrow molecular weight distribution, while the catalyst system (1)/MAO yielded a polymer with a relatively broad polydispersity index. The Table 7 summarizes the results of the copolymerization of ethylene and vinyl acetate in the presence of the catalyst systems (1)/MAO and (5)/MAO. The results were obtained by varying the catalyst concentration in the feed and by maintained constant the others parameters.

Table 7: Results for ethylene and VA copolymerization<sup>a</sup>.

Run	Catalyst (mol)	Tm (°C)	•H (J/g)	M <sub>n</sub> (Kg/mol)	Pd
66 <sup>b</sup>	3.10 <sup>-6</sup>	136,5	118,2	119,6	2,3
67 <sup>b</sup>	3.5.10 <sup>-6</sup>	134,3	74,4	601,9	1,9
71 <sup>b</sup>	4.10 <sup>-6</sup>	132,3	74,0	161,3	2,3
77 <sup>c</sup>	1.10 <sup>-6</sup>	133,4	99,0	199,3	3,2
76 <sup>c</sup>	2.10 <sup>-6</sup>	130,7	118,0	159,7	3,6
78 <sup>c</sup>	3.10 <sup>-6</sup>	132,0	125,0	65,1	4,1

<sup>a</sup>Polymerization conditions: b) cat(1) and c) cat (5), 60°C, ethylene pressure: 3bar, toluene volume: 200mL, polymerization time: 1h, cocatalyst MAO; [ ]<sub>VA</sub>=0,47mol/L.

It is very interesting to note that the behaviour of the crystallinity of the copolymers is opposite to both catalysts systems. For the catalyst system (1)/MAO, the crystallinity decreases with the increase in the catalyst concentration. The maximum value of 40% crystallinity was obtained at the lowest catalysts concentration. On the other hand, the catalyst system (5)/MAO show the highest crystallinity value of 43% that was reached at the highest catalyst concentration in feed. Additionally, for the catalyst system (1)/MAO, the melting points of the obtained polymers decrease with an increase in the catalyst concentration.

Considering the effect of catalyst concentration, it was observed the same behaviour for both systems, the higher the concentration of the catalyst, the lower the activity. However, it is possible to work at lower concentration with the catalyst system (5)/MAO than with catalyst system (1)/MAO, in order to obtained the same amount of the polymers.

### ***7.3.3.2 FTIR Spectroscopy Results***

Figure 29 shows a partial IR spectrum of the obtained polymers synthesized with the catalyst system (5)/MAO. Based on infrared (IR) spectrum of EVA, it is possible to confirm the presence of the VA in the polyethylene chain. Comparing the spectra of the copolymer with the spectra of the polyethylene the changes in PE crystalline structure can be seen. At the copolymer spectrum, it is possible to identify characteristic absorbance of some bands assigned to the VA units (1620: C=O, 1240: C-O-C=O, 1020 C-O-C=O, 610: C=O  $\text{cm}^{-1}$ ) as well as the absorbance of the ethylene groups (2920, 2820, 1470, 720  $\text{cm}^{-1}$ )<sup>56</sup>.

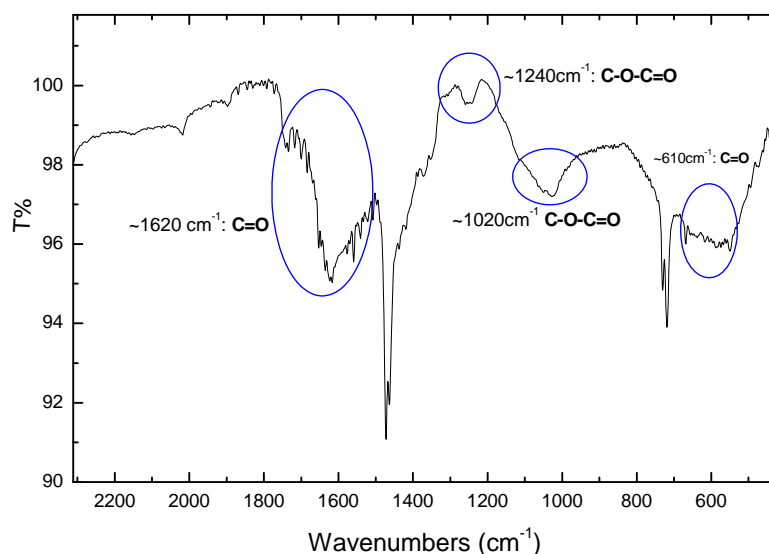


Figure 29: Partial FTIR spectrum of ethylene/vinyl acetate copolymer, zoom region: 500 and 2300  $\text{cm}^{-1}$ , polymerization conditions: cat (**5**)/MAO, 60°C, ethylene pressure 3bar, toluene volume 200mL, polymerization time 1h,  $[\text{V}_A]=0,47 \text{ mol/L}$ .

#### 7.3.4 Polymerization Tests with co-catalyst other than MAO

Lewis acids such as  $\text{B}(\text{C}_6\text{F}_5)_3$ <sup>58</sup> and MAO<sup>59-60</sup> play important roles as cocatalyst in generating highly active cationic olefin polymerization catalyst<sup>61-68</sup>. Evidences<sup>69-74</sup> argue that the nature of the active species generated during the polymerization reaction influence significantly some parameters such as catalyst activity, life time, temperature stability, chain transfer characteristic and stereoregulation.

Despite the excellent properties of MAO as a cocatalyst, the high cost and the fact that often a large excess is needed, renders it less attractive. Additionally, the main idea of this study was to reduce the co-catalyst concentration in order to make the catalyst more tolerant to the polar group<sup>75</sup>.

It was of interest to investigate the influence of the cocatalyst system on the copolymerization reaction of ethylene with vinyl acetate. The results of the copolymerization reaction of ethylene and vinyl acetate are summarized in Table 8.

Table 8: Copolymerization of VA and Ethylene in the presence of (5)/ B(C<sub>6</sub>F<sub>5</sub>)<sub>3</sub>

Run	V <sub>cat</sub> (mL)	t (h)	TIBA:B(C <sub>6</sub> F <sub>5</sub> ) <sub>3</sub>	Yields (g)	T <sub>g</sub> (°C)	T <sub>m</sub> (°C)	Activity (Kg <sub>polymer</sub> /mol <sub>Zr</sub> ·C <sub>monomers</sub> ·h)
83	2	1	1	2,42	-47,3	127,8	1160
84	4	1	1	-	-	-	0
85	2	1/2	1	1,39	59,8	-	1340
86	5	1/2	1,3	1,39	50,7	74,7	535
87	5	1/2	2	9,88	49,5	85,5	3800
89	3,5	1	1	trace	61,2	131,1	0
90	2	1	2	6,93	-	72,5	3330

Polymerization conditions: [C<sub>cat(1)</sub>]=10<sup>-6</sup> mol/mL, 30°C, ethylene pressure 4bar, toluene volume 200mL, C<sub>VA</sub>=0,47 mol/L, [TIBA]= 1mol/L

Overall, using B(C<sub>6</sub>F<sub>5</sub>)<sub>3</sub> as co-catalyst, a decrease in the catalytic activity is observed when compared with MAO as co-catalyst. This may be due to a less efficient scavenging of catalyst poisons in the case of a lower aluminium alkyl concentration<sup>75</sup>.

Very interesting to note, is the effect of the co-catalyst on the polymer properties. The obtained polymers show considerable lower melting points than the polymers obtained using MAO as co-catalyst. The molecular weights of the obtained polymers were not possible to be determined due to the poor solubility of the polymers in a set of different solvents.

Despite the reduction observed in the melting points of the obtained polymers together with their poor solubility, it was not possible to detect by NMR or FTIR spectroscopy the polar monomer incorporation. Comparing the behavior of the polymerization using MAO and using B(C<sub>6</sub>F<sub>5</sub>)<sub>3</sub> as co-catalysts, the last one is less efficient for the system ethylene-VA copolymerization.

### 7.3.5 Partial Conclusions

Copolymerization tests using ethylene and VA were carried out under different experimental conditions. Surprisingly after the addition of VA in the reactor, the catalysts (1) and (5) activated with MAO did not deactivate completely, although the polymerization activities were significantly reduced.

Analysis by FTIR and <sup>1</sup>HNMR spectroscopy of the obtained polymers revealed that in addition to the signals for polyethylene, signals corresponding to the functional group of VA were present. However, the detection by FTIR and NMR spectroscopy is not straightforward

due to heterogeneous character of the polymerization procedure.

The crystallinity of the obtained polymer is affected by the used catalyst systems. For the catalyst system (1)/MAO, the crystallinity decreases with the increase of the catalyst concentration. On the other hand, the catalyst system (5)/MAO show the highest crystallinity value of 43% and this value was reached at the highest catalyst concentration in feed.

The solubility of the copolymers is strongly affected by the presence of VA. It was not possible to dissolve the obtained polymers completely in several organic solvents. Assuming the partial solubility of the sample, it was not possible to visualize a typical  $^{13}\text{C}$ NMR spectrum in solution of the sample.

Co-catalyst other than MAO was tested in this work.  $\text{B}(\text{C}_6\text{F}_5)_3$  as co-catalysts afford less efficient profile during the ethylene and VA copolymerization. The obtained materials are insoluble in the used organic solvents and have low melting transitions.



## 7.4 Copolymerization of Ethylene with Allyl Ethers

The copolymerization of allyl ethers yield linear or branched polymers that can be used as coatings, adhesives, thermoplastics and fiber finishes<sup>76</sup>. It also may be employed as electrical products, serving as bushings standoff insulators, impregnating resins and the like<sup>76-84</sup>.

However, copolymers of ethylene and allyl ethers are very difficult to be obtained, first because of the high stability of the allyl ethers under wide range of reactions and also due to the large reactivity ratio of both monomers<sup>85,86</sup>. Considering that successful copolymerization of olefin with functional monomers have been achieved by providing steric and electronic protection on the functional groups<sup>22</sup>, copolymerization of ethylene with allyl ethers, pre-treated with alkyl aluminium were carried out in presence of the metallocene catalyst  $[\text{Me}_2\text{Si}(\text{Ind})_2]\text{ZrCl}_2$ , using MAO as cocatalyst.

The structures of three oxygen containing allyl ethers are illustrated in Figure 30. The Figure represents the different monomer structures that were pre treated with TIBA and copolymerized with ethylene.

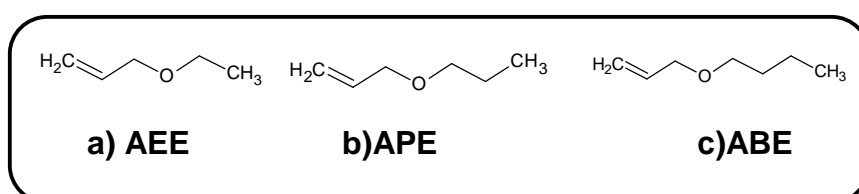


Figure 30: Structures of the oxygen containing monomers used for the copolymerization with ethylene: (a) AEE: allyl ethyl ether, (b) APE: allyl propyl ether and (c) ABE: allyl butyl ether.

### 7.4.1 Copolymerization of Ethylene with Allyl Ethyl Ether (AEE)

Due to the lack of available information in the open literature for the copolymerization of allyl ethyl ether with ethylene, it was necessary to search for the suitable copolymerization conditions. Pressure, temperature, MAO quantity and the catalyst system were included in this initial screening.

### 7.4.1.1 Effect of the Catalyst System

From the catalytic structures showed in the Figure 13, the only two ones that show activity toward the copolymerization of AEE with ethylene were catalyst (3)/MAO and catalyst (5)/MAO. The results of the catalytic activity of both catalysts in the copolymerization of ethylene and AEE are presented in Figure 31.

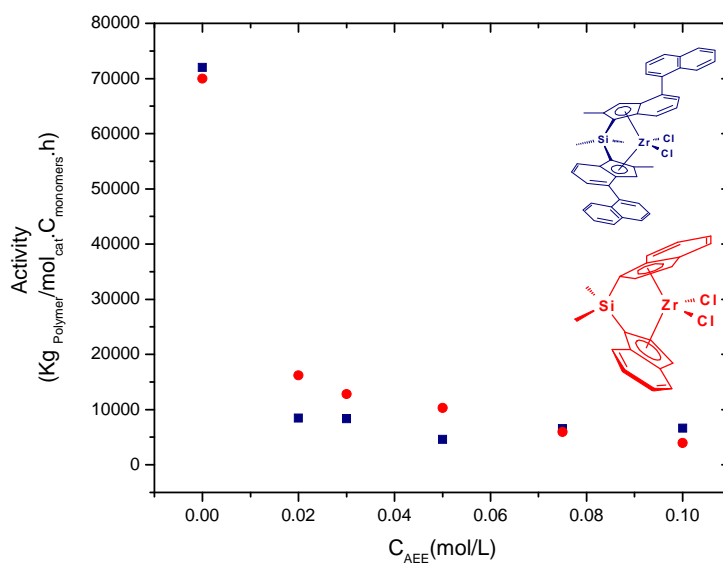
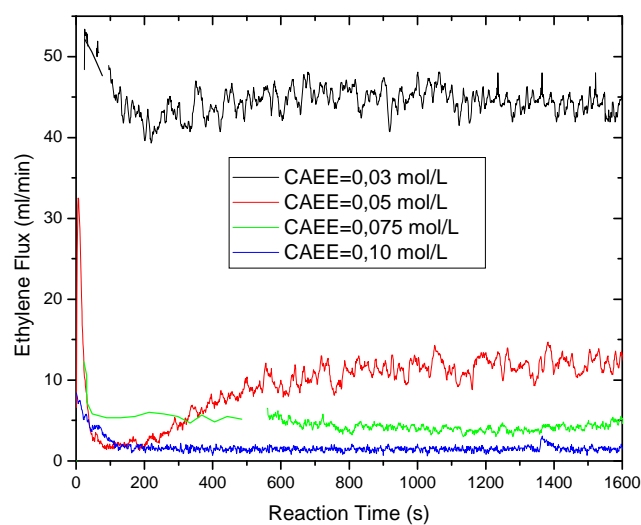
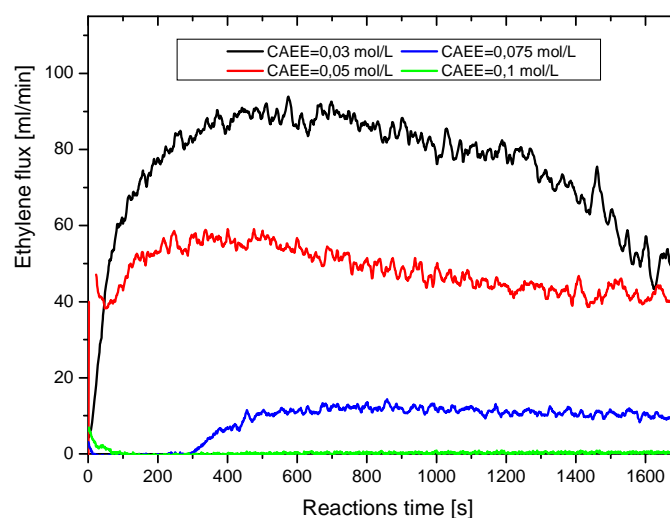


Figure 31: Catalytic activity as a function of the comonomer concentration in feed.

The catalytic activities of both systems are in the same order of magnitude and after the addition of the polar monomers, they exhibit similar deactivation behaviours. Based on the productivity of the catalytic system (3)/MAO, it is possible to conclude that this catalyst tolerates the addition of the functional monomer better at lower monomer concentration in the feed than the catalyst system (5)/MAO. Although the catalyst system (3)/MAO shows relatively better activity in almost the whole range of comonomer concentration studied, both systems are strongly influenced by the polar monomer concentration. It was observed that the higher the polar monomer concentration was, the lower the catalytic activity was. Also, this behaviour can be seen by the consumption of ethylene during the reaction for the studied systems, (Figure 32).



a)



b)

Figure 32: Ethylene flux as a function of time for two catalyst systems a) (5)/MAO and b)(3)/MAO

Comparing both systems, it is possible to say that ligands of the catalyst system influenced the polymerization behavior. The indenyl ligand substituted in the positions 2 and 4 containing catalyst system is less stable during the reaction than the system (3)/MAO. Despite the fact that catalytic activity is in the same order of magnitude, the substitution of one hydrogen in the position 2 for a methyl group and in position 4 for naphthyl group result in a lower catalytic activity at lower comonomer concentration in feed. The substitution in the indenyl ligand allows olefins to easier access to the cationic zirconium center. Unfortunately, the Lewis basic functionalities can also easily coordinate and inhibit the polymerization<sup>41</sup>.

#### 7.4.1.1.1 GPC and DSC results

Thermal analyses of the copolymers synthesized with the catalyst system (5)/MAO have shown some decrease in melting points with increase in monomer incorporation, as it can be seen in Figure 33. The majority of the AEE copolymers exhibit a semi crystalline profile. It is also possible to see the presence of second melting peaks. The lowest melting point obtained for the polymer was 98.7°C (IR=3,6%) followed by a huge loss of crystallinity. Additionally, the highest melting peak was 131°C at the smallest (0,7 mol%) polar monomer incorporation for this catalyst system, as illustrated in Figure 33.

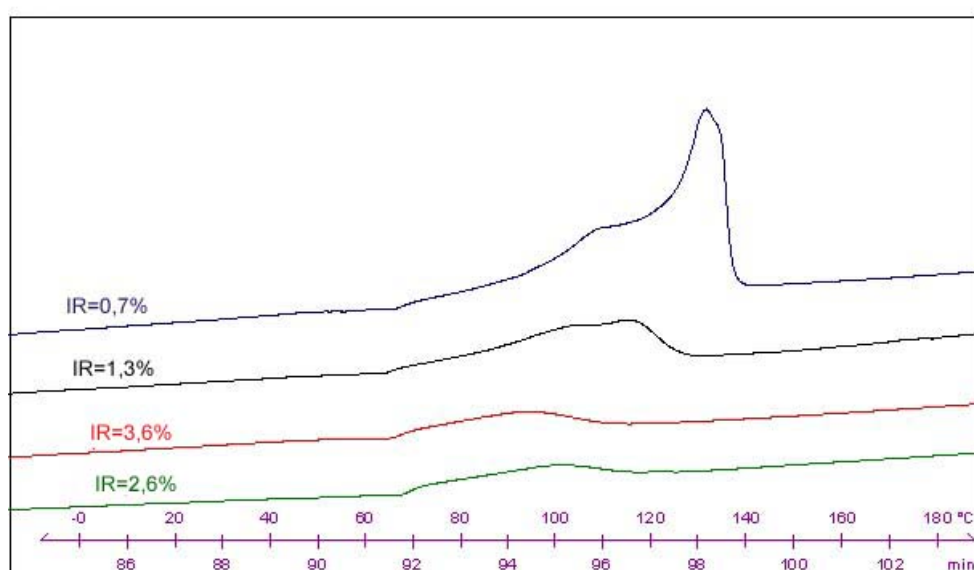


Figure 33: DSC curves of the obtained polymers in the presence of the catalyst system (5)/MAO. IR=incorporation rate

Similar results were obtained when the copolymerization of AEE and ethylene is conducted in the presence of the catalyst system (3)/MAO (Figure 34). With this system the melting points of the obtained polymers varied from 132 to 129°C. The crystallinity of the obtained polymers was also influenced by the incorporation level of the polar monomer in the polyethylene backbones. At higher level of comonomer incorporation (3,8 mol%), it was observed a lowering in the crystallinity of the polymers, as it can be seen at Figure 34. However, the lost of crystallinity observed with the catalyst (3)/MAO was not as strong as observed with the catalyst (5)/MAO.

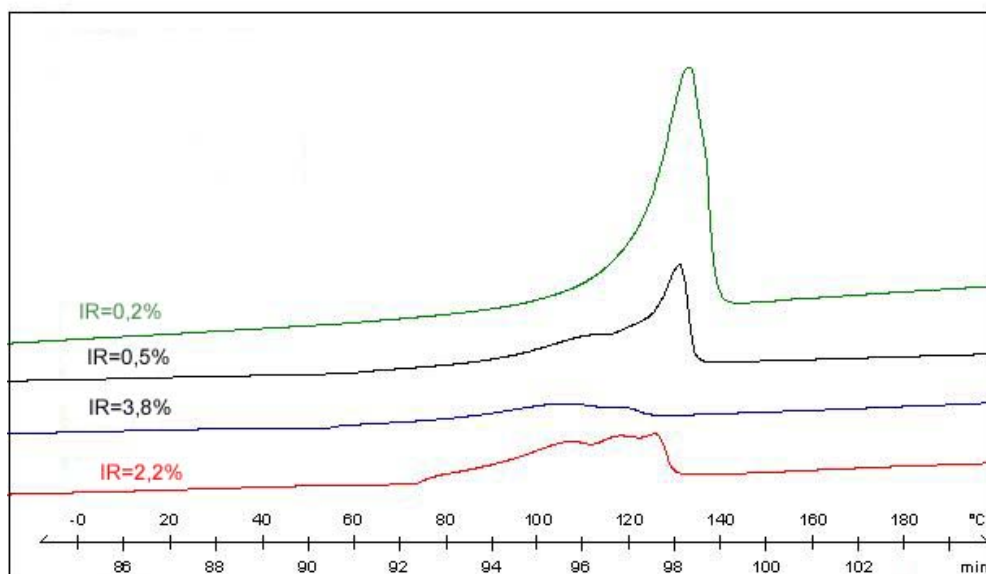


Figure 34: DSC curves of the obtained polymers in the presence of the catalyst system (3)/MAO.

The molecular weights of the obtained polymers determined by GPC showed some broadening of the polydispersity in the presence of the polar comonomer when compared to Pd of the ethylene homopolymer. For the catalyst system (3)/MAO, the molecular weight distributions remain unimodal, while for the catalyst system (5)/MAO, it is possible to see a presence of some signal at the oligomers region. The GPC results for both catalyst systems are summarized in Table 9.

Table 9 – Results of Ethylene copolymerization with AEE.

Reaction	C <sub>AEE</sub> [mol/L]	M <sub>n</sub> [kg/mol]	Pd
137 <sup>a</sup>	0,02	470	3,5
141 <sup>a</sup>	0,03	730	3,3
142 <sup>a</sup>	0,04	410	2,9
140 <sup>a</sup>	0,05	500	2
124 <sup>a</sup>	0,075	nd	nd
125 <sup>a</sup>	0,1	nd	nd
149 <sup>b</sup>	0,02	150	2,5
153 <sup>b</sup>	0,03	180	2,3
150 <sup>b</sup>	0,05	180	2,3
151 <sup>b</sup>	0,075	490	2,3
152 <sup>b</sup>	0,1	nd	nd

Polymerization conditions: <sup>a</sup>catalyst system (5)/MAO and <sup>b</sup>catalyst system (3)/MAO; reaction conditions: 60°C, 400mg MAO, V<sub>total</sub>=200mL, solvent: Toluene, nd=not determined.

The molecular weights of the obtained polymers were influenced by the incorporation of the polar monomers. The influence is clearer in the presence of the catalyst system (3)/MAO than with the catalyst system (5)/MAO. Figure 35 shows that for the catalyst systems (3)/MAO, it

was observed a tendency of increase in molecular weight with increase in the comonomer concentration.

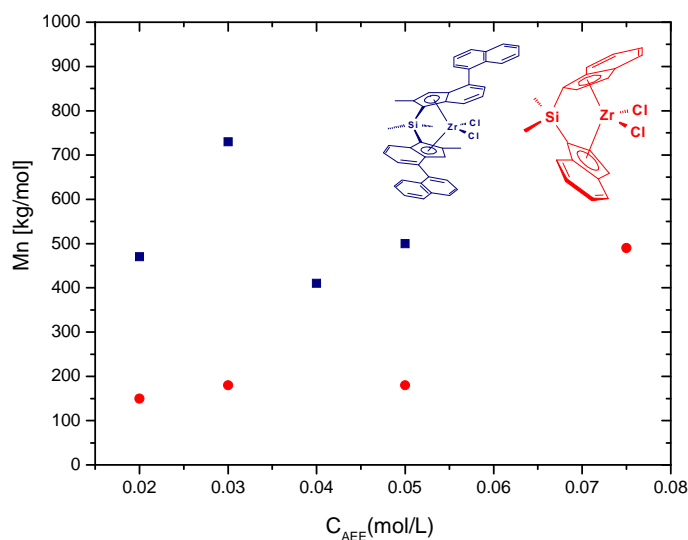


Figure 35: Molecular weights of the obtained copolymers as a function of the comonomer concentration in feed with the catalyst system (3)/MAO and (5)/MAO.

The results of the DSC together with the broadening of the molecular weight distribution, suggest heterogeneity of the copolymers at higher AEE contents. One explanation for this effect could be the formation of a different active species by a side reaction between AEE and the catalyst during the polymerization process<sup>98</sup>.

#### 7.4.1.1.2 Scanning Electron Microscopy (SEM) Results

Scanning Electron Microscope, operating with secondary electron image, shows the surface topography of the AEE-co-PE copolymers obtained with the catalyst system (3)/MAO. The results revealed in SEM studies confirm the previous results obtained by DSC and GPC. As shown in Figure 36, the copolymer surfaces are very different. The surfaces show some heterogeneity as well as a decrease in the crystallinity with an increase in the polar monomer incorporation.

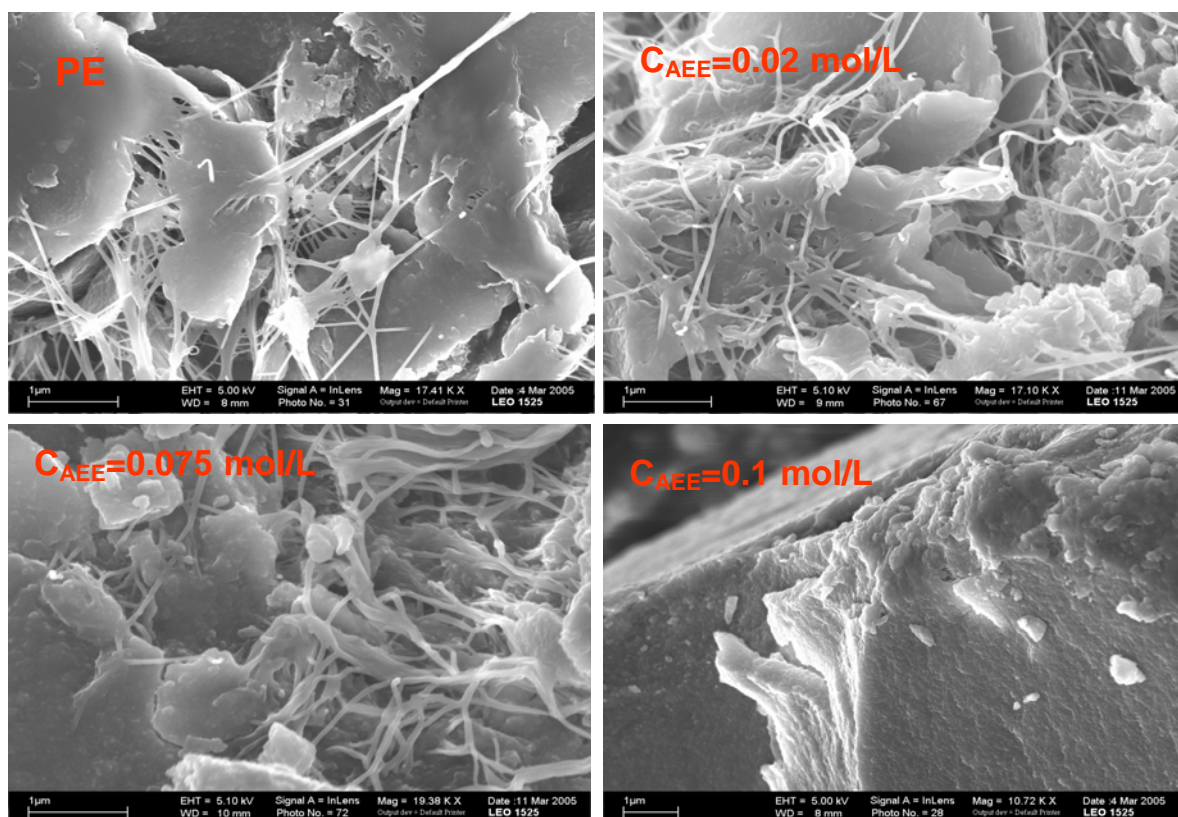


Figure 36: SEM of the obtained copolymers and PE, Polymerization conditions: 60°C, 400mg MAO, Pressure: 4 bar, Catalyst concentration:  $2 \cdot 10^{-6}$  mol/mL, cat. (3).

#### 7.4.1.1.3 <sup>1</sup>H NMR Results

The <sup>1</sup>H NMR characterization of the ethylene/AEE copolymers showed the presence of the ether group for all obtained polymers. A typical <sup>1</sup>H NMR spectrum of the obtained copolymer is present at Figure 37. The poor solubility of the polymers leads to a spectrum that not allows an easy integration of the assignments. Despite of that, the incorporation rates were calculated as the ratio between the integration of the ether assignments at  $\delta=3,7$  ppm and the assignments regarding to the polyethylene chain between  $\delta=1,2-1,45$  ppm. Additionally, the integrations were correlated with the numbers of protons that each peak represents.

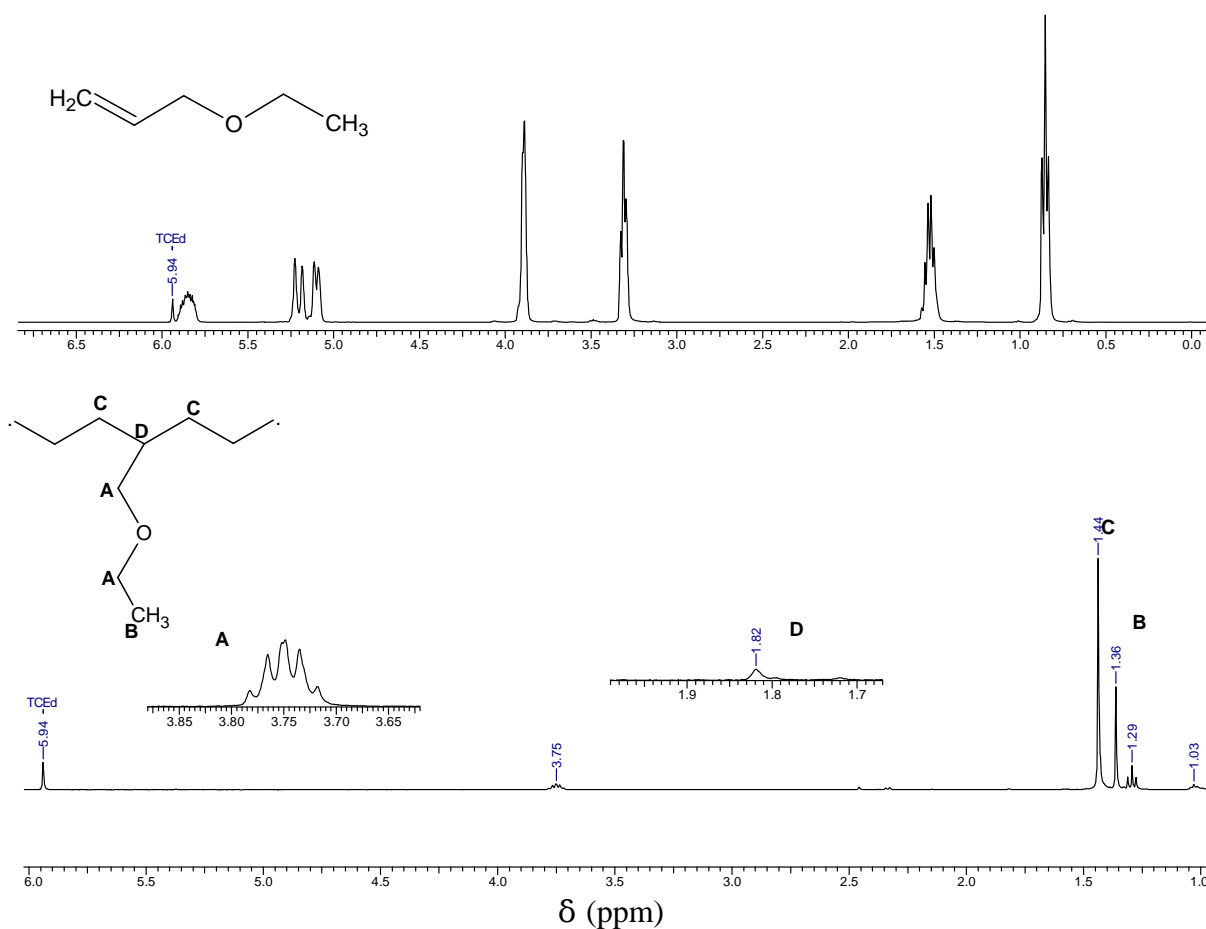


Figure 37: Upper: Typical  $^1\text{H}$ NMR of AEE monomer. Down: Typical  $^1\text{H}$ NMR of obtained copolymer. Polymerization conditions:  $60^\circ\text{C}$ , 400mg MAO, Pressure:4 bar, Catalyst concentration:  $1 \cdot 10^{-6}$  mol/mL cat. (5),  $C_{\text{AEE}} = 0,05$  mol/L

The Figure 37 also presents the  $^1\text{H}$ NMR of the allyl ethyl ether monomer. A significant observation is the complete absence of the signal referent to the vinyl group of the polar monomer between  $\delta = 5.48$  ppm and  $5.07$  ppm suggesting a complete conversion of the polar monomer.

The incorporation level for AEE in [mol-%] as a function of the polar monomer concentration in feed is giving in the Figure 38. As it can be seen, the abilities of the catalysts systems to copolymerize ethylene with AEE are different and strongly dependent on the catalyst structure. The incorporation level is between 0,1 and 16%. The highest incorporation level was obtained at the polar monomer concentration of 0,1 mol/L in the presence of the catalyst system (3)/MAO. However, this incorporation level was followed by strong catalyst deactivation.



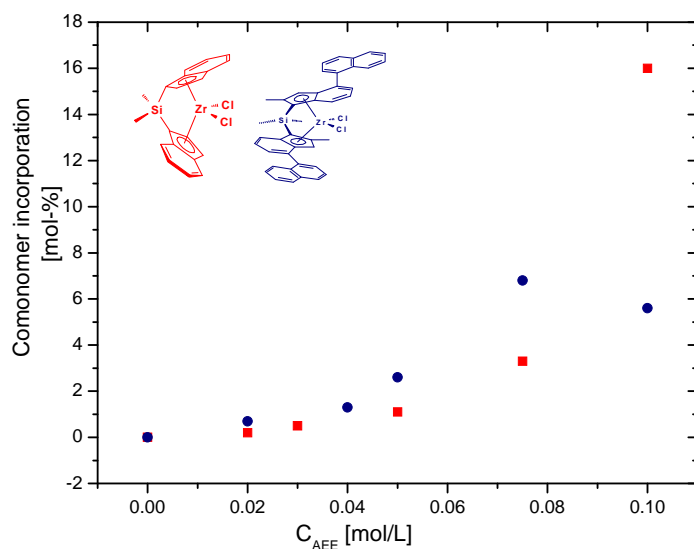


Figure 38: Comonomer incorporation (mol-%) as a function of AEE concentration in feed. Polymerization conditions: 60°C, Al/Zr=3800,  $C_{\text{cat}}=10^{-6}$  mol/mL, toluene.

For the catalyst system (5)/MAO was observed a maximum incorporation of 6.8 mol %. The incorporation rate followed different trends for both systems. The highest level of incorporation attained with the catalyst system (5)/MAO was observed at 0,075 mol/L of AEE in the feed. Additionally, when the concentration of the polar monomer was increased in the feed, the catalyst system seems to be poisoned and the incorporation rate has fallen down. The catalyst system (3)/MAO seems to be more stable in the presence of the polar group at the studied comonomer concentration range.

To gain additional insight into the system AEE-co-PE, a deep investigation of the copolymerization was performed in this work. The influence of the reaction temperature, pressure, catalyst system and co-catalyst concentration was investigated.

#### 7.4.1.2 The Temperature Effect

Three different temperatures 30, 45 and 60°C of the polymerization reactions were studied using two catalyst systems in order to assess the final properties of the obtained polymers. Considering the catalytic activity (Figure 39), it was observed that the higher the temperature of the reaction was, the higher the catalytic activity for the catalysts system (3)/MAO was. The catalyst system (5)/MAO, has presented a minimum value for the activity at 45°C. It was

observed that the catalytic activity of the system (3)/MAO was higher than the activity of the system (5)/MAO in all temperatures investigated.

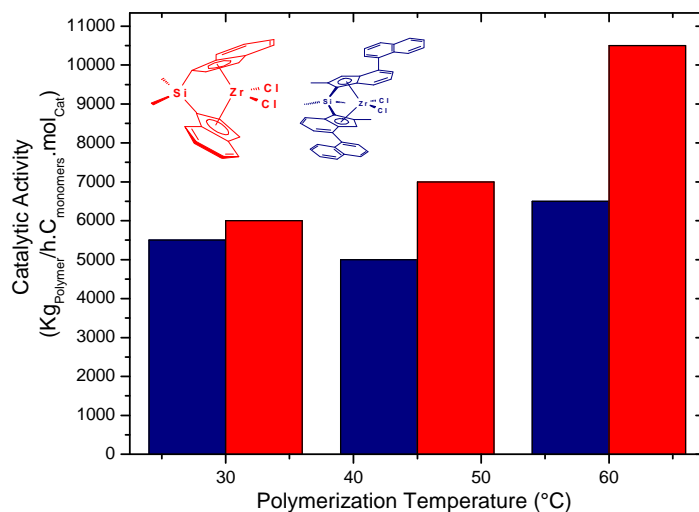


Figure 39: Catalytic activity as a function of the polymerization temperature for two catalyst systems.

The influence of the polymerization temperature on the composition of the obtained polymers was investigated by  $^1\text{H}$ NMR spectroscopy. It was observed that the temperature of the reaction influences the incorporation rates of the polar monomer. Figure 40 shows that the highest level of incorporation was obtained using the catalyst system (5)/MAO at 30°C. On the other hand, for the catalyst system (3)/MAO the highest level of incorporation was obtained at the temperature of the reaction 45°C. For the catalyst system (5)/MAO, the incorporation rates calculated using  $^1\text{H}$ NMR spectroscopy was 3,6 mol % and 2,2 mol % for the catalyst system (3)/MAO.

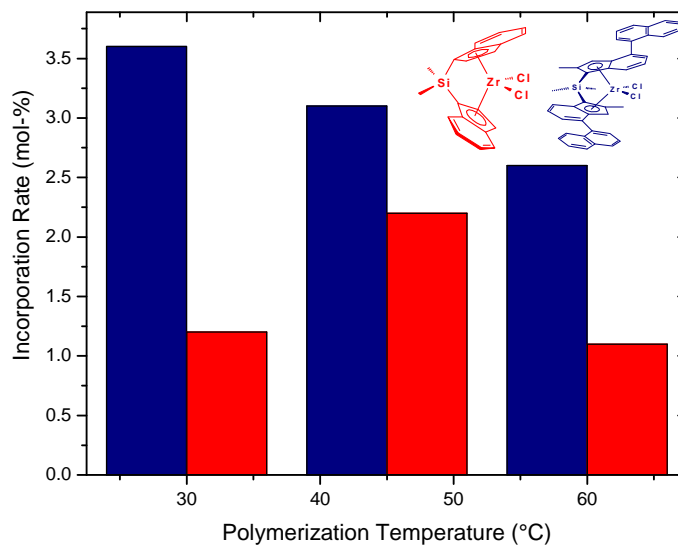


Figure 40: Incorporation rate as a function of the reaction temperature for two different catalyst systems.

The melting points of the obtained polymers did not follow any trend. The highest values were obtained when the catalyst system (3)/MAO was used. The molecular weights of the obtained polymers decrease with an increase in the temperature of the reaction (Figure 41). As it was expected, the molecular weights of the obtained polymers are higher when the catalyst system (5)/MAO was used.

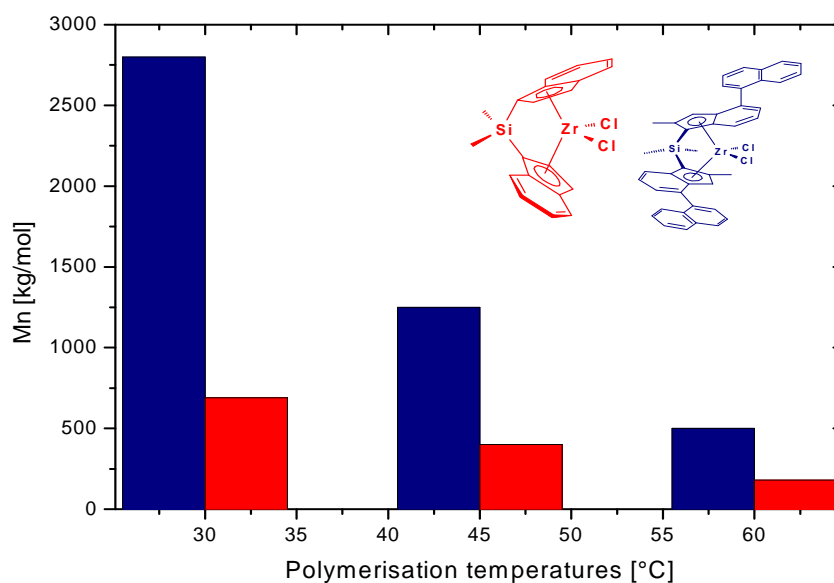


Figure 41: Molecular weight as a function of the reaction temperature for two different catalyst systems.

### 7.4.1.3 The MAO Effect

The polymerization activities with metallocene catalyst generally increase with the Al/Zr ratio, reaching a maximum value at a certain mole ratio. If the molar quantity of aluminium alkyl is increased beyond this point, the activity usually remains constant or decrease slightly<sup>31</sup>.

The influence of the amount of MAO was studied for both catalyst systems by keeping the amount of comonomer constant and increasing the MAO quantity from 200 to 400 mg. The results presented in the Figure 42, show that for both systems were observed an increase in the catalytic activity with an increase in the ratio MAO/Zr. However, the activity is higher with the catalyst system (3)/MAO than with the system (5)/MAO. In addition, the polymerization rate was low when the ratio Al/Zr was about 2000. With the increase in the MAO concentration, the catalytic activity rapidly reaches approximately twofold of its initial activity for the catalyst system (3)/MAO. This result was also observed for the copolymerization of ethylene with 10-undecen-1-ol using the same catalyst system<sup>31</sup>.

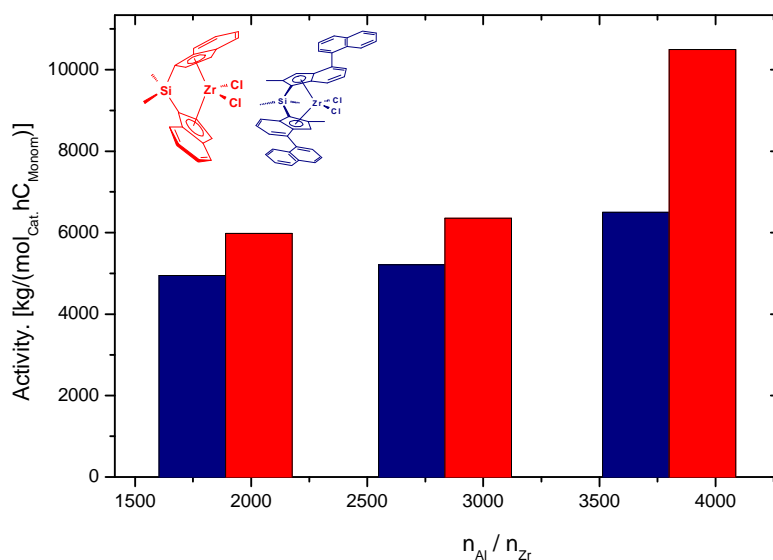


Figure 42: Catalytic activity as a function of MAO concentration in feed

The melting points of the obtained polymers show an increase trend for both systems with increase in the Al/Zr ratio, Figure 43. Additionally, the melting points of the obtained

polymers using the catalyst system (3)/MAO are relatively higher than those polymers using the catalyst system (5)/MAO.

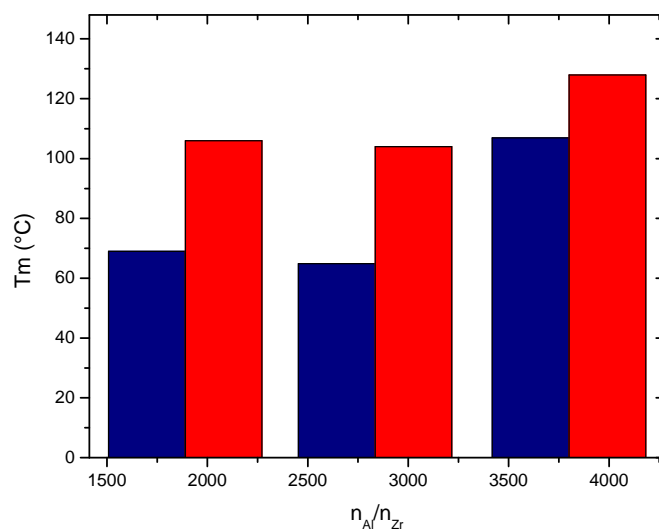


Figure 43: Melting points of the obtained polymers as a function of MAO concentration.

The incorporation rates are higher for the catalyst system (5)/MAO than for the catalyst system (3)/MAO, Figure 44. The maximum value of incorporation, 3,6 mol% was observed at 300mg MAO ( $n_{Al}/n_{Zr}=2835$ ) and using the catalyst system (5)/MAO.

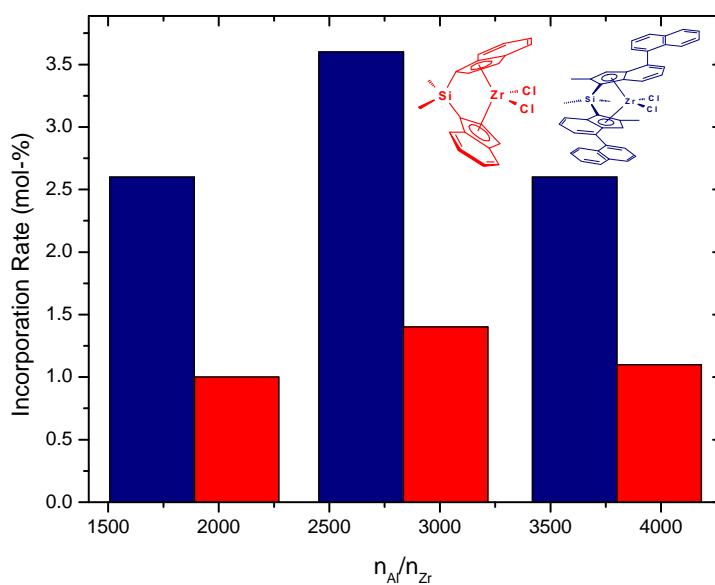


Figure 44: Incorporation rate as a function of MAO concentration.

#### 7.4.1.4 The Pressure Effect

The effect of the ethylene concentration on the catalytic activity and polymer properties was studied by varying the ethylene concentration during the polymerization reaction from 0,16 to 0,34 mol/L (2-4 bar), Table 10. It was noticed that the pressure influences the melting point, the molecular weight and the incorporation rates of the obtained polymers for both catalyst systems.

Table 10: Copolymerisation of Ethylene and AEE

Reaction	P <sub>eth</sub> (bar)	Mn(Kg/mol)	T <sub>m</sub> (°C)	IR(mol%)	Activity*
140 <sup>a</sup>	4	500	106,9	2,3	6500
133 <sup>a</sup>	3	280	108,1	2,6	10000
134 <sup>a</sup>	2	1200	63	4,5	7500
150 <sup>b</sup>	4	180	128	1,1	10500
159 <sup>b</sup>	3	2000	125,5	1,4	10000
162 <sup>b</sup>	2	460	96,1	3,8	10000

Used catalyst systems: a-(5)/MAO, b-(3)/MAO, \*-Activity unit – Kg<sub>polymer</sub>/(h.C<sub>monomers</sub>.mol<sub>Zr</sub>), C<sub>AEE</sub>=0,05 mol/L

The melting points of these polymers follow a similar pattern, Table 10. For the catalyst system (3)/MAO the melting point increased with increasing ethylene concentration. However for the catalyst system (5)/MAO the melting point increased and then decreased with increasing ethylene concentration. The maximum melting point (128°C) was observed for the catalyst system (3)/MAO at an ethylene pressure of 4 bar and the minimum value (96,1°C) at 2 bar. For the catalyst system (5)/MAO, the melting points of the polymers are lower than that obtained with the catalyst system (3)/MAO, the values are between 63 and 108,1°C, in this case followed by a high loss of crystallinity.

Figure 45 shows that both catalyst systems have similar behaviors regarding to the comonomer incorporation as a function of the ethylene pressure in the feed. The catalyst system (5)/MAO has presented the highest incorporation level of 4,5 mol% at the lowest ethylene pressure. For the catalyst system (3)/MAO the maximum incorporation was 3,8 mol% observed at 2 bar.

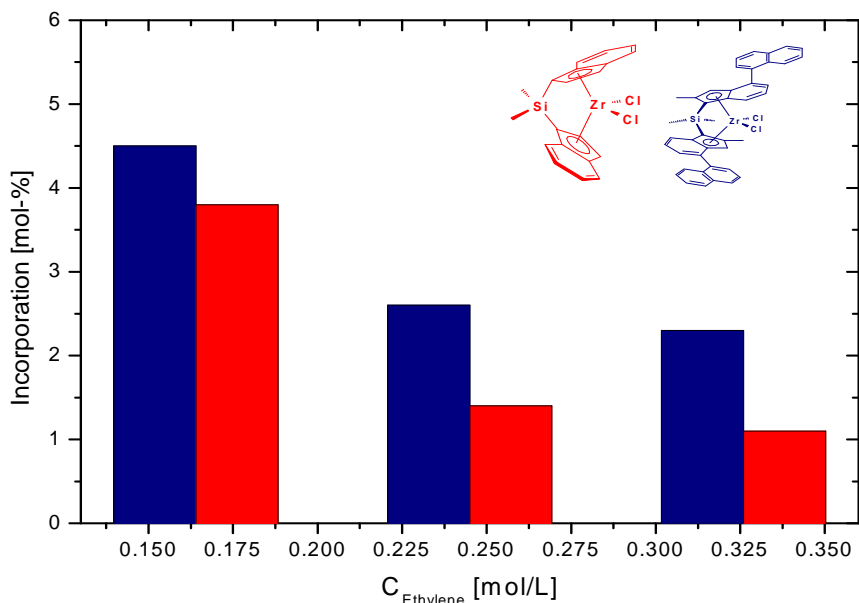


Figure 45: Incorporation rates as a function of pressure of the reaction.

#### 7.4.1.5 Partial Conclusions

The copolymerization reactions of ethylene with allyl ethyl ether using zirconium and titanium based catalysts with MAO as cocatalyst and TIBA as complexation agent were carried out in the laboratory. Copolymers with a comonomer content up to 16 mol % were synthesized using only the zirconium based catalyst. The titanium based catalyst was not active in the presence of the polar monomer on testing conditions. Probably, the oxophilic character of the comonomer has deactivated the active species of titanium based catalyst faster than the zirconium based catalyst.

Although the polar monomer was treated with TIBA, the polymerizations with zirconium based catalyst have shown a strong reduction in the catalyst activity even at lower comonomer concentration in the feed when compared with the homopolymerization of ethylene.

A complete chemical characterization of the obtained copolymers was not possible due to the poor solubility of the obtained polymers. The spectra of the obtained polymers are quite complex and did not allow an easy assignment of a well defined structure. One reason for that might be the presence of remaining aluminium oxide originated from the pre reaction of the polar comonomer with TIBA. However, the presence of signals relevant to the polar group and the polyethylene main chain in the NMR spectrum indicate that the copolymerization

proceeded.

The set of DSC, GPC, NMR and SEM results leads to a conclusion that the obtained copolymers contain two different crystalline phases that were built through different active species during the polymerization reactions. The first phase shows a melting point range from 128-134 °C and low comonomer content below 1.5mol-% and the second phase shows a broad melting transition range from 65-125°C and a comonomer content up to 16%. Copolymers with a comonomer content higher than 6 % were amorphous and show only a glass temperature in a range from 65-85 °C.

The presence of two crystalline phases in the copolymer is remarkable when the catalyst system (5)/MAO was used. The catalyst system (3)/MAO did not show this effect so strong. Besides that, the catalyst system (3)/MAO presents a high level of incorporation.

The molecular weights of the obtained copolymers are between 150 and 1200 kg/mol when the catalyst system (5)/MAO was used in the polymerization. Using the catalyst system (3)/MAO, these values are between 180 and 2800 kg/mol. These results are only an estimative value due to the fact that the GPC equipment did not use specific columns calibrated for polar groups. However, the values represent a trend in the behavior for all samples studied here.

To sum up, it was observed that the properties of the obtained copolymers closely depend on the polymerization parameters. Incorporation rates, melting points and molecular weights strongly depend on the temperature of the reaction. In general, at 45°C the incorporation of the polar monomer was relatively better than at the other temperatures studied.



## 7.4.2 Comparison between the Results of the Copolymerization of Ethylene with Allyl Propyl Ether and the Copolymerization of Ethylene with Allyl Ethyl Ether

In order to investigate the rule of a larger monomer on copolymerization, a second polar monomer with one additional methylene group after the oxygen atom in the ether structure, Figure 30 b), APE was copolymerized with ethylene. The reactions were carried out in the presence of catalyst system (5)/MAO at the same polymerization conditions applied for the previous used polar monomer AEE. The results of the activities, as well as the polymer characterizations will be discussed and compared with the previous results with AEE.

### 7.4.2.1 Effect of Comonomer Concentration

The effect of the comonomer concentration was observed by varying its concentration from 0,02 to 0,1 mol/L in the feed (Figure 46). For ethylene/APE copolymers, it was observed a steady decrease in the polymerization activity with increasing value of the comonomer concentration. On the other hand, the catalytic activity in the presence of AEE slightly decreases with an increase in AEE concentration in feed and is lower than the catalytic activity in the presence of APE in almost all concentrations studied. These results suggest that the presence of one more methylene group in the monomer structure of APE reduce in some extent the negative influence of the polar group on the catalytic activity compared with the catalytic activity in the presence of AEE.

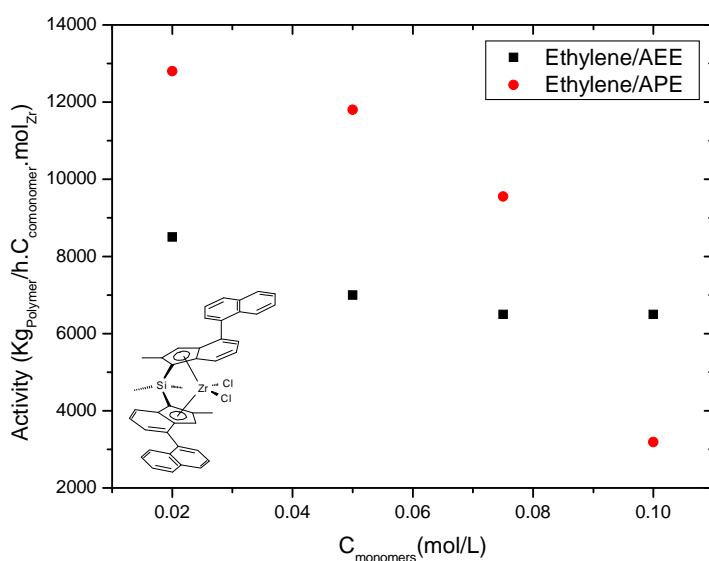


Figure 46: Catalytic activity as a function of comonomer concentration in feed.

### 7.4.2.1.1 DSC and GPC Results

The melting points of the obtained polymers measured by DSC are giving in the Figure 47. The melting points of these polymers follow similar patterns, the higher the polar monomer concentrations in feed, the lower the melting point. However, the system ethylene/APE presents a second melting peak at high comonomer concentration in the feed.

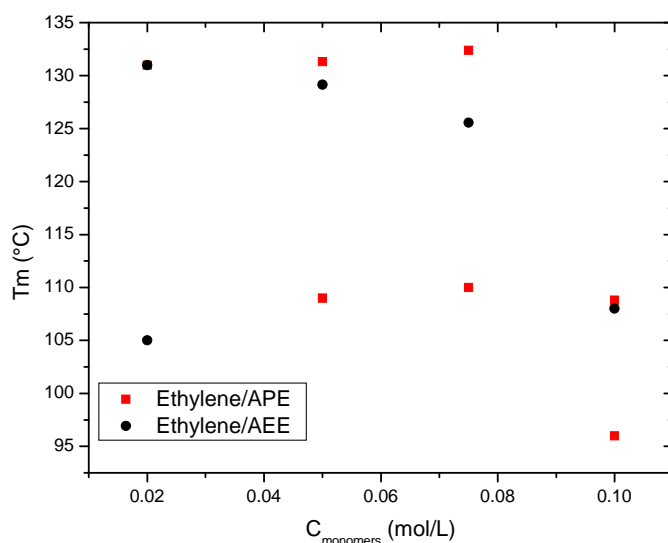


Figure 47: Melting Points of the obtained copolymers as a function of the comonomer concentration in feed.

The DSC curve of each copolymer shows a melting peak that shifts to lower temperatures with an increase in the comonomer concentration. In both cases, there is a loss of crystallinity with an increase of the comonomer concentration in the feed, as it can be seen at Figure 48. However, this effect is more evident when the polar monomer AEE was used.

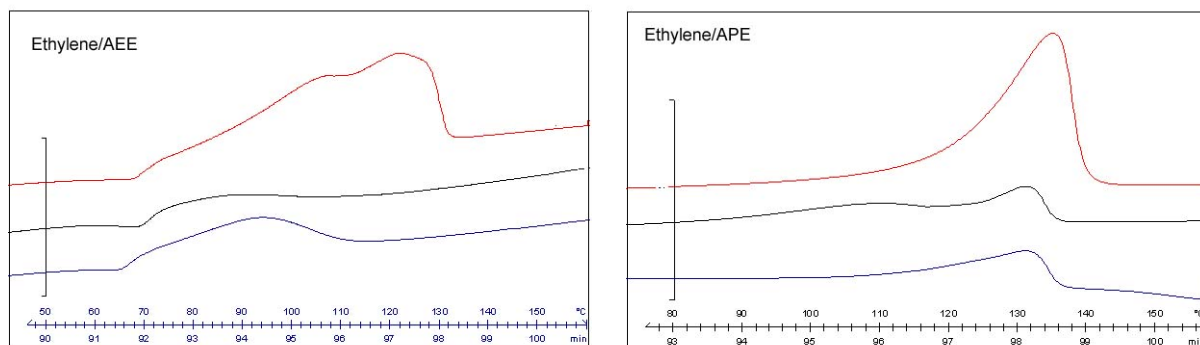


Figure 48: DSC Curves of the obtained copolymers.

Molecular weight determinations by GPC have shown a uniform distribution in all samples ( $168 < Mn_{APE}(\text{kg/mol}) < 350$  and  $150 < Mn_{AEE}(\text{kg/mol}) < 450$ ). It was observed some broadening of MWD with the presence of the polar comonomer, specially in the case of APE ( $2,4 < Pd_{APE} < 3,2$ ), although the molecular weight profiles continue as unimodal distribution. These results together with DSC results suggest some heterogeneity of copolymers at higher AEE and APE contents. Aaltonen et al<sup>26</sup> and Deffieux et al<sup>98</sup> have already observed the same behavior for the copolymerization of ethylene with 10-Undecenol.

#### 7.4.2.1.2 <sup>1</sup>H NMR Spectroscopy Results

The incorporated AEE and APE contents were determined by <sup>1</sup>H NMR. The <sup>1</sup>H NMR characterization of the produced polymer shows the presence of ether groups for all the concentration used. The maximum AEE incorporation (4,2 mol%) was followed by a significant decrease in the catalyst activity. In the case of the APE monomer, a further increase in the incorporation rate with the increase of comonomer concentration was clearly observed and at comonomer concentration of 0.1 (mol/l), APE incorporation was approximately twofold higher (8,2 mol%) than observed for AEE, Figure 49.

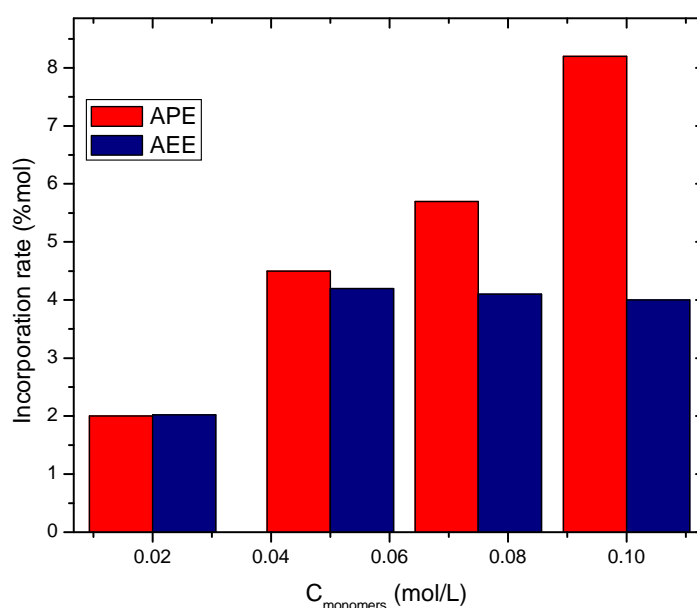


Figure 49: Incorporation rates of AEE and APE as a function of comonomer concentration in feed.

#### 7.4.2.2 Effect of Polymerization Temperature

The effect of the temperature on the copolymerization of ethylene with AEE and with APE was studied by maintaining the polar monomer concentration at 0,05mol/L, pressure at 4 bar and the ratio polar monomer:TIBA=0,5. Polymerization runs were carried out at temperatures of 30°C, 45°C and 60°C.

The activity profiles for both systems as a function of the reaction temperature are dependent on the polar monomer structure. In the Figure 50, it can be seen for the ethylene/APE system that the maximum catalytic activity was found at 45°C. In the case of AEE, the catalytic activity increase with increase in the reaction temperature. This result is in agreement with the observation from Aaltonen et al<sup>31</sup>. Additionally, it was observed by all investigated temperatures that the catalytic activity of APE is one order of magnitude higher than the catalytic activity of AEE, Figure 50.

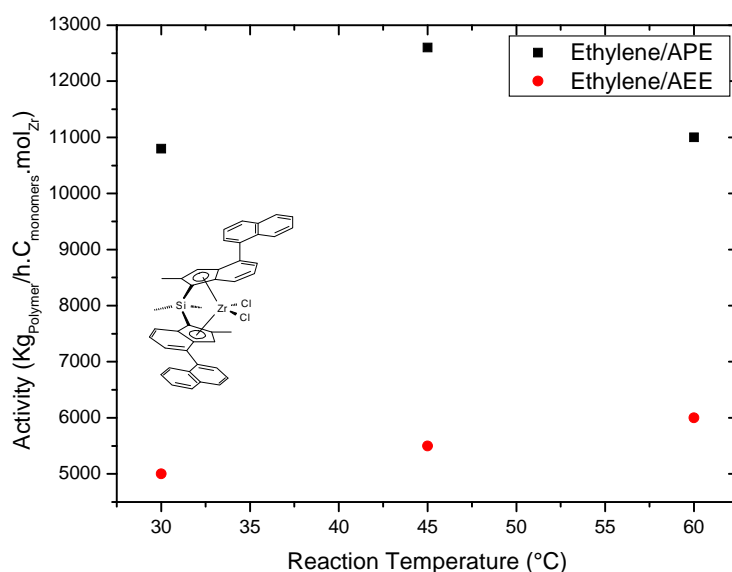


Figure 50: Catalytic activity as a function of the reaction temperature.

#### 7.4.2.2.1 DSC and GPC Results

The DSC analyses of the obtained polymers show the same profile for both systems. The lowest melting point was obtained at the highest reaction temperature. However, the smaller

polar monomer structure, the lower the melting point, as it can be seen at Figure 51.

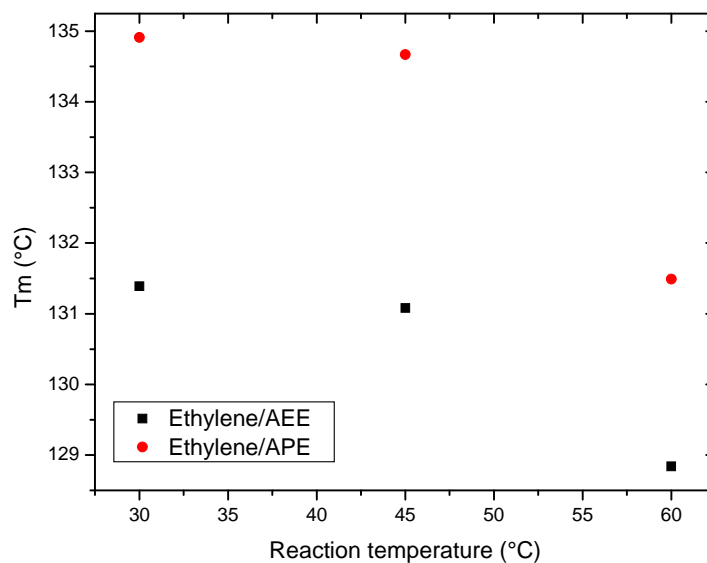


Figure 51: Melting Points as a function of the temperature of the polymerization reaction

#### 7.4.2.3 Effect of Catalyst Concentration

Later on, the effect of the catalytic concentration was studied by maintaining the others parameters constant. The catalyst amount varied in the range  $(1-3) \cdot 10^{-6}$  mol. It was observed that the catalyst activity followed the same behavior for both systems. The lowest catalyst concentration leads to the highest catalyst activity for both systems. Additionally, the activity profile shows that the catalytic activity is higher for the system ethylene/APE than for the system ethylene/AEE, Figure 52. As it was observed before, the activity is again much more dependent on the comonomer structure than the catalyst concentration.

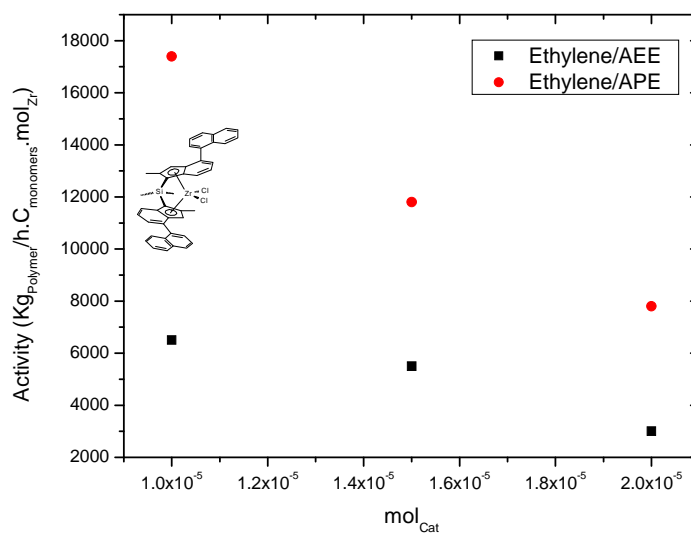


Figure 52: Catalytic activity as a function of catalyst concentration.

#### 7.4.2.3.1 DSC and GPC Results

The DSC analyses of the obtained copolymers at different catalyst concentrations show a marked decrease in the melting point for the small polar monomer (AEE) with increase in the catalyst concentration. On the other hand, the influence of the catalyst concentration on the physical properties of the obtained polymers in the presence of APE is relatively negligible. Figure 53 shows the DSC profile for both systems.

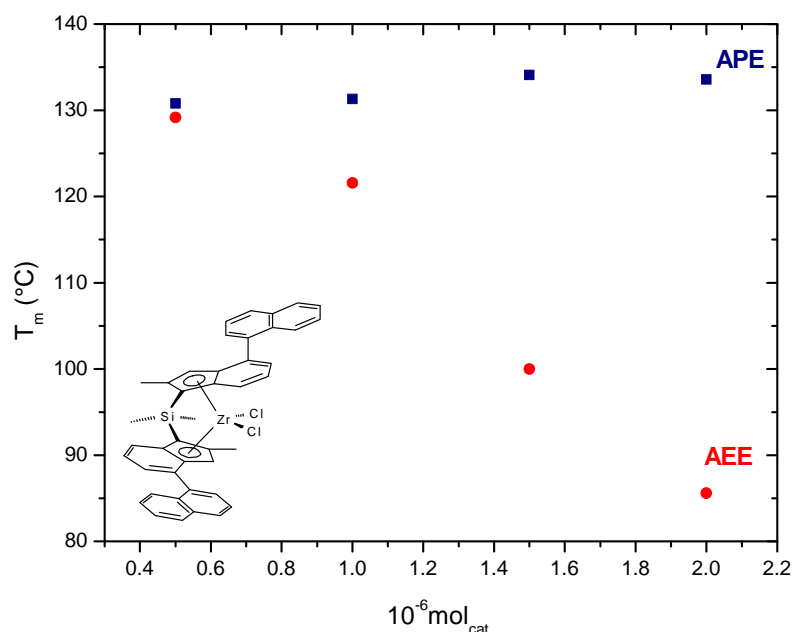


Figure 53: Melting Points as a function of catalyst concentration.

#### 7.4.2.4 Partial Conclusions

The copolymerization of ethylene with APE was carried out using the catalyst system (5)/MAO. Efforts to use titanium based catalysts in the copolymerization reaction of ethylene with APE was unsuccessfully. Although the polar monomer was pretreated with TIBA, the reactions with the zirconium based catalyst have shown a strong reduction in the catalyst activity even at lower comonomer concentration in the feed when compared with the homopolymerization with ethylene.

Some interesting observations can be withdrawn from a direct comparison of the behavior of the used comonomers, APE and AEE. For APE, the incorporation values highly depend on the comonomer concentration in feed. Additionally, the physical properties of the ethylene/APE copolymers strongly depend on the reaction temperature and slightly depend on the catalyst concentration. In the case of the AEE copolymer composition, we have seen an opposite behavior. The catalyst concentration exerts influence on the physical properties of the obtained polymers while the comonomer concentration influence is negligible.

As already mentioned and explained in the previews section (7.4.1.5), a complete chemical characterization of the obtained copolymers was not possible due to the poor solubility of the obtained polymers.

The presence of more than one crystalline phase in the copolymer is remarkable when the polar monomer AEE was used. The use of a larger monomer did not show this effect so strong. Besides that, the APE system presents higher level of incorporation at the same polymerization conditions compared with AEE.

To sum up, it was observed that the properties of the obtained copolymers are close dependent on the polymerization parameters. Incorporation rates, melting points and molecular weights strong depend on the polar monomer structure. Progression from AEE to APE yields an increasing activity.



### 7.4.3 Comparison of the Results obtained in the Copolymerization of Ethylene with AEE, APE and ABE respectively

It is very interesting to note that from the free radical perspective, the homopolymerization of the allylic monomers is very unlike, and if it does occur, it polymerizes at rather low rates<sup>87-88</sup>. The catalyst system (3) activated with MAO has proved to be able to copolymerize ethylene with AEE and also with APE. Using this previous finding, the above mentioned catalyst was used to investigate the copolymerization of ethylene with the polar monomer ABE (Figure 30c).

#### 7.4.3.1 Determination of TIBA:Allyl Ether Ratio and TIBA:Allyl Ether Pre Contact Time

Subsequently, a systematic study involving two parameters, pre contact time and molar ratio between the polar monomer and TIBA was carried out in order to find optimum conditions for the further polymerizations. The molar ratio between the polar monomer and the protecting agent was the first parameter to be investigated in this study. A set of experiments were conducted in order to find a ratio that minimize the amount of the protecting agent. Based on previous achievements using other monomers, the pre reaction time between the polar monomer and TIBA of 30 minutes was chosen for the experimental runs. The results are presented in the Figure 54.

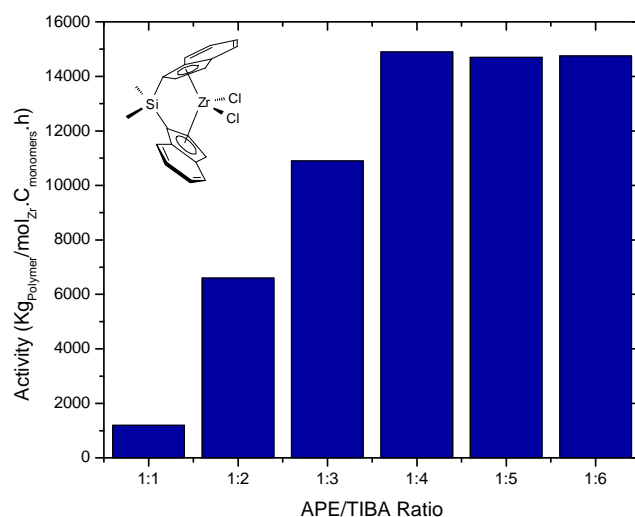


Figure 54: Catalytic activity as function of APE/TIBA Ratio. Polymerization conditions: 60°C, ethylene pressure: 4bar, toluene volume:200mL, polymerization time:30min, cocatalyst MAO;  $[A]_{APE}/[T]_{TIBA}$  pre contacted for 30 min.

Based on the results presented in the Figure 54, the use of TIBA in concentration that fulfil the ratio  $[\text{allyl ether}]/[\text{TIBA}] = 1:3$  leads to the best possible results, regarding to the satisfactory catalytic activity for the copolymerization of APE and Ethylene system. Additionally, the choice was also based on the small amount of TIBA in the pre reaction that allowed all the used monomer to be copolymerized with ethylene without significant decrease in the catalytic activity.

The following reactions used the same ratio between the polar monomers and TIBA in order to compare the influence of the others parameters on the experimental data. It is important to remember that there are three different monomers structures (AEE, APE, ABE) as well as different reactivity behaviours. It means that, in some cases, it was necessary to work with different allyl ether/TIBA ratios or with other experimental conditions to obtain comparable results in the copolymerization of these allyl ethers with ethylene.

Further on, the influence of the pre contact time between TIBA and the polar monomer on the polymerization process as well as on the final characteristic of the obtained polymers was also investigated. The pre contact time for the pre reaction of APE and TIBA varied between 1 minute and 24 hours. The other parameters, such as pressure, reaction temperature, MAO and the ratio  $[\text{APE}]/[\text{TIBA}] = 1:3$  were maintained constant during the polymerization process. The results of the set of experiments with the catalyst system (3)/MAO are shown in Table 11.

Table 11: Ethylene polymerization with the catalyst system (3)/MAO in the presence of APE<sup>a</sup>

Reaction	V <sub>APE</sub> (ml)	V <sub>TIBA</sub> (ml)	Time (h)	Activity*
174	5	15	24	293
175	5	15	2:30	3050
176	5	15	2:00	3770
177	5	15	1:00	7590
178	5	15	0,5	13200
179	5	15	0,016	70900

<sup>a</sup>Polymerization conditions: 60°C, ethylene pressure:4bar, toluene volume:200mL, polymerization time:30min, cocatalyst MAO;  $[\text{APE}]/[\text{TIBA}] = 1:3$ , \* (Kg<sub>Polymer</sub>/mol<sub>Zr</sub>.C<sub>monomers</sub>.h).

The activity of the catalyst strongly depends on the precontact time between APE and TIBA, Figure 55. It was observed that the longer the reaction time between the polar monomer and the protecting agent was, the lower the catalytic activity was. As it can be seen in Table 11,

the pre contact time of 30 minutes gives high activities for the subsequent copolymerizations runs.

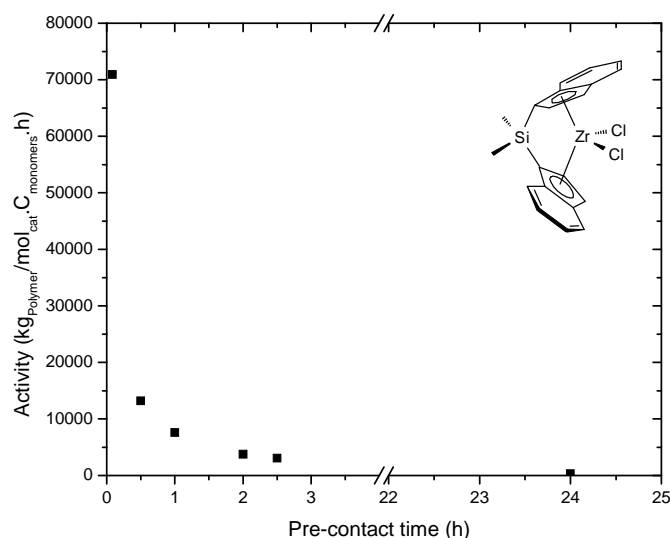


Figure 55: Catalytic activity as function of Pre Contact Time. Polymerization conditions:60°C, ethylene pressure:4bar, toluene volume: 200mL, polymerization time: 30min, cocatalyst MAO; [APE]/[TIBA]=1:3.

On the other hand, the physical properties of the obtained polymers seem to be independent of the pre contact time. The melting points ( $T_m$ ) and molecular weights of the copolymers determined by DSC and GPC respectively are indicated in Table 12.

Table 12: Ethylene polymerization with the catalyst system (3)/MAO in the presence of APE<sup>a</sup>

Reaction	$x_{APE}$	$T_m$ (°C)	$\Delta H$ (J/g)	$M_w$ (Kg/mol)	Pd
174	0,07	135,0	111,0	142,5	2,0
175	0,07	135,8	109,5	106,1	2,1
176	0,07	134,0	102,7	105,9	2,0
177	0,07	133,2	105,2	84,5	2,2
178	0,07	135,5	109,5	109,9	2,0
179	0,07	138,2	104,6	112,6	2,1

<sup>a</sup>Polymerization conditions: 45°C, ethylene pressure:4bar, toluene volume:200mL, polymerization time:1h, cocatalyst MAO; [APE]/[TIBA]=1:3.

The molecular weights, melting points and heats of fusion of the obtained polymers remain practically unchanged and unaffected by the changes in the pre contact time.

With these preliminary results in hand, it was decided to undertake the following copolymerizations of ethylene with AEE, APE and ABE respectively, using the polar monomer/TIBA molar ratio of 1:3 and the pre contact time of 30 minutes.

#### ***7.4.3.2 Effect of Comonomer Structure***

The distinguishing effect of the ethyl, propyl or butyl groups connected to the oxygen atom in the structure of the allyl ethers on the catalytic activity were compared during the copolymerization of the respective monomers with ethylene.

In an effort to shed some light on this aspect of polymerization, experiments were conducted at three different temperatures using the catalyst system (3)/MAO. At each temperature, the copolymerization series were performed by varying the concentration of the polar monomer in feed, Figure 56, 57 and 58. Temperature effect on the catalytic activities, melting points, polymer molecular weights and molecular weights distributions were studied. These experiments point out that progression from AEE to ABE yielded an increasing activity at 45°C and 60°C. As observed by Waymouth *et al.*<sup>25</sup>, a shortening of methylene spacer length cause a steady decrease in the catalytic activity.

A significant observation is that the efforts to copolymerize ethylene with AEE, APE and ABE respectively, in absence of TIBA at the same experimental conditions were unsuccessful with no catalytic activity. The main reason for this behaviour is a strong complexation between the Lewis acid component of the used catalyst and the non bonded electron pairs on the oxygen atom of the polar monomer, in preference to that between the catalyst and the  $\pi$  electrons of the double bonds<sup>22</sup>. From this observation, we assume that this interaction can be minimized if a protecting agent such as TIBA could shield the electron pairs of oxygen atom in the comonomer structure.

Despite the fact that the presence of TIBA is mandatory to run the set of experiments, it was observed that the polar group was not completely shield by the protecting agent. This observation is supported by the systematic decrease in the catalytic activity with increase in the polar monomer in feed. Moreover, the protection strategy was satisfactory and leads to a considerable higher catalytic activity.

Comparing the set of experiments run at the temperatures 30, 45 and 60°C, Figure 56, 57 and 58, it is possible to see that the highest catalytic activity values for all monomers was

obtained at the temperature of 60°C. Additionally, it was observed that the copolymerization of ethylene with the biggest monomer structure, ABE yields the highest catalytic activity at 45°C and 60°C. On the contrary, with the smaller monomer structure, AEE, the catalytic activity was significantly low at all temperatures investigated.

Figure 56 shows that the system ethylene-co-ABE has the highest catalytic activity at 30°C and at the lowest comonomer concentration of 0,02 mol/L, followed by the system ethylene-co-APE and ethylene-co-AEE. Over the concentration of 0,02mol/L, the catalyst activities follow the sequence APE>ABE>AEE. Up to a comonomer concentration of 0,07 mol/L, the catalytic activity towards the system ethylene-co-ABE shows a systematic decrease.

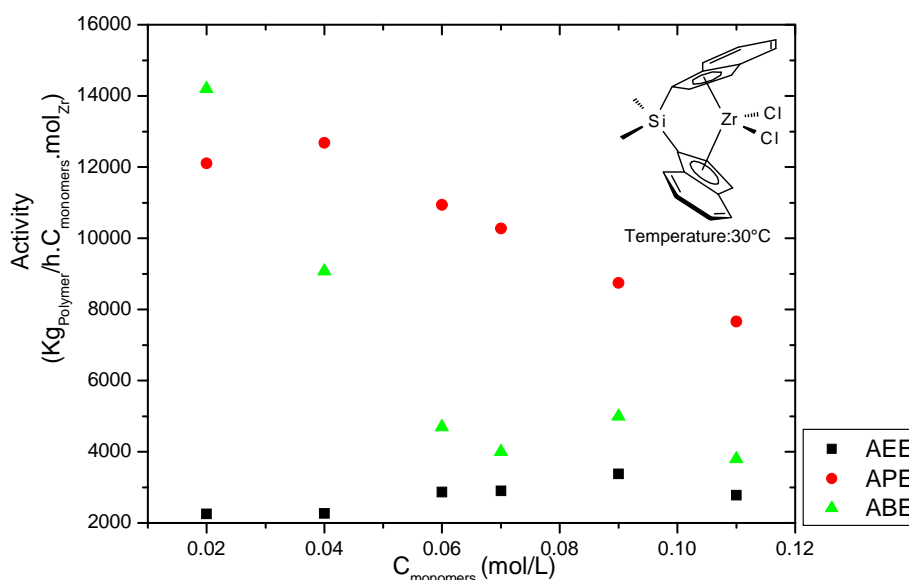


Figure 56: Catalytic activity as function of comonomer concentration at 30°C. Polymerization conditions:30°C, ethylene pressure:4bar, toluene volume:200mL, polymerization time:0,5h, cocatalyst MAO; [APE]/[TIBA]=1:3

Surprisingly, the system ethylene-co-AEE behaves in a different manner. The catalyst activity at these experimental conditions, increase with the increase in the polar monomer concentration in feed until 0.09 mol/L and decrease after this concentration. Additionally, the catalytic activity with the system ethylene-co-ABE was approximately 7 times higher than with the system ethylene-co-AEE and 1,3 times higher than with the system ethylene-co-APE at comonomer concentration of 0,02 mol/L.

Comparing the results obtained for the system ethylene-co-APE at 45°C Figure 57, with those results obtained at 30°C, Figure 56, it is clear that the catalyst partly lost its activity. The data obtained at the temperature of 45°C shows that the catalytic activity with the system ethylene-co-APE has plunged. This effect was the opposite from that observed for the systems ethylene-co-AEE and ethylene-co-ABE. It was observed for both systems an increase in the catalytic activity with increase in the reaction temperature in almost the whole range of comonomer concentration studied.

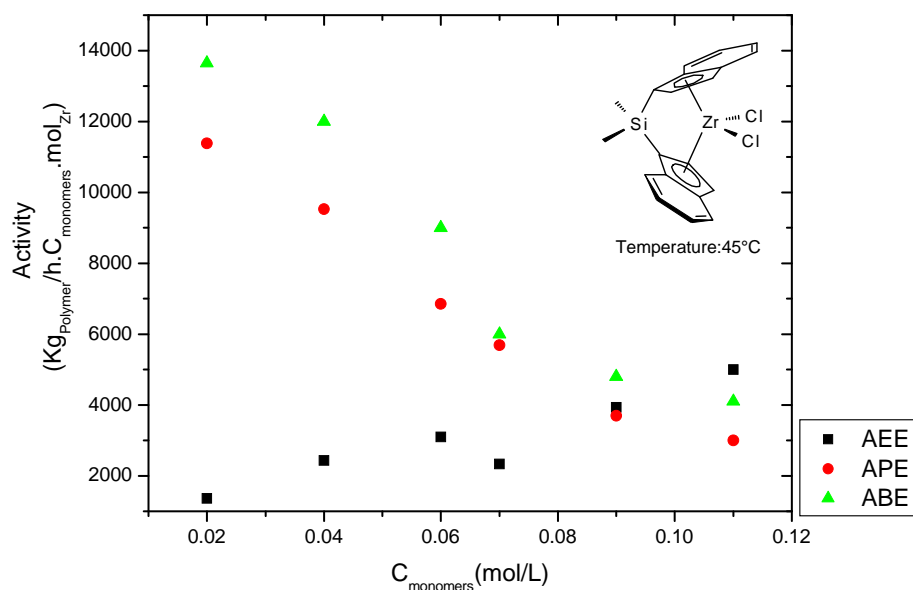


Figure 57: Catalytic activity as function of comonomer concentration at 45°C. Polymerization conditions: 45°C, ethylene pressure:4bar, toluene volume:200mL, polymerization time:0,5h, cocatalyst MAO; [APE]/[TIBA]=1:3

The effect of the comonomer concentration at 60°C on the catalytic activity was also studied, Figure 58. The results of the copolymerization with the polar monomer AEE at 60°C show the opposite tendency of the copolymerization results at 30°C and 45°C, the catalytic activity decrease slightly with the increase in comonomer concentration in feed. However, the activities values are relatively higher than those activities values obtained at 30°C and 45°C at low concentration in feed.

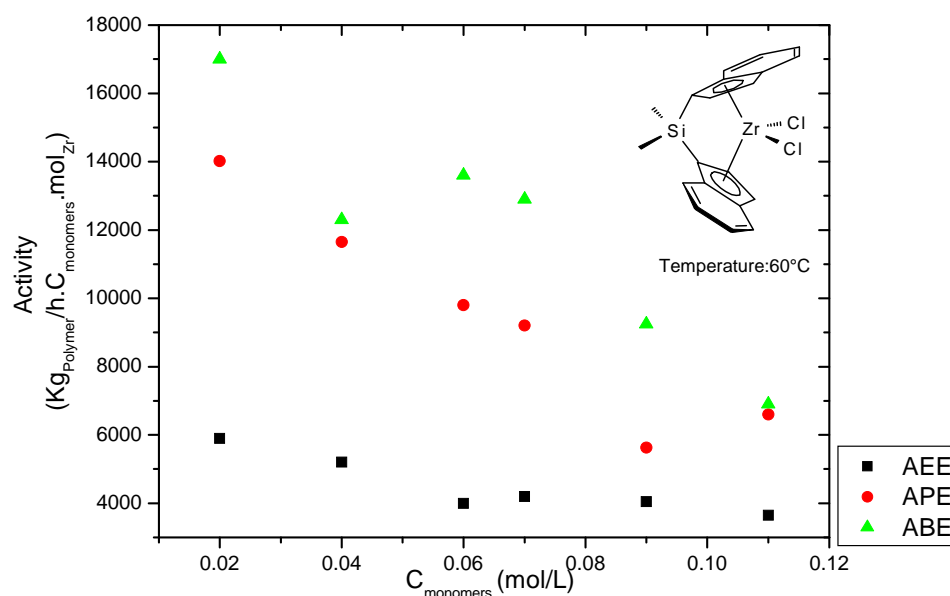


Figure 58: Catalytic activity as function of comonomer concentration at 60°C. Polymerization conditions: 60°C, ethylene pressure 4bar, toluene volume 200mL, polymerization time 0,5h, cocatalyst MAO; [APE]/[TIBA]=1:3

The last finding contrasts to the results obtained for the systems ethylene-co-APE and ethylene-co-ABE. In these both systems, the catalytic activities are strongly affected by the variation of the comonomer concentration in feed and show a sharp decrease in the catalyst activity as the comonomer concentration increase. Interesting to note is that for the system with ABE at 60°C, it was observed not only a better catalytic activity but also more tolerance of the catalyst system to the presence of this polar monomer. This observation is supported by the fact that the lost of activity was 55% at 60°C (refers to the final activity, at the highest comonomer concentration in feed), 71 % at 30°C and 70% at 45°C.

The catalytic activity for the system ethylene-co-APE at 30°C was slightly higher than those activities obtained at 45°C and 60°C for all concentrations over 0.02 mol/L. In addition, the catalyst shows more tolerance towards this polar monomer at 30°C than at 45°C or at 60°C in the wide range of comonomer concentration studied. This implies that the great majority of the active centers remain active during the copolymerization at 30°C. Additionally, at 30°C the catalytic activity increased up to C<sub>APE</sub> of 0,04 mol/L, followed by a decrease at high comonomer concentrations. This behaviour was similar to that observed for the copolymerization of ethylene with  $\alpha$ -olefins<sup>89-92</sup>. Several explanations have been considered

to explain this short increase in the catalytic activity. First of all, it is considered the better solubility of the copolymer in comparison with that of the ethylene homopolymer, which may favour monomer diffusion to the active site of the catalyst. A second approach considers the increase in the rate constant of ethylene insertion with the addition of the comonomer. After a certain monomer concentration, the reaction rates slow down, probably due to the lower insertion rates of APE than that ones with ethylene<sup>89,93</sup>.

Taking in consideration the above experimental data, it becomes clear that the different behaviour of the catalyst system (3)/MAO towards different monomers can be associated with a physical phenomenon relative to the monomer diffusion in the lower crystalline copolymer structure that changes the accessibility of the monomers to the active site<sup>102</sup>. The smallest monomer AEE leads to the lowest catalyst activity. The decrease observed for the copolymerization of ethylene with polar monomers depends on the monomer size because smaller monomer shows stronger intermolecular inhibitive interaction<sup>103</sup>.

#### **7.4.3.2.1 <sup>1</sup>HNMR, <sup>13</sup>CNMR, FTIR and Elemental Analyses Results**

For the copolymer, the incorporation of the comonomer was evidenced by the presence of the functional group as well as the absence of the comonomer vinyl group for all obtained polymers by <sup>1</sup>HNMR and later on by FT-IR.

The <sup>1</sup>HNMR spectrum of the monomer and the obtained PE-co-APE copolymer are given in Figure 59. The spectrum of the copolymer with a typical signal at  $\delta_2=3,64$  and  $\delta_1=3,62$  ppm belonging to C<sub>1</sub> and C<sub>2</sub> in the ether structure (CH<sub>2</sub>=CH-CH<sub>2</sub>-C<sub>1</sub>H<sub>2</sub>-O-C<sub>2</sub>H<sub>2</sub>-R). The complete disappearance of the multiplet at  $\delta=5.48$  ppm and at  $\delta=5.07$  ppm, indicated the total conversion of this group.



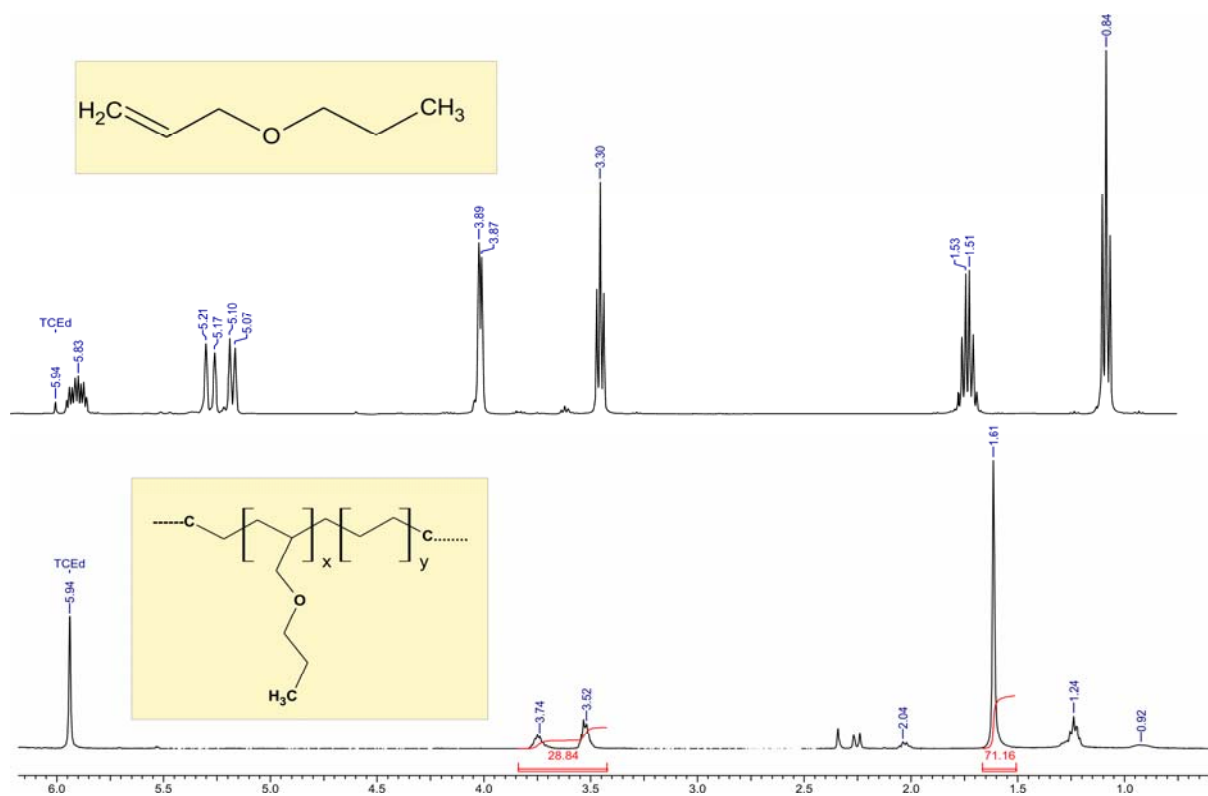


Figure 59 a)- Upper -  $^1H$  NMR of APE; b)-Down -  $^1H$  NMR of the obtained copolymer at 30°C, Polymerization conditions: ethylene pressure:4 bar, toluene volume:200mL, polymerization time: 0,5h, cocatalyst MAO;  $[APE]/[TIBA]=1:3$ , APE:TIBA pre contact time of 30 min.

It is worth to notice that several homopolymerizations were carried out at similar reaction conditions in the presence of the same catalyst system without TIBA. The aim was to verify how the polar monomers in the absence of TIBA affect the catalytic activity. In absence of TIBA, homopolymerization of these polar monomers does not occur. When the ether group was protected with TIBA, it was observed some catalytic activity towards the polar monomers. Besides that, the homopolymerization of APE lead to a yellow polymeric product in contrast to the white polymers obtained in the copolymerization with ethylene.

Comparison of the  $^1HNMR$  spectrum of the homopolymer derivate from APE with the spectrum of the corresponding APE monomer (giving in the Figure 59a), showed that the homopolymerization has occurred. Particularly, the absence of the vinyl resonances between 5.07 and 5.21 ppm indicated total convention of the monomer, see Figure 60.

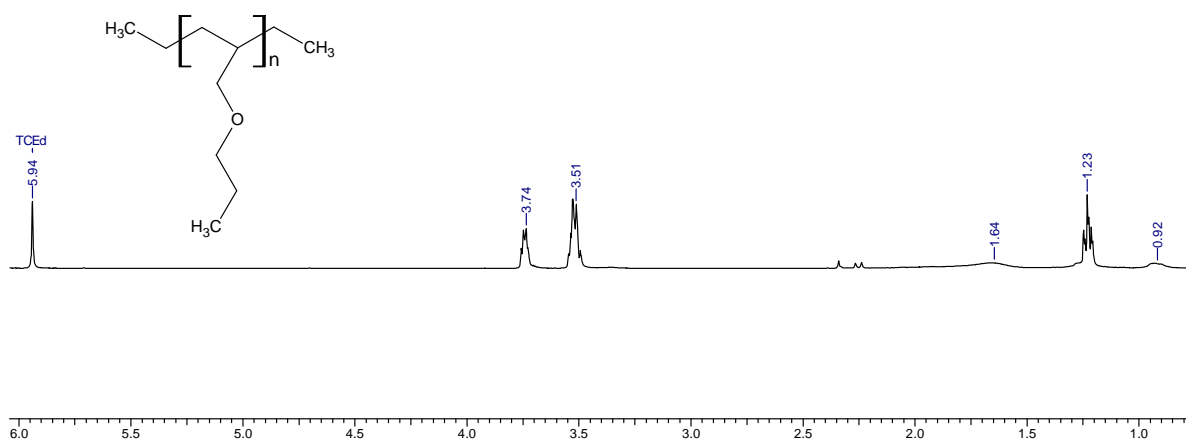


Figure 60:  $^1\text{H}$  NMR of homoAPE polymer at  $30^\circ\text{C}$ , Polymerization conditions: toluene volume: 100mL, polymerization time: 0,5h, cocatalyst MAO;  $[\text{APE}]/[\text{TIBA}]=1:3$ , APE:TIBA precontacted for 30 min.

Figure 61 shows a  $^{13}\text{C}$ NMR DEPT pulse spectrum of the copolymer that was taken to confirm if the polar group are introduced in the polyethylene main chain. Using this analysis it was possible to confirm the formation of a truly copolymer. The resonance at 33.42 ppm assigned to methine carbon is definitely a proof that a copolymerization proceeded well.

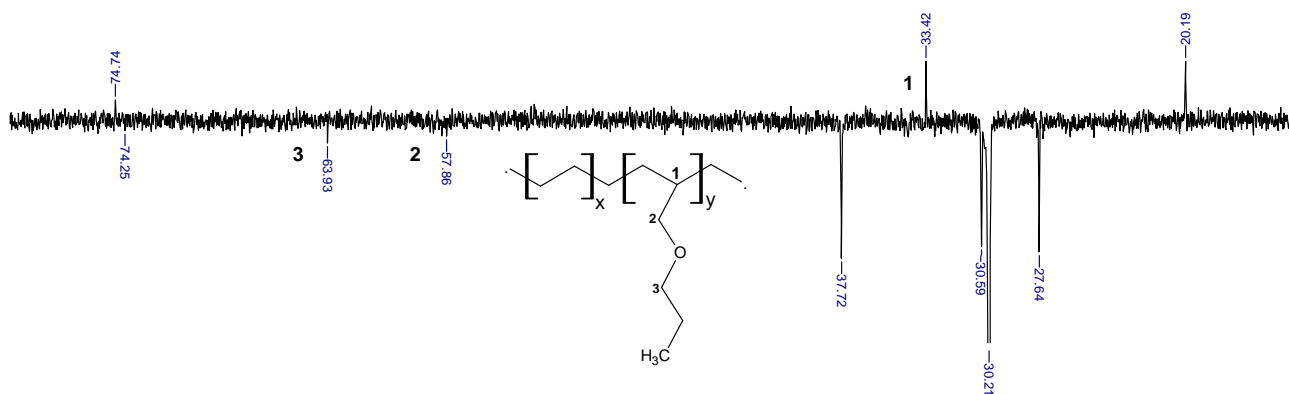


Figure 61:  $^{13}\text{C}$  NMR (DEPT) Spectrum of ethylene-co-APE copolymer obtained at  $30^\circ\text{C}$ , Polymerization conditions: toluene volume:100mL, polymerization time:0,5h, cocatalyst MAO;  $[\text{APE}]/[\text{TIBA}]=1:3$ , APE:TIBA pre contact time of 30 min.

Fourier Transform Infrared (FTIR) spectroscopy results also confirm the presence of the ether group in the obtained copolymers. The partial FT IR spectrum of the obtained copolymer is giving in Figure 62. Blank experiments were carried out using homopolymer

of polyethylene. A comparison of the FTIR spectrum of the obtained copolymer with the FTIR spectrum of the material used in the blank experiments shows two new absorptions peak at 1024 and 1014  $\text{cm}^{-1}$  belonging to C-O-C vibration stretching modes of the ether group. The remaining absorbance bands suggest disordered crystalline polyethylene segments, probably due to the inclusion of the ether group into the polymer crystal<sup>86</sup>.

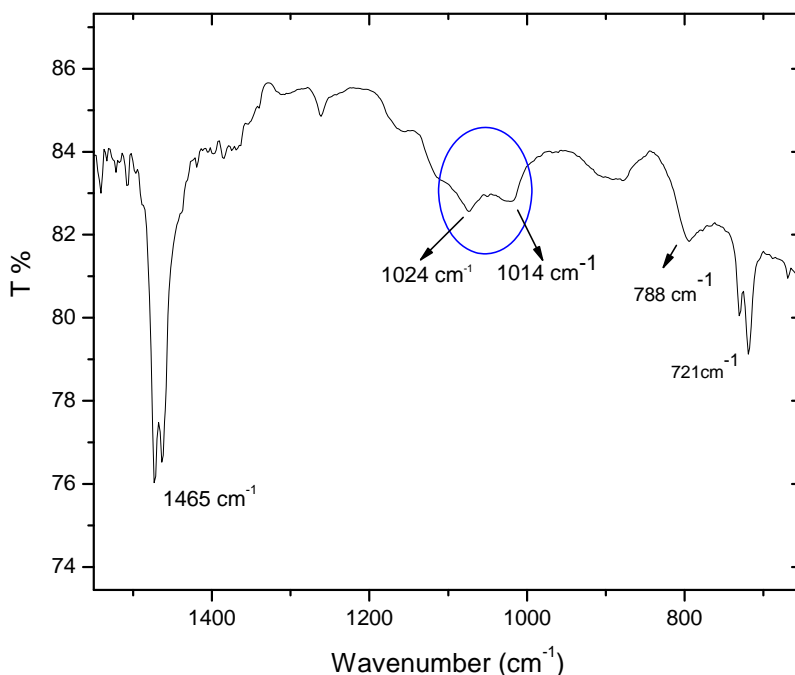


Figure 62: Partial FTIR Spectrum of APE at 30°C. Polymerization conditions: ethylene pressure: 4 bar, toluene volume:200mL, polymerization time:0,5h, cocatalyst MAO;  $[\text{APE}]/[\text{TIBA}]=1:3$ , APE:TIBA precontacted for 30 min.

As mentioned early, the polymeric materials obtained from the copolymerization of ethylene with allyl ethers (AEE, APE, ABE) in the presence of the catalyst system (3)/MAO are only partially soluble in the common organic solvents. Due to this limited solubility, it was not possible to obtain a well-resolved NMR spectrum in solution of the obtained polymers. The observation of the poor solubility of the polymers suggests that a solid state analysis could be helpful to estimate the incorporation rate of the polar group into the polyethylene main chain.

The differences in the nature of the curves explain the general influence of the reaction conditions on the incorporation of the polar group in the polyethylene main chain. Generally, the elemental analysis of the obtained polymers showed that the mol percent of

oxygen present in the polymers increase with an increase in the comonomer concentration in feed.

The elemental analysis of the ethylene-co-ABE copolymers synthesized at 30°C showed higher incorporation levels than those ethylene-co-ABE copolymers synthesized at temperatures (45°C and 60°C) in almost the whole range of concentration studied, Figure 63. These results could be an explanation for the low catalytic activity observed during the copolymerization at this temperature. It is worth noting that the lowest incorporation rates were determined at 60°C over the wide range of the comonomer concentration in feed in contrast to the high catalyst activity observed at this temperature.

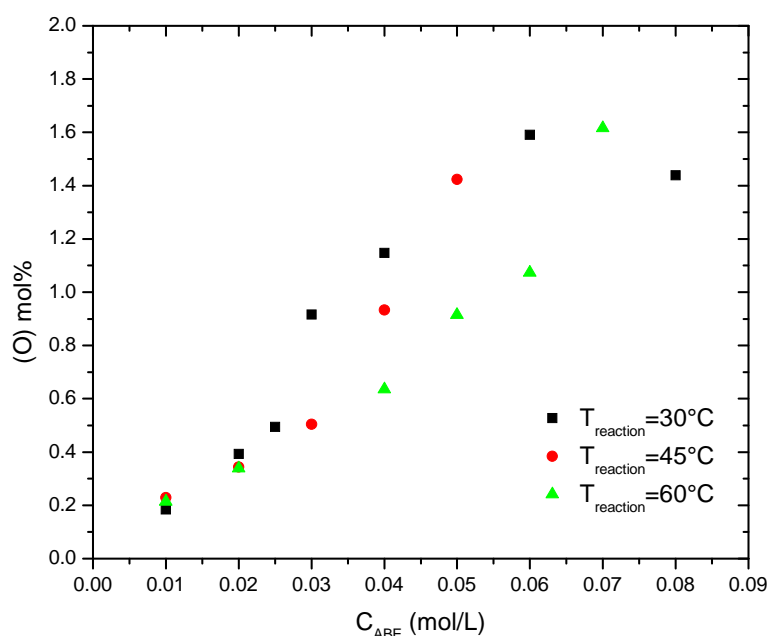


Figure 63: Elemental analysis of the obtained PE-co-ABE copolymer as function of ABE concentration.

Comparing the data obtained with the system APE, Figure 64, it is possible to conclude that the reaction temperature exerts a minor influence on the incorporation of the polar monomers into the polyethylene main chain. The very similar nature of the curves at 30°C, 45°C and 60°C also contribute to corroborate this finding. The highest comonomer incorporate of 1.6 mol % was obtained at 60°C. We have also noticed that the oxygen incorporation was reduced for comonomer concentration higher than 0.07 ml/L that could indicate difficulties to the incorporation at high comonomer concentration. Additionally, it is

interesting to report that a significant catalyst deactivation occurred at high comonomer concentration.

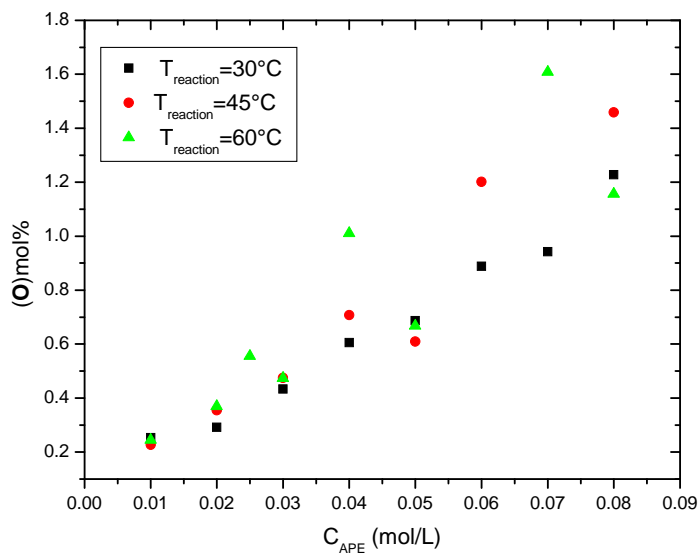


Figure 64: Elemental analyses of the obtained PE-co-APE copolymer as function of APE concentration.

Figure 65 illustrates the incorporation rates of AEE into the polyethylene main chain at different AEE concentrations and temperatures. It is worth to note that the incorporation level obtained for the copolymers synthesized at 30°C and 45°C are practically unaffected by either the increase in the comonomer concentration or reaction temperature. On the other hand, the incorporation rates of the copolymers synthesized at 60°C systematically increases with increase of AEE contents, reach a maximum value (1.56 mol%) then decrease to 1.4 mol% at  $C_{AEE} = 0.06$  mol/L.

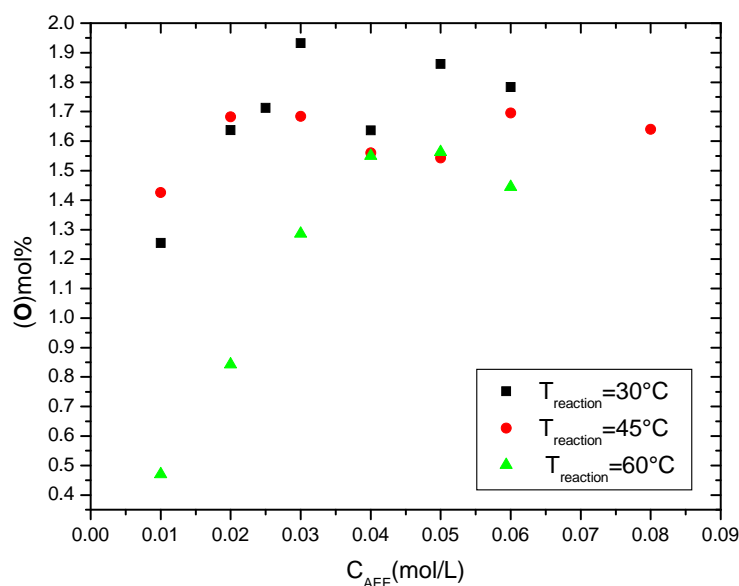


Figure 65: Elemental analyses of the obtained polymers PE-co-AEE Copolymer as function of AEE concentration.

#### 7.4.3.2.2 GPC and DSC results

It is very interesting to compare the DSC results of the obtained polymers, having similar comonomer concentration but prepared at different reaction temperatures. Generally, it was observed that the melting points of the polymeric materials are dependent on comonomer concentration and temperature.

By comparison of the melting behaviours at different temperatures, it is possible to see a decrease trend on melting point with increase in comonomer in feed. Additionally, it was also observed the presence of two melting peaks at specific comonomer concentration and temperature.

In the presence of ABE, Figure 66, the majority of the copolymers obtained at 30°C exhibits semi crystalline profile, while the polymers obtained at 45 °C show just one melting point in almost the whole range of concentration studied. The polymer obtained at 60 °C show the highest melting point at  $C_{ABE}=0.02$  mol/L. Additionally, it was observed a second melting point for all ABE concentrations higher than 0.05 mol/L.

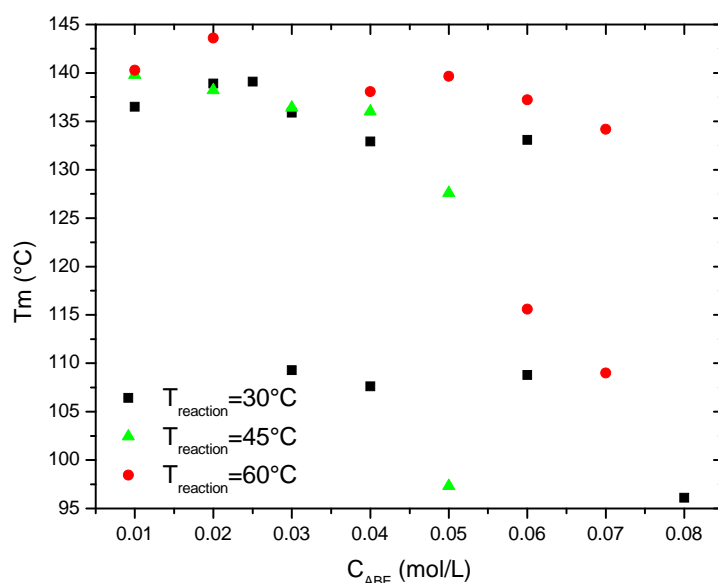


Figure 66: Melting points of the obtained copolymers as function of ABE concentration at different reaction temperatures.

Figure 67 shows that the melting points of the polymers synthesized in the presence of APE follow the same trend observe for the polymers obtained with ABE. The melting points are in the range of 143.6°C – 99.4°C and decrease with the increase in comonomer concentration in feed.

The lowest melting point was obtained for the copolymers obtained in the reaction at 45 °C. However, in the case of ABE system, the lowering in the melting points was followed by a large loss of crystallinity while a similar behaviour was not observed for the APE system.

The polymer obtained at 60 °C exhibited a single melting peak in the whole range of concentrations studied. On the other hand, the polymers obtained at 30 °C and 45 °C present a semi crystalline melting behaviour, especially in the concentration range over 0.03 mol/L of APE in feed.

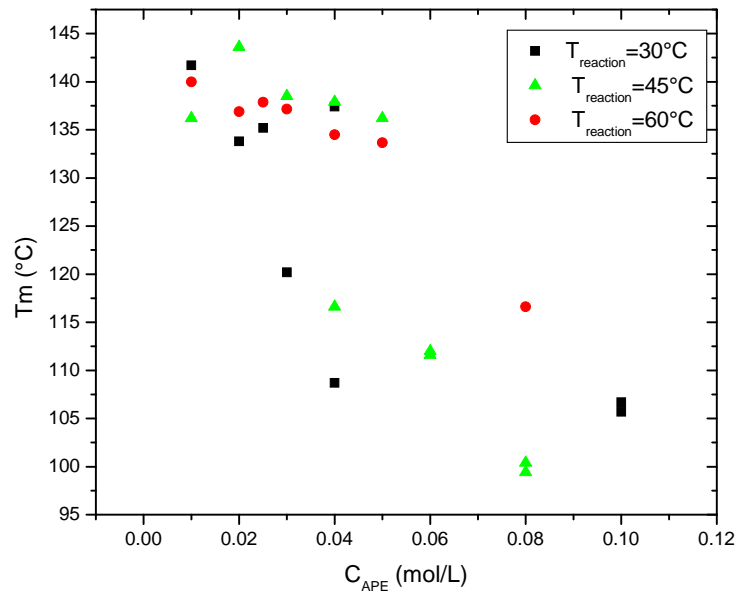


Figure 67: Melting points of the obtained copolymers as function of APE concentration at different reactions temperatures.

Figure 68 show that the great majority of the ethylene-AEE copolymers exhibit a wide melting profile. The melting points of the polymers are in the range of 141,2°C – 89,7 °C. Additionally, most of the copolymers synthesized at 60°C present a second melting peak in concentration over 0,02 mol/L in feed and decrease with the increase in comonomer concentration in feed.



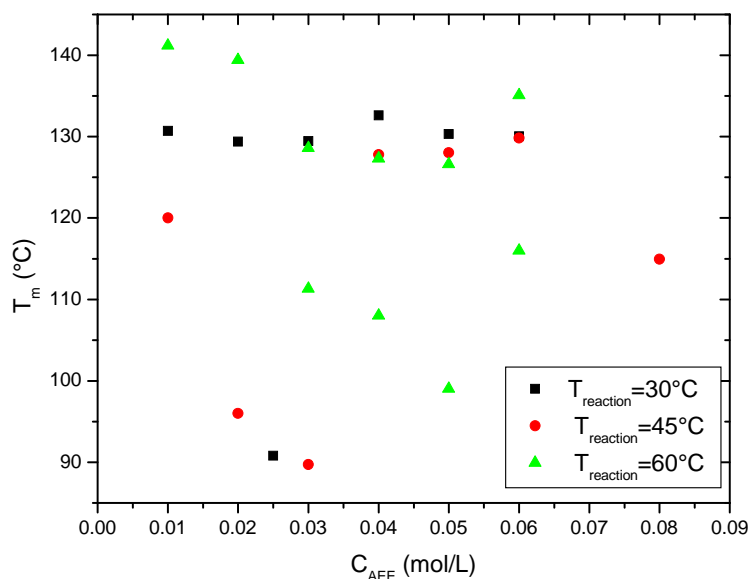
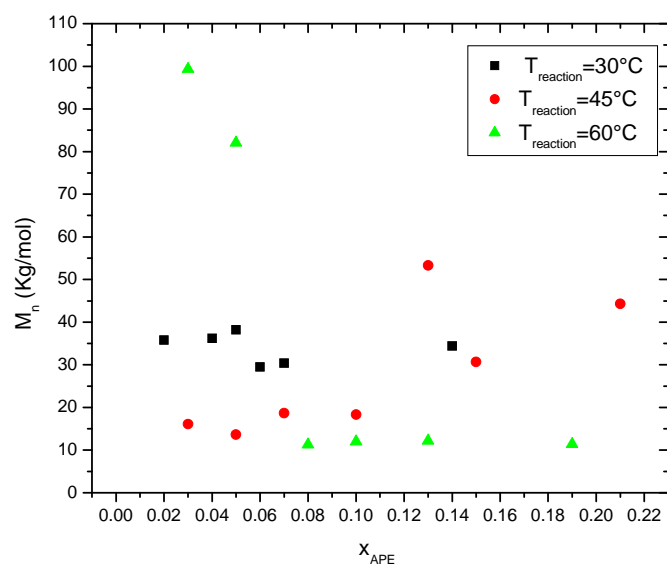
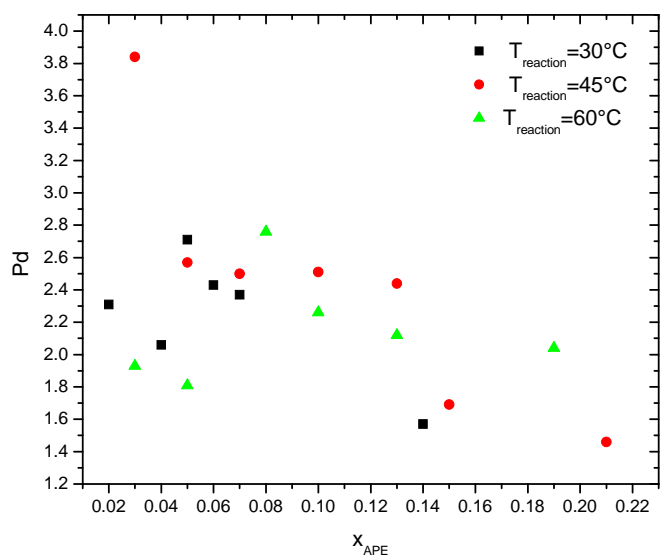


Figure 68: Melting points of the obtained copolymers as function of AEE concentration at different reactions temperatures.

The structure of the polar monomers and the reaction temperatures exert influence on the molecular weights and molecular weights distributions of the obtained polymers. The copolymerizations of ethylene with APE at three different temperatures with different monomer feed rates lead to polymeric products with reasonably narrow molecular weight distribution ( $1.4 < P_d < 3.8$ ) and high molecular weights ( $10 < M_n < 100$ ) Kg/mol, Figure 69. Specifically, the reactions conducted at  $60^\circ C$  lead to polymeric products with significant high molecular weights ( $80 < M_n < 100$ ) Kg/mol at lower comonomer concentration in feed ( $x_{APE} = 0.02$  and  $0.05$ ) respectively. However, over the molar fraction of APE of  $0.08$ , the molecular weights of the obtained polymers reach the lowest level ( $11.3$  Kg/mol) observed for all temperatures and remain almost unchanged with variation in the polar monomer concentration in feed.



a)



b)

Figure 69: a)Molecular weights of the obtained copolymers as function of APE concentration at different reactions temperatures, b) Polydispersity indexes of the obtained copolymers as function of APE concentration at different reactions temperatures

Figure 70 show that in case of the copolymerization of ethylene and ABE, among three temperatures studied, the polymers obtained at 60°C show the highest molecular weights (75<Mw<250) Kg/mol with narrow molecular weight distributions (1.5<Pd<2.5). The reactions run at 45°C and 30°C respectively afford polymers with moderate molecular weights (18<Mw<73) Kg/mol with relatively broad molecular weight distributions (1.4<Pd<4). The last finding contrasts to the general behavior observed for ethylene/ $\alpha$ -olefin

copolymers synthesized with the same catalytic system and similar experimental conditions<sup>90</sup>.

It is worth to note that the reactions run at 30°C and 45°C have shown very similar behaviors, it was observed an increase in the molecular weight of the obtained polymers with an increase in polar monomer concentration in feed. Additionally, in these reactions the molecular weight distribution behaves in opposite manner, decrease with an increase in the comonomer concentration in feed.

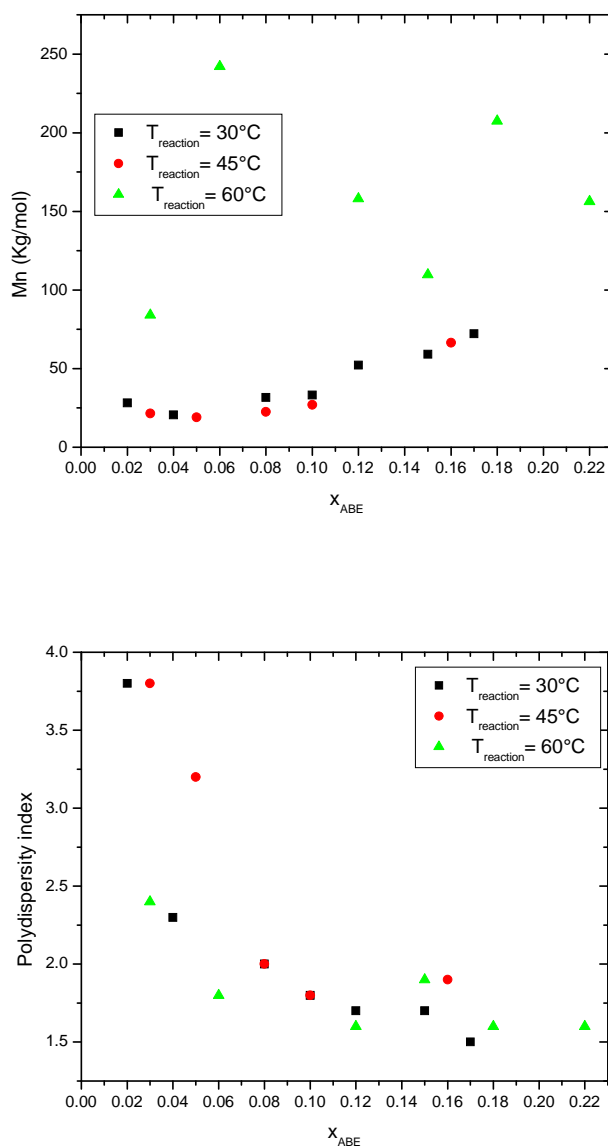


Figure 70: a)Molecular weights of the obtained copolymers as function of ABE concentration at different reactions temperatures, b) Polydispersity indexes of the obtained copolymers as function of ABE concentration at different reactions temperatures

In addition, the molecular weights of polymers produced at 60°C have remained practically

unaffected by the variation in the comonomer concentration in feed, the polydispersity index are narrow ( $1.4 < P_d < 2.8$ ) and decrease with an increase of the polar monomer concentration in the feed.

The molecular weight of the polymeric material resulting from the copolymerization of ethylene with AEE was not possible to be determined. It was not possible to dissolve these materials completely in the common organic solvent suitable to GPC analysis.

### **7.4.3.3 Partial Conclusions**

A series of copolymers containing oxygen was synthesized by direct copolymerization of ethylene with allyl ethers (AEE, APE and ABE). These monomers can be copolymerized with ethylene in excellent yields by the catalyst system  $\text{Me}_2\text{SiInd}_2\text{ZrCl}_2/\text{MAO}$  using TIBA as protecting agent. The ability of this catalyst system to copolymerize allyl ethers with ethylene could allow the development of a wide range of new materials.

In general, different parameters such as reaction temperature, comonomer concentration as well as comonomer structure have great influence on the catalytic activities. The difficulty to be copolymerized with ethylene follows the sequence:  $\text{AEE} > \text{APE} > \text{ABE}$ , which is directly relative to the steric nature of the functional group.

The protection method which can be used to prevent catalyst deactivation offers several advantages, such as facility to be removed and solubility in the polymerization medium. However, despite the fact that the presence of TIBA is mandatory to run the set of experiments, it was observed that the polar group were not completely shield by the protecting agent. This observation is supported by the systematic decrease in the catalytic activity with the increase in the polar monomer in feed. Moreover, the protection strategy was satisfactory and leads to a considerable higher catalytic activity.

It is interesting to note that AEE-co-ethylene copolymers synthesized at AEE:TIBA=1:3 ratio have shown reduced solubility in organic solvents used in GPC analysis. Due to that, the determination of the molecular weights of the copolymers was not possible to be carried out in the laboratory.

APE-co-ethylene and ABE-co-ethylene copolymers have shown a decrease in the solubility with the increase in comonomer content in the copolymer. In many cases, a fractionation of the copolymer could be occurred that leads to approximated molecular weight values of the copolymers. Besides this fact, GPC results have shed some lights on the role of comonomer concentration on the copolymers properties.

A lowering in the melting point was observed for all copolymers synthesized. Additionally, the presence of two melting peaks at particular reaction conditions suggests some heterogeneity of the obtained polymers.

## 7. 5 Copolymerization of Ethylene with MODE

In a continuation of our effort to copolymerize ethylene with polar monomers, three catalyst systems, two bridged with the spatially opened active sites  $\text{Me}_2\text{SiInd}_2\text{ZrCl}_2$ ,  $\text{Ph}_2\text{Si}(\text{OctHFlu})(\text{Ind})\text{ZrCl}_2$  and one diimine ligand (Ni diimine), illustrated in Figure 13, represented the different catalyst systems that were tested in the copolymerization of ethylene with MODE. Additionally, triisobutylaluminium (TIBA) was used as protecting agent by insulating the functional group from the active site during the copolymerization reaction. The results obtained with these catalysts systems are present in this section. The structure of MODE (2,7-Octadienylmethylether) is depicted in Figure 71.

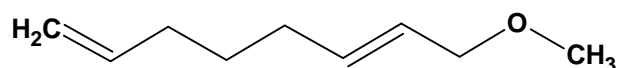


Figure 71: 2,7-Octadienylmethylether (MODE)

### 7.5.1 Results with the Catalyst System (3)/MAO

#### 7. 5.1.1 Determination of MODE:TIBA Ratio

A sequence of experimental steps was carried out in order to determine the suitable copolymerization conditions of MODE with ethylene. In a first step, a copolymerization of MODE and ethylene in absence of the protecting agent TIBA was tried without significant achievements. Afterwards, a set of copolymerization runs were carried out in order to find an optimum ratio between MODE:TIBA that lead to a production of a considerable amount of polymer. The reaction output quantity should be enough to allow further investigation on the physical properties of the obtained polymers. The experiments were run by varying TIBA concentration in feed, while the concentration of MODE was maintained constant. The results are present in Table 13.

Table 13: Ethylene polymerization with  $\text{Me}_2\text{SiInd}_2\text{ZrCl}_2/\text{MAO}$  in the presence of MODE<sup>a</sup>

Reaction	$V_{\text{MODE}}(\text{mL})$	$V_{\text{TIBA}}(\text{mL})$	Activity ( $\text{kg}_{\text{Pol}}/\text{mol}_{\text{cat}}\cdot\text{h}\cdot\text{C}_{\text{monomers}}$ )
334	5	0	0
335	5	1,5	0
336	5	10	1120
337	5	5	1380
338	5	2,5	0
339	5	3,75	0

<sup>a</sup>Polymerization conditions: 60°C, ethylene pressure 4bar,  $[\text{cat}] = 10^{-3}\text{mol/L}$ , toluene volume 200mL, polymerization time: 1h, cocatalyst MAO; MODE:TIBA precontacted time of 30 min.

Considering the catalytic activity as screening parameter, there is a clear indication that the best ratio MODE:TIBA is 1:1, Table 13. Having established the most appropriate MODE:TIBA ratio for the polymerization, the effects upon polymer properties due to variation of the different experimental conditions were studied.

### 7. 5.1.2 Effect of the Reaction Temperature and MODE Concentration

The previous determined MODE:TIBA (1:1) was used in a series of copolymerization reactions to investigate the influence of the polymerization temperature and concentration of MODE in the feed on the polymer properties. A dried toluene solution of MODE (1mol/L) was added to a toluene solution of TIBA at room temperature for 30 min under argon atmosphere. Copolymers of ethylene and MODE were synthesized at two different temperatures and different MODE concentrations in feed. These results are provided in Table 14.

Table 14: Ethylene polymerization with  $\text{Me}_2\text{SiInd}_2\text{ZrCl}_2/\text{MAO}$  in the presence of  $\text{MODE}^x$

Reaction	$C_{\text{MODE}}(\text{mol/L})$	$x_{\text{MODE}}$	Yields (g)	Activity ( $\text{kg}_{\text{Pol}}/\text{Mol}_{\text{cat}}\cdot\text{h}\cdot C_{\text{monomers}}$ )
332 <sup>a</sup>	0,025	0,07	2,9	509
343 <sup>a</sup>	0,03	0,08	1,7	313
344 <sup>a</sup>	0,04	0,10	1,6	304
345 <sup>a</sup>	0,05	0,13	0,97	182
346 <sup>a</sup>	0,06	0,15	0,59	114
384 <sup>b</sup>	0,015	0,04	0,79	1000
381 <sup>b</sup>	0,025	0,06	0,86	1060
383 <sup>b</sup>	0,04	0,09	0,34	406
382 <sup>b</sup>	0,05	0,11	0,28	326

<sup>x</sup>Polymerization conditions: a)60°C and b)45°C, ethylene pressure:4bar, toluene volume:200mL, polymerization time:1h, cocatalyst MAO; MODE:TIBA=1:1, MODE:TIBA precontacted for 30 min.

Clearly, the presence of the comonomer has a significantly influence on the catalytic activity at the investigated experimental conditions. The effect of the reaction temperature is also observed using the same catalyst system. An increase in the polymerization temperature caused a decrease in the catalytic activity. The catalyst activity at 45°C, at the same MODE concentration in feed (reactions 332 and 381), is 1 order of magnitude higher than the catalyst activity of the reaction at 60°C. Figure 72 shows a decrease trend in the catalytic activity in the presence of the protected functional monomer at both studied temperatures.

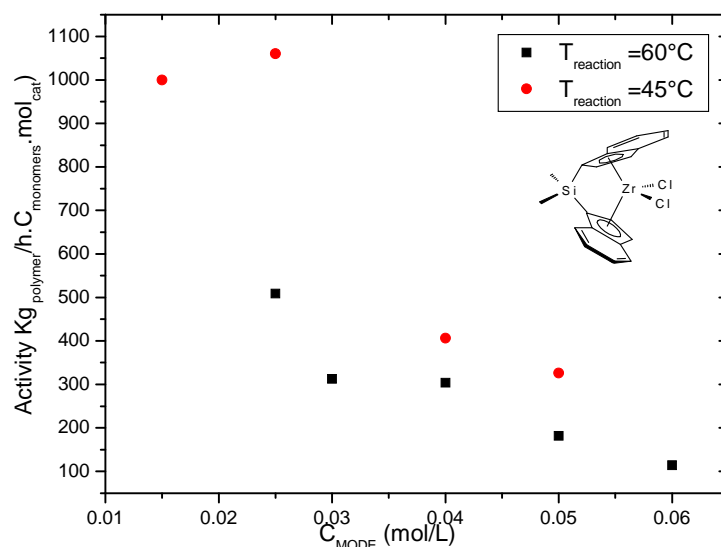


Figure 72: Polymerization activity as a function of MODE concentration in feed.

### 7. 5.1.2.1 GPC and DSC Results

The physical properties (melting point, molecular weight and polydispersity index) of the obtained polymers are summarized in the Table 15.

Table 15: Ethylene polymerization with  $Me_2SiInd_2ZrCl_2/MAO$  in the presence of  $MODE^x$

Reaction	$C_{MODE}$ (mol/L)	$T_m$ ( $^\circ C$ )	$\Delta H$ (J/g)	$M_n$ (Kg/mol)	Pd
384 <sup>a</sup>	0,015	133	120,8	181,8	3,2
381 <sup>a</sup>	0,025	136	122,5	160,8	2,3
383 <sup>a</sup>	0,04	116,6	0,22	157,0	2,2
382 <sup>a</sup>	0,05	100	n.d.	n.d.	n.d.
332 <sup>b</sup>	0,025	141,2	152,3	108	2,8
343 <sup>b</sup>	0,03	134,2	148,0	102	3,1
344 <sup>b</sup>	0,04	131,7	147,6	75	2,7
345 <sup>b</sup>	0,05	131	126,4	113	2,4
346 <sup>b</sup>	0,06	128	2,4	n.d.	n.d.

<sup>x</sup>Polymerization conditions: <sup>a</sup>45 $^\circ C$  and <sup>b</sup>60 $^\circ C$ , ethylene pressure:4bar, toluene volume:200mL, polymerization time:1h, cocatalyst MAO; MODE:TIBA=1:1;MODE:TIBA precontacted for 30 min, n.d= not determined.

The physical properties of the copolymers seem to be temperature dependent. At 45 $^\circ C$ , it is clear possible to observe a decrease trend in both molecular weight and melting point with an increase in comonomer in the feed (Table 15). These results agree with the general behavior of ethylene/ $\alpha$ -olefin copolymers when the amount of the  $\alpha$ -olefin incorporated increase<sup>93,94,99</sup>. Additionally, some narrowing of the polydispersity index was also observed with an increase concentration of the polar group in feed. On the other hand, at 60 $^\circ C$ , the molecular weight



partially follows the same behavior, with one exception ( $C_{\text{MODE}}=0,05$  mol/L). It is interesting to note that the copolymers obtained at 60°C showed lower molecular weights than the copolymer synthesized at 45°C. This behavior is due to the fact that in polymerization reaction both propagation and termination steps are affected by the reaction temperature. At low temperatures the propagation is favored and leads to higher molecular weights<sup>100</sup>.

Figure 73 shows the influence of the variation of comonomer concentration in feed on the melting points of the obtained polymers at 60°C and 45°C. The melting points decrease with the increase of the comonomer concentration. In general, using this catalyst, it can be seen that the lower the polymerization temperature, the lower the melting point.

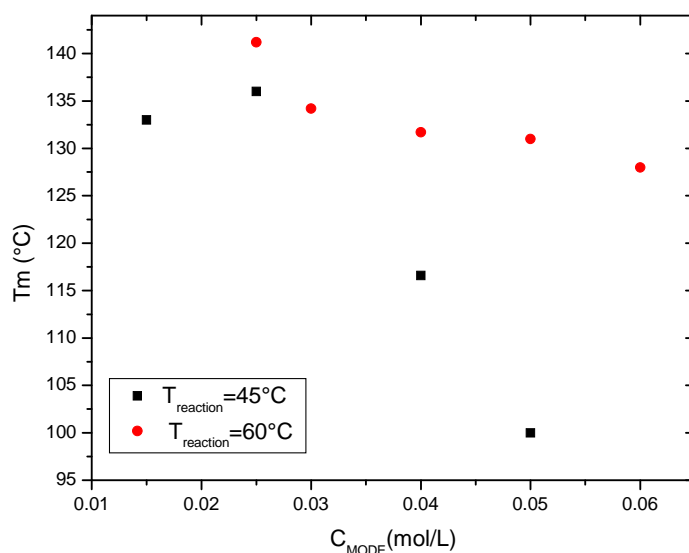


Figure 73: Melting points of the obtained polymer as function of comonomer concentration in feed at different temperatures in the presence of (1)/MAO catalyst system.

#### 7.5.1.2.2 <sup>1</sup>H NMR, <sup>13</sup>C NMR and Elemental Analysis (EA) Results

A preliminary <sup>1</sup>H NMR of the obtained polymer, Figure 74, shows a presence of peaks that are consistent with MODE incorporation  $\delta=3,37$ ppm ( $\text{CH}_3$ -; methyl group) and  $\delta=3,93$ ppm ( $\text{CH}_2$ -O; methylene group), this effect was confirmed by <sup>13</sup>C NMR, Figure 75. The presence of peaks corresponding to the methyl group (57,63 ppm) as well as methylene for polar tail at 73,49 ppm, suggest that a copolymer is formed.

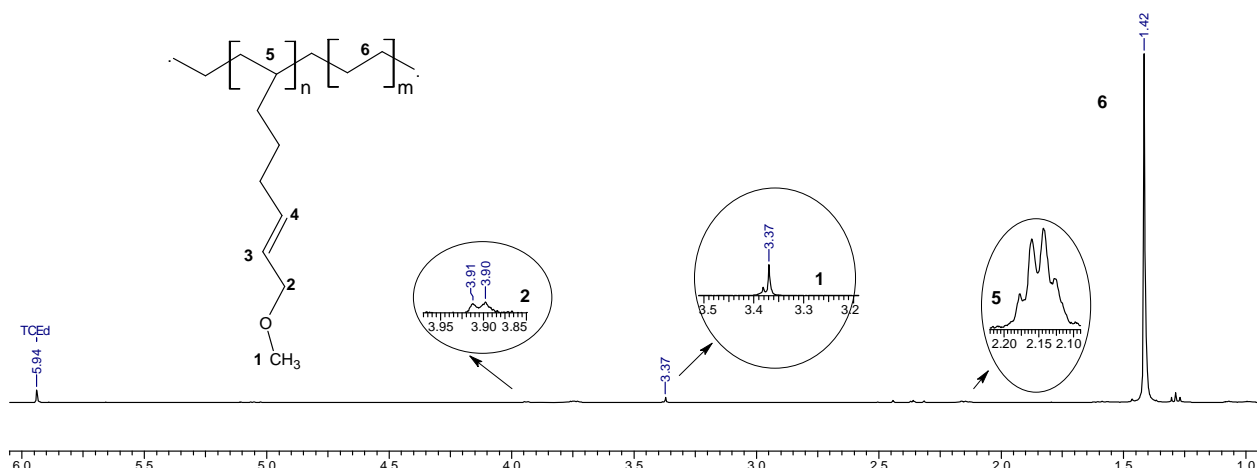


Figure 74: <sup>1</sup>H NMR spectrum of an ethylene-MODE copolymer. Polymerization conditions: 60°C, ethylene pressure:4bar, toluene volume:200 mL, polymerization time:1h, cocatalyst MAO; MODE: TIBA=1:1; MODE:TIBA precontacted for 30 min, run 345

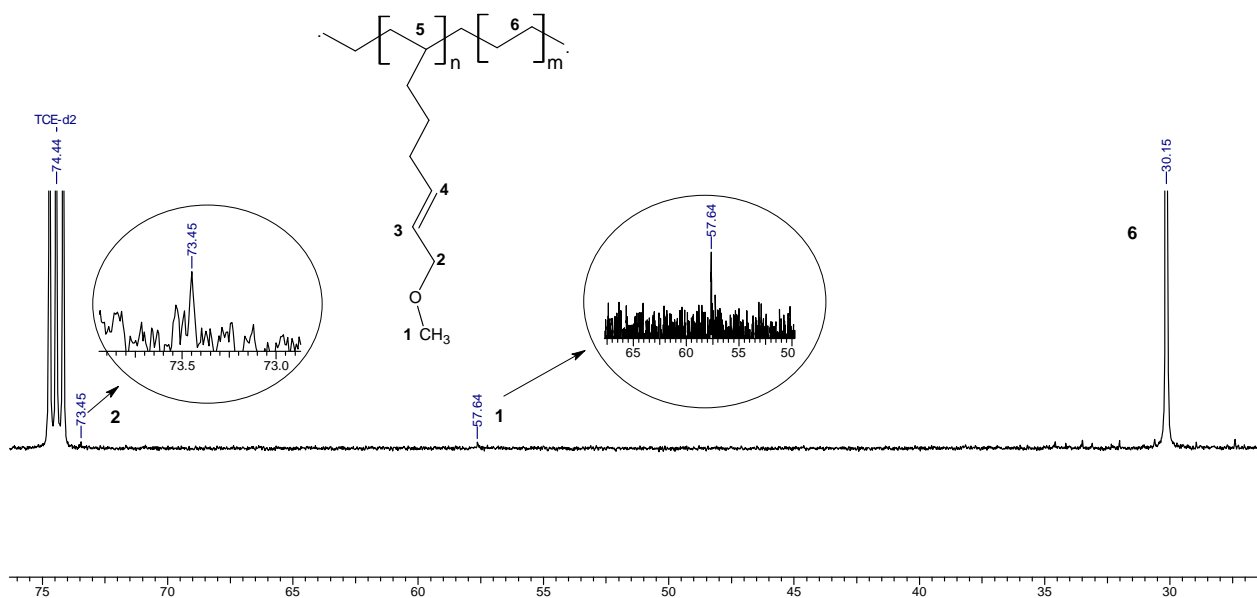


Figure 75: <sup>13</sup>C NMR spectrum of an ethylene-MODE copolymer. Polymerization conditions: 60°C, ethylene pressure:4bar, toluene volume:200mL, polymerization time:1h, cocatalyst MAO; MODE: TIBA=1:1;MODE:TIBA precontacted for 30 min, run 345

The incorporated functional group contents were determined by elemental analyses. The effect of MODE concentration on the comonomer incorporation is shown in Table 16. As expected, the incorporation rates of MODE into the polyethylene main chain increase with an increase in the MODE concentration in the reaction media. MODE concentration of 0,05 mol/L ( $x_{\text{MODE}}=0,13$ ) in the reaction media leads to a maximum incorporation rates of 0,45 mol %.

Table 16: Ethylene polymerization with Me<sub>2</sub>SiInd<sub>2</sub>ZrCl<sub>2</sub>/MAO in the presence of MODE<sup>a</sup>

Reaction	x <sub>MODE</sub> in feed	MODE (mol %) <sup>x</sup> in polymer
332	0,07	0,08
343	0,08	0,27
344	0,10	0,38
345	0,13	0,45
346	0,15	n.d.

<sup>a</sup>Polymerization conditions: 60°C, ethylene pressure 4bar, toluene volume 200mL, polymerization time 1h, cocatalyst MAO; MODE: TIBA=1:1; MODE:TIBA precontacted for 30 min, <sup>x</sup>Elemental Analysis.

The results of EA together with thermal analyses results have demonstrated the general correlation of increased branch contents to decrease melting point and heats of fusion for this series of copolymers. This behavior is in agreement with the behavior observed by copolymers of ethylene with propylene<sup>104,105</sup>, vinyl chloride<sup>106</sup> and acrylic acid<sup>107</sup>. In these cases, sharp melting profiles exhibited by high density polyethylene become broad transitions with increase levels of the comonomer incorporation<sup>94,108</sup>.

#### 7. 5.1.2.3 Fourier Transform Infrared (FTIR) Spectroscopy Results

Fourier Transform Infrared (FTIR) spectroscopy confirms the presence of the ether group. The asymmetric stretch reflective of the ether pendant group is observed at  $\approx 1112\text{cm}^{-1}$  and  $1073\text{ cm}^{-1}$  as well as the double bonds at  $1639\text{ cm}^{-1}$  of MODE structure. The remaining absorbance bands in the FTIR spectrum suggest the disordered crystalline structure of polyethylene segments. Particularly the strong bands at  $\approx 722, 970, 1458$  suggest the inclusion of the ether group into the polymer crystal<sup>86,108</sup>. The FTIR spectrum of the obtained polymer is giving at Figure 76.

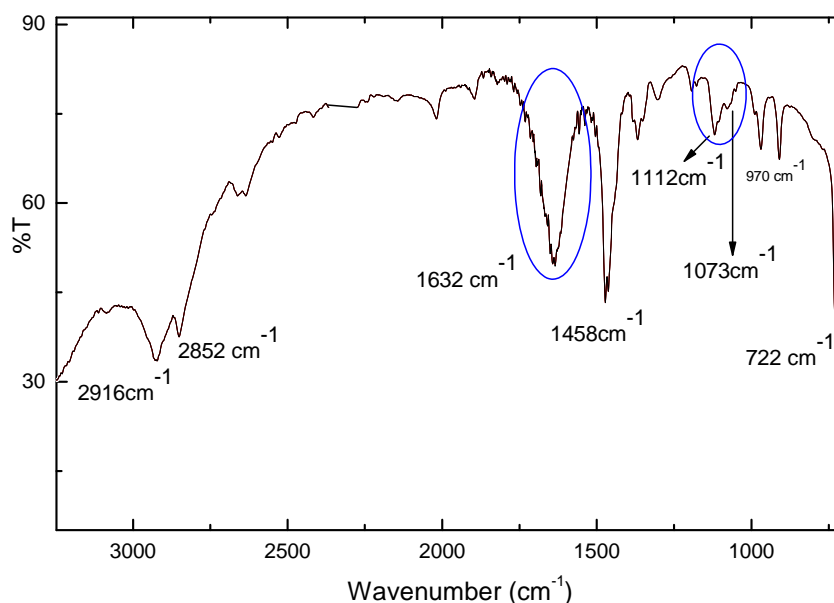


Figure 76: IR spectrum of the obtained polymer in KBr pellets, PE-co-MODE. Polymerization conditions: 60°C, ethylene pressure 4bar, toluene volume 200mL, polymerization time 1h, cocatalyst MAO; MODE:TIBA=1:1; MODE:TIBA precontacted for 30 min.

### 7. 5.2 Results with the Catalyst System $\text{Ph}_2\text{Si}(\text{OctHFlu})(\text{Ind})\text{ZrCl}_2/\text{MAO}$

The effect of variation in polymerization temperature and MODE concentration on catalytic activity during the copolymerization of ethylene with MODE, using the system (2)/MAO, is present in Table 17. Polymerization temperature was varied from 30 to 90°C. It was found that the catalyst activity is temperature dependent and the catalyst shows the highest activity at 90°C, Figure 77. It was also observed a strong decrease in the polymerization activity in the presence of the polar monomer when compared with the homopolymerization of ethylene using the same catalyst system at all temperature studied.

Table 17: Ethylene polymerization with  $\text{Ph}_2\text{Si}(\text{OctHFu})(\text{Ind})\text{ZrCl}_2/\text{MAO}$  in the presence of  $\text{MODE}^{\text{a, b, c, d}}$

Reaction	$C_{\text{MODE}}$ (mol/L)	Yields (g)	$x_{\text{MODE}}$	Activity ( $\text{kg}_{\text{pol}}/\text{Mol}_{\text{cat}} \cdot \text{h} \cdot C_{\text{monomers}}$ )
380 <sup>a,y</sup>	0	3,55	0	56200
376 <sup>a</sup>	0,015	0,78	0,05	990
375 <sup>a</sup>	0,025	0,18	0,10	223
379 <sup>a</sup>	0,03	0,62	0,09	767
377 <sup>a</sup>	0,04	0,20	0,14	239
378 <sup>a</sup>	0,05	0,60	0,18	699
365 <sup>b,y</sup>	0	3,87	0	71300
362 <sup>b</sup>	0,015	0,79	0,07	1160
363 <sup>b</sup>	0,025	1,49	0,09	2120
364 <sup>b</sup>	0,04	0,48	0,12	656
366 <sup>b</sup>	0,05	0,20	0,15	253
391 <sup>c,y</sup>	0	1,92	0	45400
388 <sup>c</sup>	0,015	3,09	0,05	5740
387 <sup>c</sup>	0,025	0,44	0,09	789
389 <sup>c</sup>	0,04	0,32	0,14	544
386 <sup>d</sup>	0,015	0,20	0,05	186

<sup>a</sup>Polymerization conditions: a)45°C, b)60°C, c)90°C and d)30°C, ethylene pressure: 4bar, toluene volume: 200mL, polymerization time: 1h, cocatalyst MAO;  $\text{MODE}:\text{TIBA}=1:1$ ,  $\text{MODE}:\text{TIBA}$  precontacted for 30 min, y) polymerization time:5min.

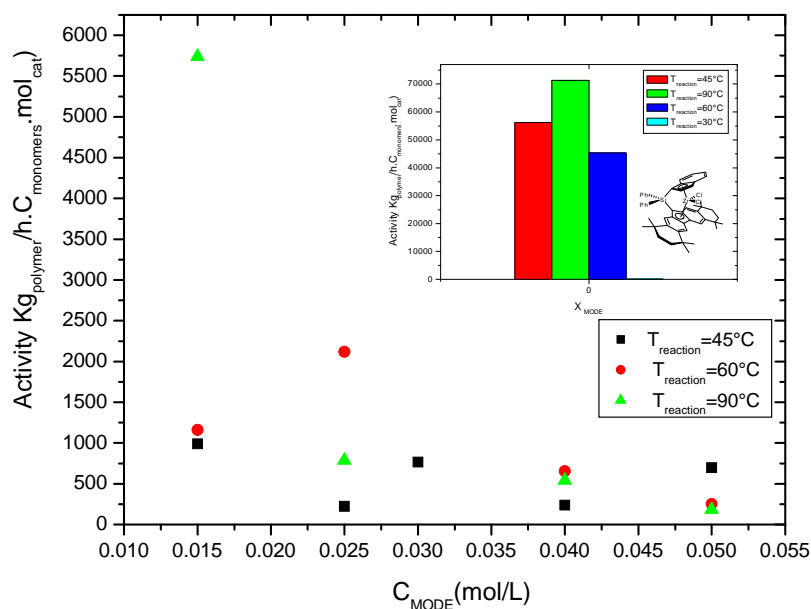


Figure 77: Activity as function of the MODE concentration in feed at different reaction temperatures.

Figure 78 presents the effect of variation in the polymerization temperature using the same concentration of MODE in feed. At this condition, it was observed that the catalyst efficiency increases directly with the increase in temperature. Additionally, it was not observed a

considerable difference in the catalytic activity between 45°C and 60°C, showing small sensibility of the system at these temperatures.

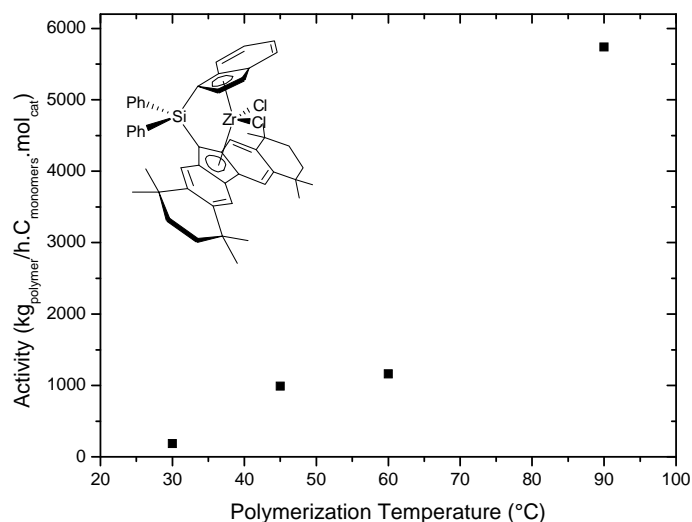


Figure 78: Catalytic activity as a function of the polymerization temperature.  $[ ]_{\text{MODE}}=0,015\text{mol/L}$

### 7. 5.2.1 $^{13}\text{C}$ NMR and $^{13}\text{C}(\text{DEPT-135})\text{NMR}$ Spectroscopy Results

The  $^{13}\text{C}$ NMR and  $^{13}\text{C}(\text{DEPT-135})\text{NMR}$  spectra of the obtained polymer show a presence of the assignment regarding to the presence of MODE structure in the obtained copolymer. Besides the presence of the sign at  $\delta = 30,24$  ppm (C6) typical for the PE structure, three news signs were found. The chemical shifts at  $\delta = 57,59$  ppm and  $\delta = 73,43$  ppm and  $\delta = 36,97$  ppm can be assigned respectively to the methyl group carbons (C1), methylene group near by oxygen atom (C2) and methine (C5) that is the ramification containing carbon. The presence of the methine carbon, confirmed by  $^{13}\text{C}(\text{DEPT-135})\text{NMR}$  spectra, Figure 79, assures the formation of the copolymer.

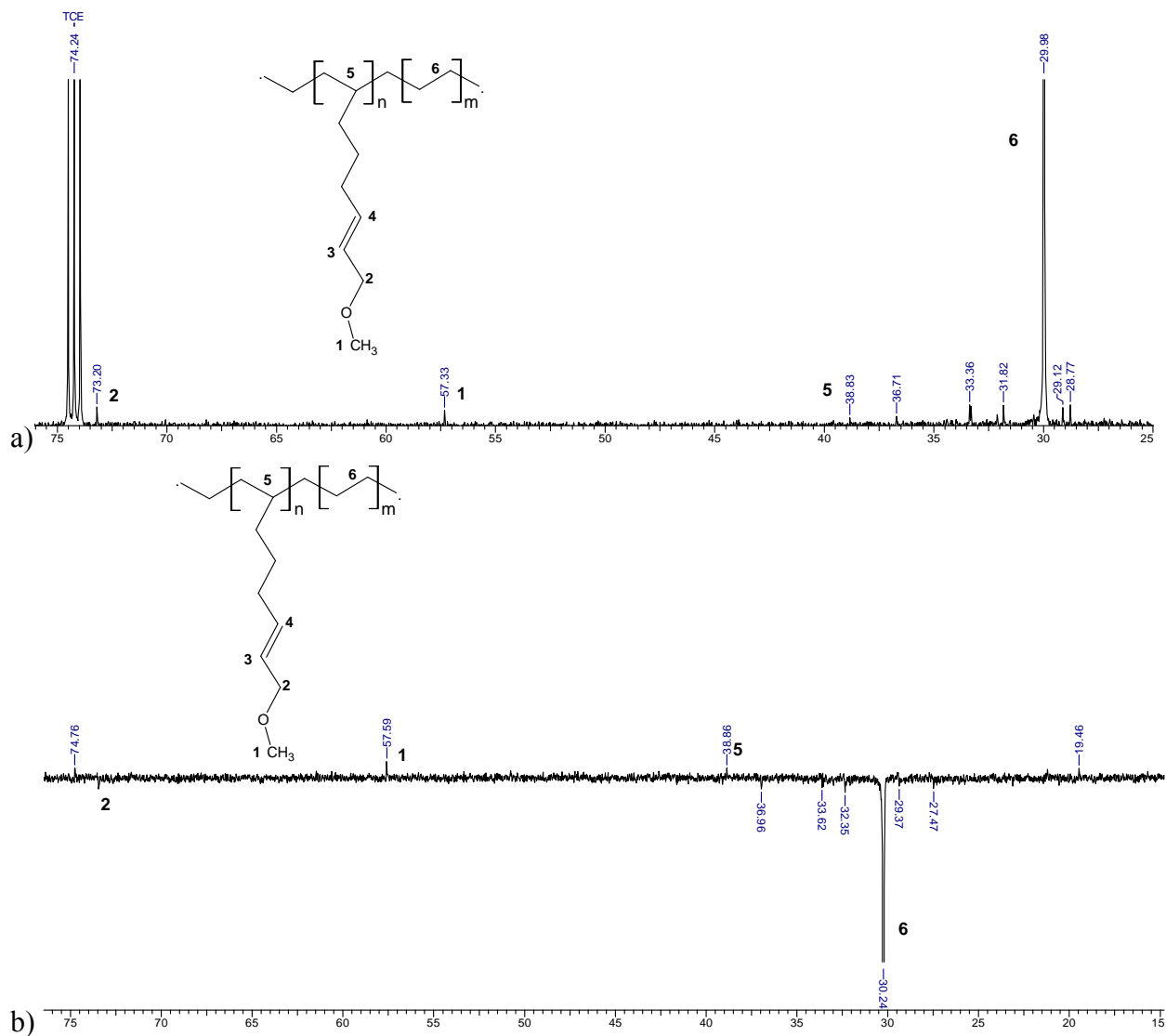


Figure 79: A typical  $^{13}\text{C}$  NMR spectra of the obtained polymer. (run 388) a)  $^{13}\text{C}$  NMR, b)  $^{13}\text{C}$  (DEPT-135) NMR

### 7.5.2.2 GPC and DSC Results

The physical properties of the obtained polymers are summarized in the Table 18.

Table 18: Ethylene polymerization with  $\text{Ph}_2\text{Si}(\text{OctHFlu})(\text{Ind})\text{ZrCl}_2/\text{MAO}$  in the presence of  $\text{MODE}^{\text{a,b,c,d}}$

Reaction	$C_{\text{MODE}}$ (Mol/L)	$\Delta H$ (J/g)	$T_m$ ( $^{\circ}\text{C}$ )	$M_n$ (Kg/mol)	Pd
380 <sup>a,y</sup>	0	152,7	138,1	1102,1	5,9
376 <sup>a</sup>	0,015	133,6	134	505,2	5,4
375 <sup>a</sup>	0,025	82,0	128,8	n.d.	n.d.
379 <sup>a</sup>	0,03	120,6	132	555,3	2,6
377 <sup>a</sup>	0,04	90,8	127,9	306,0	2,9
378 <sup>a</sup>	0,05	76,2	127,7	n.d.	n.d.
365 <sup>b</sup>	0	169,1	140,6	894,1	3,6
362 <sup>b</sup>	0,015	125,5	135,7	573,7	3,2
363 <sup>b</sup>	0,025	112,7	132,3	496,5	5,0
364 <sup>b</sup>	0,04	96,5	129,0	360,0	3,0
366 <sup>b</sup>	0,05	87,0	127,5	233,0	3,2
391 <sup>c,y</sup>	0	63,0	140	n.d.	n.d.
388 <sup>c</sup>	0,015	100,2	133,2	n.d.	n.d.
387 <sup>c</sup>	0,025	11,5	125,4	n.d.	n.d.
389 <sup>c</sup>	0,04	2,4	122,6	n.d.	n.d.
386 <sup>d</sup>	0,015	4,3	118,1	n.d.	n.d.

<sup>a</sup>Polymerization conditions: a) 45 $^{\circ}\text{C}$ , b) 60 $^{\circ}\text{C}$ , c) 90 $^{\circ}\text{C}$  and d) 30 $^{\circ}\text{C}$ , ethylene pressure: 4bar, toluene volume: 200mL, polymerization time: 1h, cocatalyst MAO;  $\text{MODE:TIBA}=1:1$ ;  $\text{MODE:TIBA}$  pre contacted for 30 min, y) 5min. n.d.= not determined.

Overall, the copolymer molecular weight is reduced in the presence of the functional protected monomer. However, the molecular weight distributions of the obtained copolymers remain relatively broad in the whole range of composition investigated. It is also observed that the copolymers synthesized at 60 $^{\circ}\text{C}$  showed slightly higher molecular weights than the copolymers that obtained at 45 $^{\circ}\text{C}$ . The similar behavior was observed for the copolymers synthesized in the presence of the catalyst system  $\text{Me}_2\text{SiInd}_2\text{ZrCl}_2/\text{MAO}$  in the previous section.

In addition, a lowering of  $T_m$  is observed. The DSC curves of the copolymers show a single melting peak that shift to lower temperatures with an increase in  $\text{MODE}$  concentration in the feed, Figure 80. The presence of only one melting peak is taken as evidence of the absence of phase separation and suggests that the obtained copolymers are fairly homogeneous<sup>101</sup>.



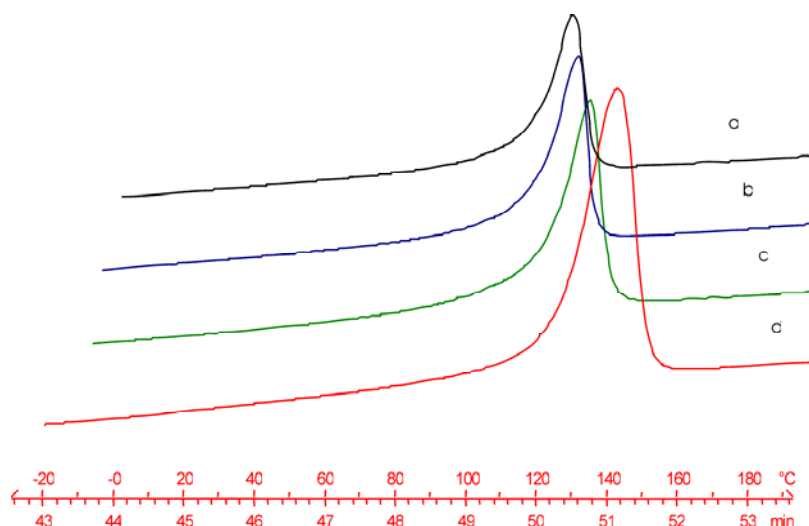


Figure 80: DSC curves of the obtained polymers at 60°C: a)  $[ ]_{\text{MODE}} = 0,05$ , b)  $[ ]_{\text{MODE}} = 0,04$ , c)  $[ ]_{\text{MODE}} = 0,025 \text{ mol/L}$ ; d) PE

Comparing the melting behavior at the different temperatures is clearly possible to see that the higher the concentration of MODE in feed was, the lower the melting point was, Figure 81.

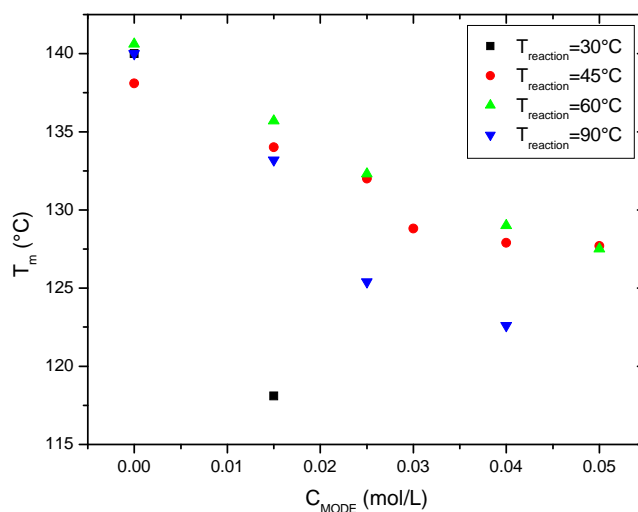


Figure 81: Melting Point of the copolymers as a function of MODE concentration in feed.

### 7. 5.2.3 Fourier Transform Infrared (FTIR) Spectroscopy Results

In the IR Spectrum of the copolymer showed in Figure 82, the presence of MODE bands appears to be clear. The copolymer spectrum was compared with that one obtained in a blank experiment using polyethylene synthesized at the same experimental conditions. The asymmetric stretch reflective of the ether pendant group is observed at  $1123 \text{ cm}^{-1}$  and  $1071 \text{ cm}^{-1}$ . Additionally, the double bonds ( $1638 \text{ cm}^{-1}$ ) in MODE structure can also be observed.

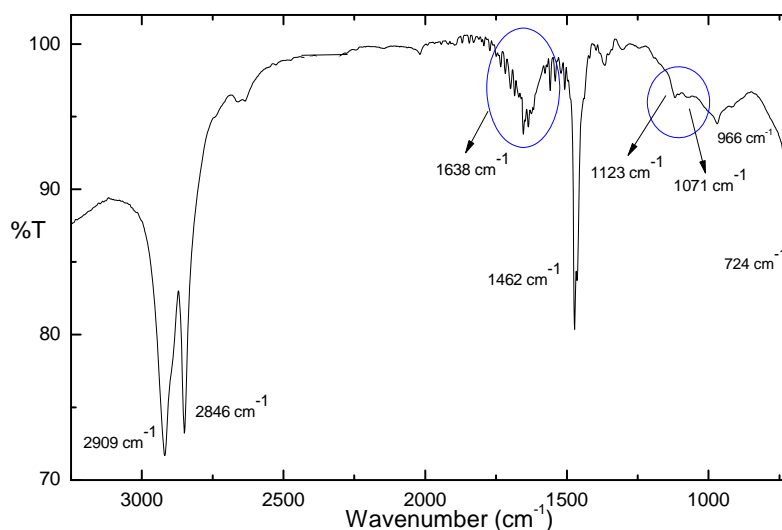


Figure 82: IR spectrum of an ethylene-MODE copolymer (Reaction 363): polymerization conditions: 60°C, ethylene pressure:4bar, toluene volume:200mL, polymerization time:1h, cocatalyst MAO; MODE: TIBA=1:1; MODE:TIBA pre contacted for 30 min.

### 7. 5.3 Catalyst System Ni diimine/MAO Results

Ethylene homopolymerization and copolymerization with MODE were performed with the less oxophilic catalyst system Ni diimine using MAO as co-catalyst. The initial idea was trying the direct approach in the copolymerization with a polar group in absence of the protecting agent. The experiments show that it is not possible to copolymerize MODE without TIBA as a protecting agent.

#### 7. 5.3.1 Effect of Comonomer Concentration

Take the above results into account, a copolymerization of ethylene and MODE protected with TIBA was carried out to compare the performance of the late transition system with the previous results with the catalyst system (2)/MAO and (4)/MAO. The results of the catalyst activity are provided in Table 19.

Table 19: Ethylene polymerization with MODE in the presence of Ni diimine/MAO<sup>a</sup>

Reaction	C <sub>MODE</sub> (mol/L)	x <sub>MODE</sub>	Yields(g)	Activity (kg <sub>Pol</sub> /Mol <sub>cat</sub> .h.C <sub>monomers</sub> )
357	0,015	0,04	1,4	138
355	0,025	0,07	1,8	171
356	0,03	0,08	0,80	78,7
358	0,04	0,10	0,40	36,4
353	0,05	0,13	0,18	15,1
359 <sup>b</sup>	0	0	2,58	9500

<sup>a</sup>Polymerization conditions: 60°C, ethylene pressure 4bar, toluene volume 200mL, polymerization time 1h, cocatalyst MAO; MODE:TIBA=1:1, MODE:TIBA precontacted for 30 min, b) polymerization time:5min.

Figure 83 shows that the catalytic activity decreases sharply (by 1 order of magnitude) with the introduction of the protected monomer in feed.

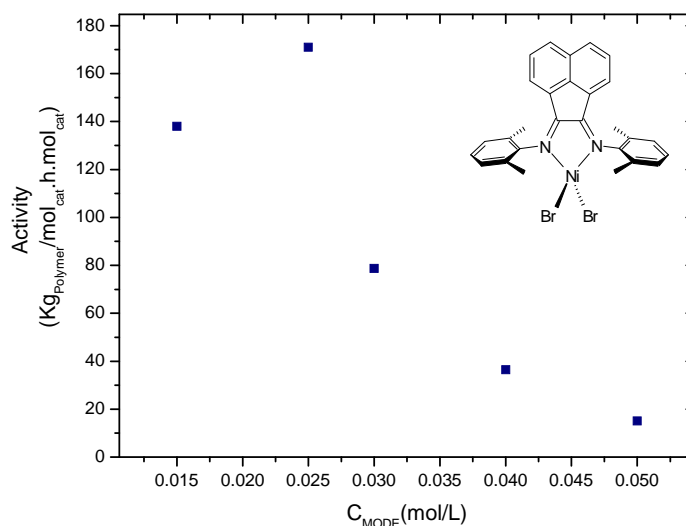


Figure 83: Polymerization Activity as a function of MODE concentration in feed.

### 7. 5.3.2 GPC and DSC Results

The melting point behavior, the molecular weights and molecular weight distributions of the obtained polymers are summarized in Table 20.

Table 20: Ethylene polymerization with MODE in the presence of Ni diimine/MAO.<sup>a</sup>

Reaction	$x_{MODE}$	$T_m$ (°C)	$T_g$ (°C)	$M_w$ (Kg/mol)	Pd
357	0,04	87,5	-47,7	24,8	1,6
355	0,07	92,1	-45,7	24,6	1,7
356	0,08	88,5	n.d.	23,6	1,6
358	0,10	92,3	n.d.	23,2	1,6
353	0,13	91,5	-36,5	22,4	1,7
359	0	128,5	n.d.	18,8	1,6

<sup>a</sup>Polymerization conditions: 60°C, ethylene pressure 4bar, toluene volume 200mL, polymerization time 1h, cocatalyst MAO; MODE:TIBA=1:1;MODE:TIBA precontacted for 30 min.

The obtained polymers have lower molecular weights than those polymers obtained with the previous metallocene systems (**3**)/MAO and (**2**)/MAO, as it was expected. Although the increase of MODE concentration in the feed leads to a strong reduction in the catalytic activity, it seems that it did not influenced the polyethylene microstructure. This statement is supported by the fact that a strong variation was not observed of the melting points (variation

from 87,5 to 92,3°C) and did not lead to a noticeable change in the molecular weights (ranged from 24,8 until 22,4 Kg/mol) of the polymers. No broadening of the polydispersity index was observed in contrast to PE/MODE copolymers obtained with the catalyst system (3)/MAO and (2)/MAO.

### 7.5.3.3 $^1\text{H}$ NMR and $^{13}\text{C}$ NMR Spectroscopy Results

All measured  $^{13}\text{C}$ NMR spectra of the copolymers produced with the Ni-diimine catalyst system have two new signals at 57,59 ppm (C1) and 73,54 ppm (C2). These signals, characteristic for the ether group of MODE, do not exist in PE (run 359). The  $^{13}\text{C}$ NMR spectrum of obtained copolymer is giving in Figure 84.

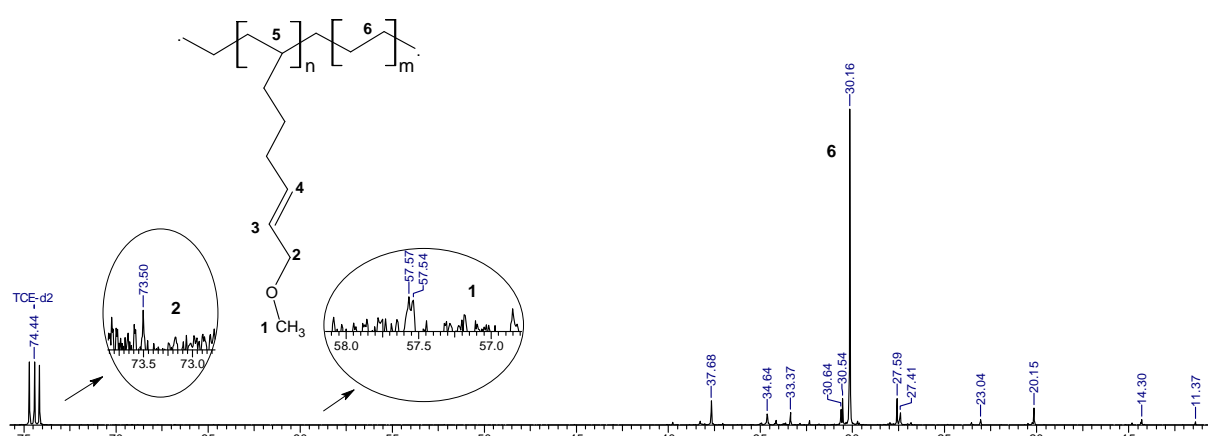


Figure 84:  $^{13}\text{C}$  NMR spectrum of an ethylene-MODE copolymer obtained with the catalyst system (3)/MAO. Polymerization conditions: 60°C, ethylene pressure:4bar, toluene volume:200mL, polymerization time:1h, MODE:TIBA=1:1, MODE:TIBA precontacted for 30 min.

The  $^1\text{H}$ NMR spectrum (Figure 85) of the resulting copolymer indicates a signal at 3,36 ppm which belongs to methyl protons (C1) of the functional group of MODE and 3,93 ppm which belongs to methylene protons (C2) closed to the “O” atom.

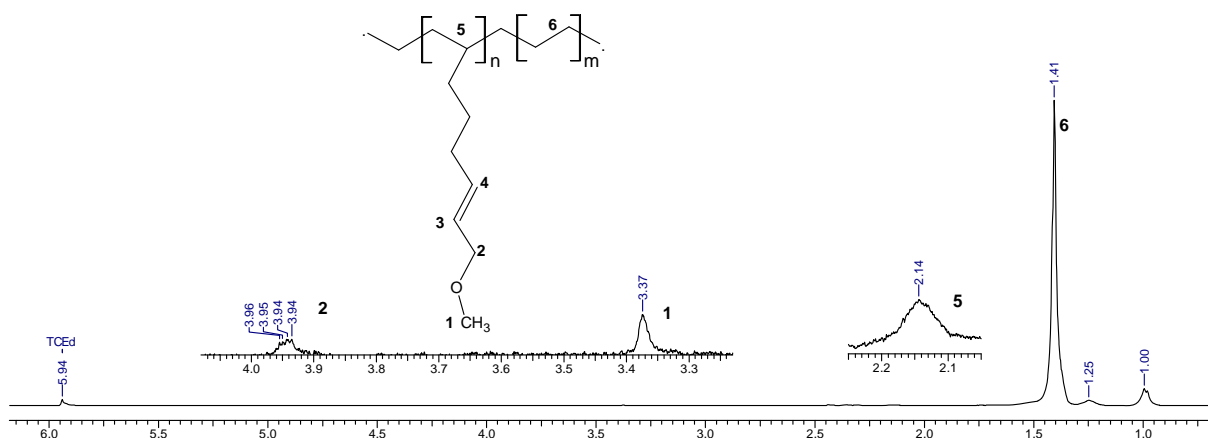


Figure 85:  $^1\text{H}$  NMR spectrum of an ethylene-MODE copolymer. Polymerization conditions: 60°C, ethylene pressure:4bar, toluene volume:200mL, polymerization time 1h, MODE:TIBA=1:1, MODE:TIBA precontacted for 30 min.

### 7. 5. 3.4 Fourier Transform Infrared (FTIR) Spectroscopy Results

The IR spectrum of the sample confirm some changes in the crystalline structure of the polymers, as it can be seen in the Figure 86. The spectrum of the copolymer shows a band in  $1641\text{ cm}^{-1}$  that can not be seen in the PE spectrum. It might be assigned to the double bond present in the MODE structure. Additionally, it is clear that the intensity and structure of the bands in between  $723$  and  $1641\text{ cm}^{-1}$  have changed in the presence of the protected functional monomer. Another evidence of the presence of the functional group is the intensity of the stretching regarding to oxygen at  $1103\text{ cm}^{-1}$ .

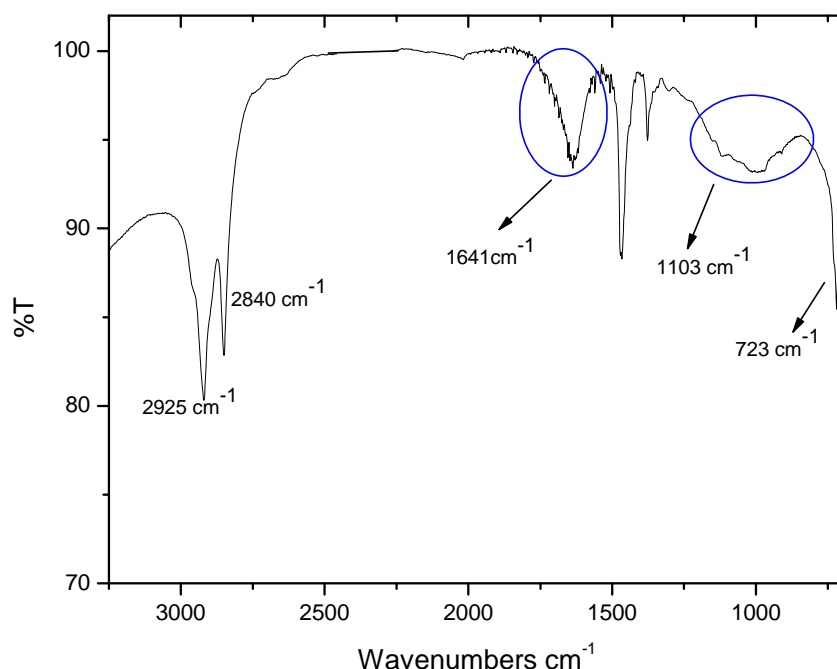


Figure 86: FTIR spectrum of the obtained copolymer, run 358.

### 7.5.4 Comparison among the Used Catalysts Systems

Considering the catalysts systems that were used in this work, it is clear that the catalyst system (2)/MAO has showed the best performance regarding catalytic activity during the copolymerization of ethylene with MODE. It may be due to the fact that this highly substituted catalyst system has less difficulty to insert monomers with polar group. The active sites are not deactivated during the polymerization process. The second best performance was observed with the catalyst system (3)/MAO followed by the catalyst system (4)/MAO.

Additionally, efforts to copolymerize MODE with ethylene in the presence of the catalyst (**1**) and (**5**) were performed without any achievements. A comparison of the catalytic activities of used systems that have yield polymer is shown in Figure 87.

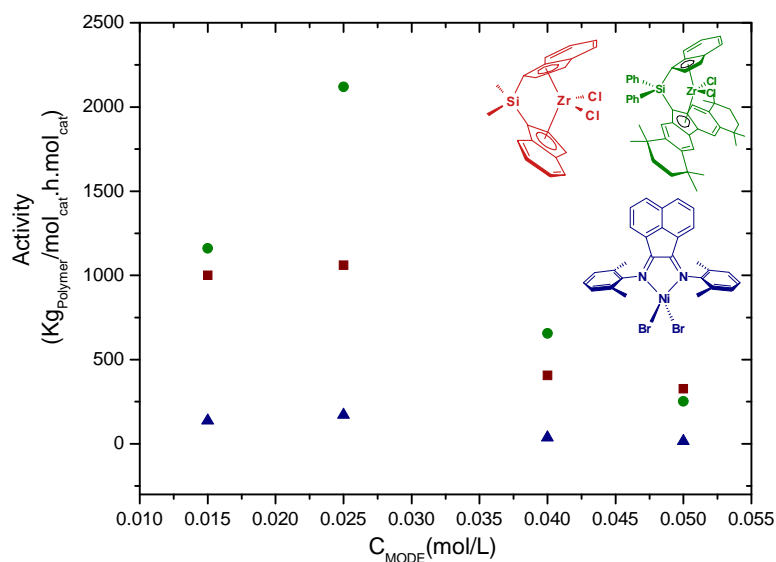


Figure 87: Catalyst activity as function of the MODE concentration in feed for different catalysts.

A comparison of the incorporation rates determined by elemental analyses can be seen at the Table 21.

Table 21: Ethylene polymerization with MODE<sup>f</sup> in the presence of the catalysts system<sup>a, b and c</sup>.

Reaction	$C_{MODE}$ (mol/L)	MODE (mol%)
332 <sup>a</sup>	0,025	0,08
343 <sup>a</sup>	0,03	0,27
344 <sup>a</sup>	0,04	0,38
345 <sup>a</sup>	0,05	0,45
346 <sup>a</sup>	0,06	n.d.
365 <sup>b</sup>	0	n.d.
362 <sup>b</sup>	0.015	0,09
363 <sup>b</sup>	0.025	0,24
364 <sup>b</sup>	0.04	0,25
366 <sup>b</sup>	0.05	0,47
357 <sup>c</sup>	0,015	n.d.
355 <sup>c</sup>	0,025	n.d.
356 <sup>c</sup>	0,03	n.d.
358 <sup>c</sup>	0,04	n.d.
353 <sup>c</sup>	0,05	n.d.
359 <sup>c</sup>	0	n.d.

<sup>f</sup>Polymerization conditions: 60°C, ethylene pressure 4bar, toluene volume 200mL, polymerization time 1h, cocatalyst MAO; MODE:TIBA=1:1; MODE:TIBA precontacted for 30 min, catalyst system a)(**3**)/MAO, b)(**2**)/MAO, c)(**4**)/MAO. n.d.=not determined

The incorporation rates determined by EA showed above are in the same order of magnitude for both catalysts system (2)/MAO and (3)/MAO. The highest incorporate rate was found using the catalyst system (2)/MAO and that is 0.47% in mol, confirming the better performance in activity for the same catalyst system. The incorporation level for the catalyst system (4)/MAO was not possible to be determined neither by  $^1\text{H}$ NMR nor EA. Although, it is possible to see the changes in the structure of the polymer obtained in the presence of the catalyst system (4)/MAO, when the physical properties ( DSC, GPC, IR) are analyzed.

### 7.5.5 Partial Conclusions

Ethylene was copolymerized with 2,7-Octadienylmethylether (MODE) using metallocene and a less oxophilic catalyst/MAO system. A comparison between the catalyst activities for the copolymerization of ethylene with MODE shows the following decrease order (4), (3) and (2).

The optimal mixing ratio between MODE and TIBA was determined using the catalyst system (1)/MAO, the following reactions were run with the same ratio in order to compare the behavior of the different systems. The ratio 1:1 (MODE:TIBA) has shown the highest catalyst activity. All reactions were carried out with and without TIBA. The presence of TIBA is mandatory to yield copolymers.

Although, the catalyst systems (3) and (2) show different activities at the same reaction temperature, the level of MODE incorporation remains similar for both systems. For the catalyst system (4), using the same characterization techniques, it was not possible to determined the level of incorporation of MODE into the PE backbone. However, its clear that a copolymer was synthesized, based on the FT-IR and NMR analyses of the obtained polymer.

## 7.6 Copolymerization of Ethylene with HBE and DBE

Functional groups directly attached to the backbone chain of high polymers are often less reactive than if these groups were not attached to a polymer. This reduced reactivity is caused by the steric hindrance or by the fact that all or part of the polymer chain interferes with the reactivity of individual functional group<sup>95-97</sup>.

Same cases have been studied in which the reactivity or activity of a functional group is unaffected by its neighboring group or more importantly by the polymer main chain. In such cases, the reactivity or functional groups are separated from the polymer main chain by a *spacer* group. Frequently, this spacer group is flexible; for example, a few methylene groups are effective in separating the functional group from the polymer backbone chain<sup>95-97</sup>.

On the basis of NMR data showing the degree of electronic influence of the ester substituent on the double bond, Purgett and Vogl conclude that a spacer of between 3 and 6 methylene units is necessary between the two functionalities for polymerization to occur<sup>95-97</sup>. This value is consistent with restrictions observed by others researchers for other types of monomers (for relatively less polar silicon substituents, one CH<sub>2</sub> group is necessary; for dialkylamines, two)<sup>21</sup>.

Knowing in advance that long spacer between the double bond and the functionality is one strategy to prevent the catalyst deactivation during the copolymerization of ethylene and polar monomers, two new monomers with sufficient spacer between the polar group and the double bond were synthesized in the work group of Dr. Prof. Emma Thorn and used in the copolymerization with ethylene. See Figure 88.

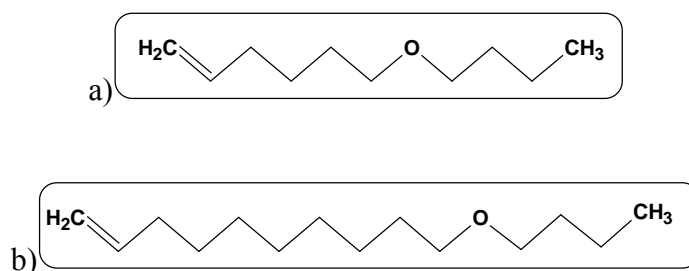


Figure 88: a)5-hexenyl butyl ether (HBE) and b)9 decenyl butyl ether (DBE)

It is also very important to emphasize that the design of the HBE and DBE monomers has



allowed producing copolymers with ethylene without the use of protection/deprotection strategy (Lewis acid complexation using TIBA).

### 7.6.1 Copolymerization Results of Ethylene with HBE

The effect of the addition of HBE monomer, Figure 88 a), into the reaction medium during ethylene polymerization was investigated in the presence of the catalytic system (3)/MAO and the results are provided in Table 22.

Table 22: Ethylene polymerization with HBE<sup>a</sup> in the presence of the catalyst system (3)/MAO

Reaction	C <sub>HBE</sub> (mol/L)	T(°C)	t (min)	Zr(mol)	Activity (Kg <sub>polymer</sub> /mol <sub>Zr</sub> ·C <sub>monomers</sub> ·h)
302	0,01	60	90	2E-06	54600
301	0,025	60	10	2E-06	1405

<sup>a</sup>Polymerization conditions: 60°C, ethylene pressure: 4bar, toluene volume: 200mL, cocatalyst MAO; [HBE]=1mol/L.

The results presented in the Table 22 shows that the long space between the double bond and the functional group provide not only an efficient protection of the catalyst system but also one way to copolymerize ethylene with oxygen containing ethers. It was observed that the higher the concentration of the polar group in the feed was, the lower the catalytic activity was.

#### 7.6.1.1 <sup>1</sup>HNMR and FTIR Spectroscopy Results

The <sup>1</sup>HNMR spectrum of the obtained copolymer is presented in the Figure 89. The spectrum shows the presence of the ether group between 3,4 and 3,8 ppm , as well as the presence of the methine group at 2,01 ppm suggesting that a copolymer was synthesized.

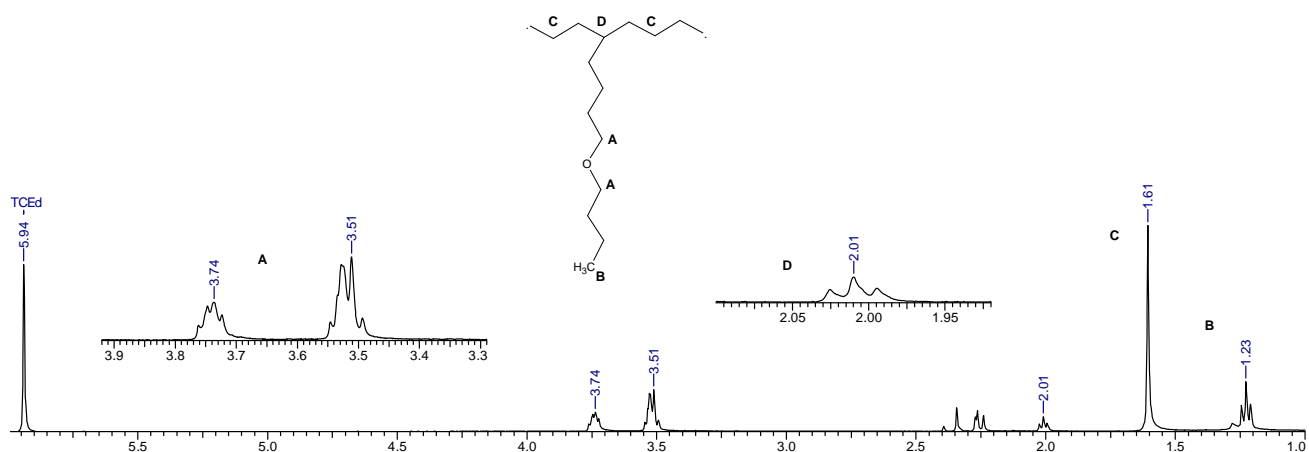


Figure 89: <sup>1</sup>H NMR spectrum of the obtained copolymer, Polymerization conditions: 60°C, ethylene pressure: 4bar, toluene volume:200mL, cocatalyst MAO; [HBE] = 1 mol/L

The presence of the ether group can be also confirmed by Fourier Transform Infrared (FTIR) spectroscopy. The copolymer spectrum was compared with that one obtained in a blank experiment using polyethylene synthesized at the same experimental conditions. The asymmetric stretch reflective of the ether pendant group is observed at  $\approx 1123$  and  $1064 \text{ cm}^{-1}$ . The remaining absorbance bands in the FTIR spectrum suggest the disorder crystalline structure of polyethylene segments. Particularly the strong bands at  $\approx 720$ ,  $968$ ,  $1466$  suggest the inclusion of the ether group into the polymer crystal<sup>90</sup>. The FTIR spectrum of the obtained copolymer is giving at Figure 90.

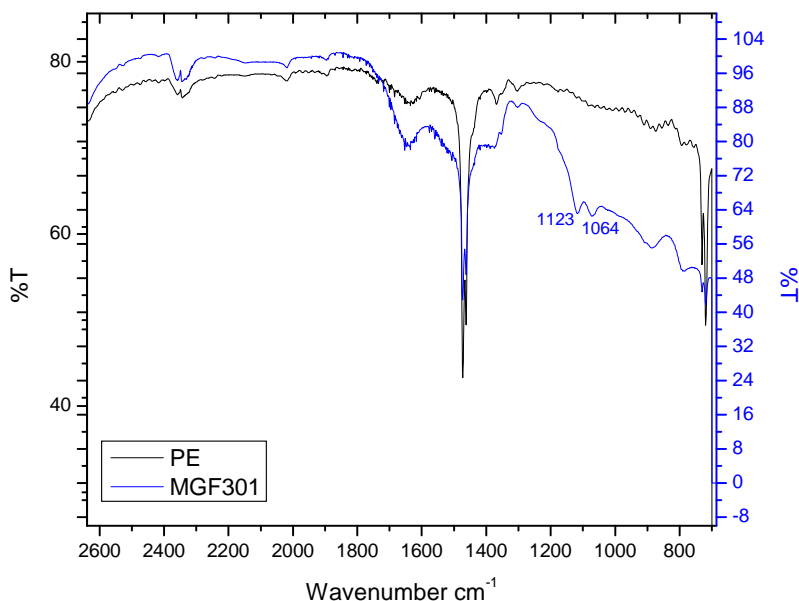


Figure 90: FTIR spectrum of the obtained copolymer, Polymerization conditions: 60°C, ethylene pressure: 4bar, toluene volume:200mL, cocatalyst MAO;  $[ ]_{\text{HBE}} = 1 \text{ mol/L}$

#### 7.6.1.2 Elemental Analyses, GPC and DSC Results

Thermal analyses of the copolymers were performed using DSC. The melting points of the obtained copolymers are respectively 132 and 139 °C, the lowest melting point was observed with the highest comonomer concentration. Both copolymers exhibit a single melting temperature. The presence of only one melting peak suggests the absence of macroscopic phase separation. This observation leads to a conclusion that the polymers are fairly homogeneous.

The influence of the HBE concentration on the molecular weight was also studied. It was observed a decrease in the molecular weight with the increase in the polar comonomer concentration in the reaction, although the molecular weights distribution broadens slightly, Table 23. The lowering of the melting point and molecular weight with an increase in the incorporation of the polar group agrees with the general behavior observed for ethylene/ $\alpha$ -olefins copolymers<sup>89</sup>.

Table 23: Ethylene polymerization with (3)/MAO catalyst system in the presence of HBE<sup>a</sup>

Reaction	C <sub>HBE</sub> (Mol/L)	T <sub>m</sub> (°C)	M <sub>w</sub> (10 <sup>3</sup> Kg/mol)	Pd	EA(% mol)
302	0,01	139	194	2,9	0,14
301	0,025	132	105	5,0	0,60

<sup>a</sup>Polymerization conditions: 60°C, ethylene pressure 4bar, toluene volume 200mL, cocatalyst MAO; [HBE]=1mol/L; EA=Elemental analysis.

The highest incorporation rate, determined by elemental analyses, was found while the highest comonomer concentration was used. However, the highest incorporation rate, 0,60 mol %, was followed by a strong decrease in the catalytic activity.

### 7.6.2 Copolymerization Results of Ethylene with DBE

A second polar monomer structure synthesized, Figure 88 b, with a longer space between the ether group and the double bond was tested in the copolymerization of ethylene with the catalyst system (3)/MAO. The results summarized in the Table 24 show that despite the fact that it was not necessary the presence of the protecting agent, at the same copolymerization conditions, the higher the comonomer concentration, the lower the catalytic activity, reactions 311 and 312. Concentration over 0,03 mol/L of the monomer decrease drastically the catalytic performance.

Table 24: Ethylene polymerization with the catalyst system (3)/MAO in the presence of DBE<sup>a</sup>

Reaction	C <sub>DBE</sub> (mol/L)	Time (min)	Zr(mol)	Activity (Kg <sub>polymer</sub> /mol <sub>Zr</sub> ·C <sub>monomers</sub> ·h)
308	0,005	10	1E-6	130880
309	0,01	10	2E-6	79300
310	0,02	30	0,5E-6	152720
311	0,02	30	2E-6	3760
312	0,03	30	2E-6	2440
313	0,05	60	4E-6	540

<sup>a</sup>Polymerization conditions: 60°C, ethylene pressure:4bar, toluene volume:200mL, cocatalyst MAO, [DBE]=1mol/L.

Comparing the results obtained in the copolymerization of ethylene with DBE and HBE, respectively, it was observed that the monomer containing the lengthiest spacer between the double bond and the functional group is more detrimental to the catalyst system.

### 7.6.2.1 <sup>1</sup>H NMR, GPC and DSC Results

The melting points ( $T_m$ ) of the obtained copolymers determined by DSC and molecular weights of the produced copolymers determined by GPC are indicated in Table 25. The melting points are in between 126 and 137°C. The lowest melting point was obtained at the highest comonomer concentration in feed.

The molecular weights of the obtained copolymers are relatively high ( $117 < M_w < 346$ ) with a narrow polydispersity ( $2 < P_d < 4$ ). It is unexpected that the molecular weights of the copolymer slightly increase with an increase in the polar monomer concentration in feed, runs 311 and 312.

The highest incorporation rate 0,6 mol%, was observed at the lowest catalytic activity, run 313 and the lowest comonomer incorporation 0,3 mol % was observed at the highest catalyst activity, run 310.

Table 25: Ethylene polymerization with the catalyst system (3)/MAO in the presence of DBE<sup>a</sup>

Reaction	C <sub>DBE</sub>	T <sub>m</sub> (°C)	M <sub>w</sub> (10 <sup>3</sup> Kg/mol)	Pd	IR (mol%)
308	0,005	137	307	4,0	nd
309	0,01	137	117	3,4	nd
310	0,02	135	183	2,4	0,3
311	0,02	131	125	3,3	nd
312	0,03	132	130	2,2	nd
313	0,05	126	346	2,0	0,6

<sup>a</sup>Polymerization conditions: 60°C, ethylene pressure:4bar, toluene volume:200mL, cocatalyst MAO, [DBE]=1mol/L.

A typical <sup>1</sup>H NMR spectrum of the obtained copolymer is shown at the Figure 91. The spectrum shows the presence of the ether group between 3,3 and 3,8 ppm, as well as the presence of the methine group at 2,10 ppm suggesting that a copolymer has been synthesized.

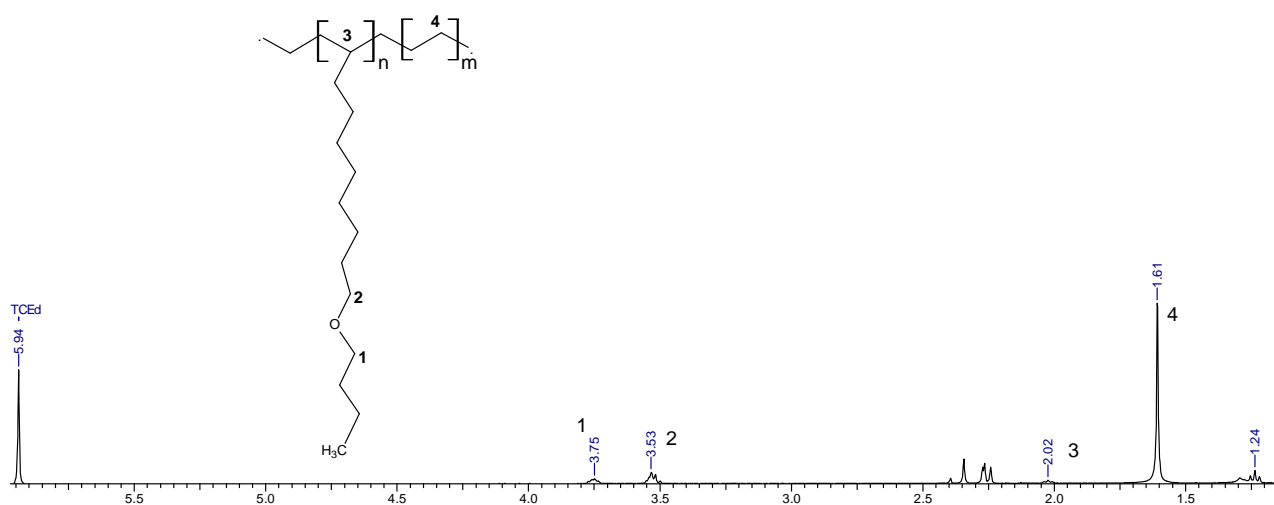


Figure 91:  $^1\text{H}$ NMR spectrum of the obtained copolymer, Polymerization conditions:  $60^\circ\text{C}$ , ethylene pressure 4bar, toluene volume 200mL, cocatalyst MAO;  $[\text{DBE}] = 1\text{mol/L}$

### 7.6.3 Partial Conclusions

The results presented herein lead to a conclusion that the monomer design is a fundamental tool to prevent catalyst deactivation during the polymerization process. The previous results with the copolymerization of ethylene with ethers, allyl ethers and MODE show that the presence of protecting agent is mandatory to prevent catalyst poisoning. Design the monomer structure is possible to circumvent this problem. Incorporation of the ether group into the polyethylene main chain was achieved in a simple and direct copolymerization process.

The experimental results clearly show that the performance of the catalyst system (3)/MAO in the ethylene/HBE copolymerization is absolutely better than the performance with system ethylene/DBE. The optimum activity was achieved using a designed monomer that has 4 methylene spacers between the functional group and the double bond. The monomer containing the longest spacer (8 methylene spacer) between the double bond and the functional group presents almost the same incorporation rates, but shows a quickly deactivation of the catalyst system.

## 8. Conclusions

The focus of this study was the copolymerization of ethylene with polar monomers. The primary objective of this work was to find a suitable metallocene catalyst that can promote the copolymerization of ethylene with polar monomers such as ester (MMA and VA) and ethers (allyl ethers(AEE, APE and ABE), MODE, HBE and DBE). The MMA-co-ethylene and VA-co-ethylene are well known and different synthesis methods to obtaining these polymers are reported in the open literature. However, the investigation of allyl monomers could be considered a pioneered work and the three monomers (MODE,HBE and DBE) were used in this work for the first time for copolymerizations with ethylene.

Several attempts were carried out to achieve copolymerizations of ethylene with polar monomers. Polar monomers with desirable functional groups such as –COOR and R-O-R can provide strong interactions with different materials as well as substrates having polar surfaces. However, the copolymerization of the non polar ethylene with polar monomers is not straightforward. Different approaches might be employed to prevent the catalyst deactivation during the polymerization. Two of them were used in this work: The protection chemistry route and the designed monomer structure strategy. Both routes were considered satisfactory for the purpose of this work, reducing the catalyst deactivation and effectively incorporate the polar monomers in the polyethylene main chain.

The results obtained in this work agree with the previous knowledge that the catalyst activity toward functionalized monomers depend on different parameters such as the kind of metallocene, co-catalyst, protecting agent, the functionality itself, the length of the methylene spacer between the double bond and the functional group, as well as the steric nature of the functional group.

Five different catalyst systems were investigated to compare their effectiveness for the copolymerization of these monomers with ethylene. The difficulty to be copolymerized with ethylene follows the sequence: VA>MMA>AEE>MODE>APE>ABE>DBE>HBE, which is directly relative first to the functionality itself and secondly to the nature of the functional group.

Some restrictions regarding to the solubility of the polymers have hindered the determination

of microstructure, the actual incorporation rates by  $^1\text{H}$ NMR as well as the molecular weights of the polymers obtained at special conditions with AEE. Besides that the incorporation rates measured using elemental analyses are considerable high and might be enough to boost the original polyethylene properties and broaden its application range.



## 9 Experimental Section

### 9.1 General Procedures

Polymerizations were carried out in a Büchi BEP 280 laboratory autoclave with a Type I glass pressure vessel, Figure 92. The stirring speed was 250 rpm, and the partial pressure of ethylene was 4 bar, the temperature was adjusted with a heat jacket connected to a thermostat allowing adjustment of the polymerization temperature with an accuracy of  $\pm 0.5$  °C. During the polymerization runs, the ethylene pressure was kept constant. The ethylene consumption was monitored with a Brooks 5850 TR mass flow meter.

Before the polymerization experiment, the reactor was dried under vacuum at 95 °C for 1 h and then cooled down to the desired reaction temperature. Subsequently, the reactor was charged with toluene, MAO and comonomer solution up to a volume of 200 mL, followed by ethylene to the desired feed composition. The polymerization was started by injection of the catalyst solution.

In the case of MMA and VA it was used another method to run the copolymerization reactions. The monomers were treated with TIBA, at monomer/TIBA ratio 1/1, under inert atmosphere separately. Subsequently, the reactor was charged with toluene, MAO and ethylene to the desired feed composition, followed by injection of the catalyst solution. The copolymerization starts with the introduction of the monomer/TIBA solution into the reaction.

After the desired polymerization time, the reaction was quenched by addition of 5-10 mL ethanol. The polymer was isolated by filtering, washed with ethanol and dried over night under vacuum.

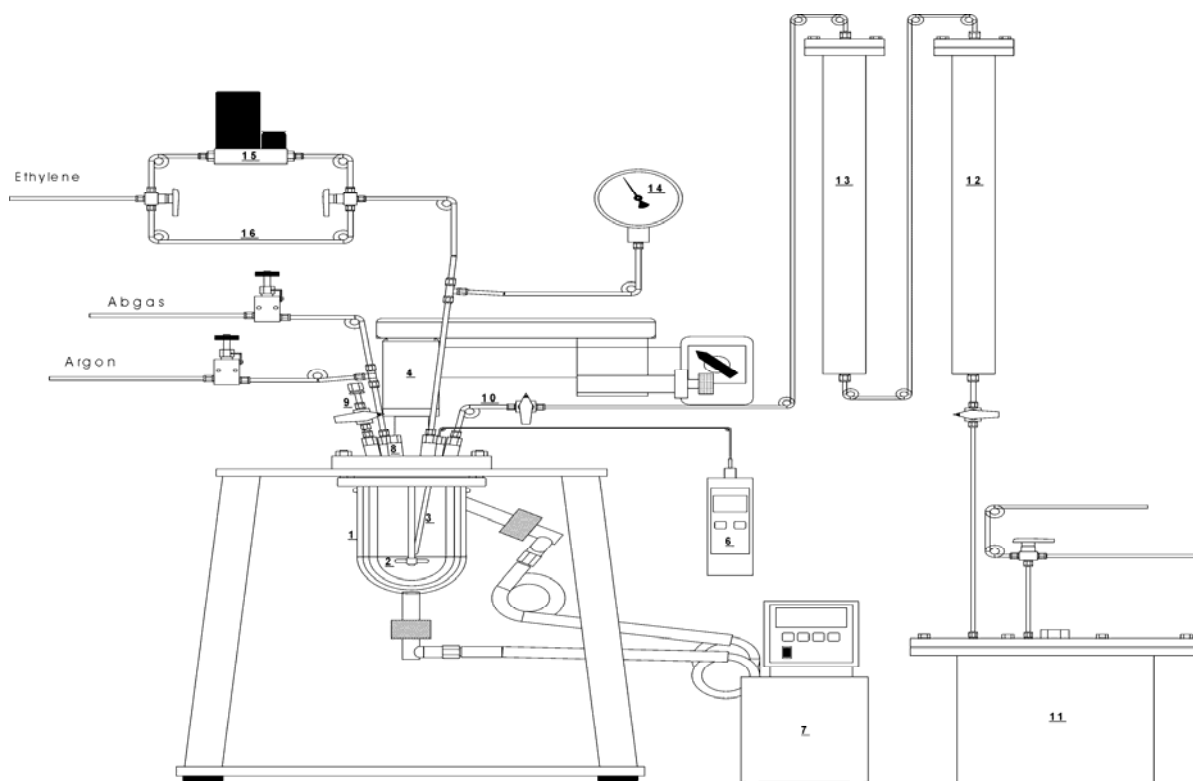


Figure 92: Reactor used for polymerization reaction: 1-autoclave, 2- mixer, 3 and 6- thermometer, 4- motor, 7- thermostat, 8-argon/vacuum release valve, 9-septum/pressure lock, 10-toluene, 12 and 13-toluene columns, 14-ethylene, 15-mass flow meter.

## 9.2 Chemicals

All reactions and manipulations were carried out under an atmosphere of nitrogen by using Schlenk-type techniques.

## 9.3 Gases

Argon (Linde, purity 99,99%) was purified by passing through a Messer Oxisorp cartridge. Ethylene (Linde, purity ) were purified by BASF R3-11 catalyst and 3Å molecular sieve.

## 9.4 Comonomers

The comonomers, allyl ethers (ethyl, propyl and butyl substitution patterns), MODE, HBE and DBE as a solution in toluene were further purified with molecular sieves (3 Å) for 72 hours and stored under argon atmosphere. MMA and VA were dried over CaH<sub>2</sub> over night following by distillation prior to use.

## 9.5 Methylaluminoxane (MAO)

Methylaluminoxane (MAO) was purchased from Crompton as a solution in toluene containing trimethylaluminum (TMA). The solution was filtered, the solvent condensed, and the residue dried in vacuum yielding solid TMA-reduced MAO.

## 9.6 Triisobutylaluminium (TIBA)

TIBA used as a protection agent was purchased from Aldrich and used as 1mol/L solution in toluene.

## 9.7 Solvents

Toluene used for polymerization as well as for preparation of the catalyst and comonomers solutions, was purchased from different suppliers, dried over potassium hydroxide and further purified passing through molecular sieves (4 Å) containing column and BASF-Catalyst R3-11 containing column in sequentially.

## 9.8 Catalysts

The metallocene catalysts used in this work were synthesized in our workgroup according to general literature procedures or purchased. The metallocene *rac*-[Et(IndH<sub>4</sub>)<sub>2</sub>ZrCl<sub>2</sub>] was purchased from Witco. The complexes *rac*-[Me<sub>2</sub>Si(2-Me-4-(1-Naph)Ind)<sub>2</sub>]ZrCl<sub>2</sub> and Dimethylsilyl-(tert-butylamido)-(tetramethyl-1-η<sup>5</sup>-cyclopentadienyl)-titaniumdichloride were purchased from Boulder Scientific Inc. The catalyst precursors were stored under inert atmosphere and their solutions were prepared in dry toluene before use into polymerizations.

## 9.9 Safety

All the chemical products that have been used in this work were disposed according to the following Germany regulation Chemikaliengesetz and Gefahrstoffverordnung<sup>39</sup>.

Chemical Substance	Classification	Risk Phrases	Safety Phrases
Acetone	F	11-36-66-67	9-16-26
Allyl Ethyl Ether	F, Xi	11-36/37/38	16-26
Allyl Propyl Ether	F, Xi	11-36/37/38	13-26-36/37/39
Allyl Butyl Ether	F, Xi	11-36/37/38	
Ethylene	T	48/23-38-36	22-29-36/37/39
Ethanol	F	11	7-16
Calcium Hydroxid	C	22-35	26-36/37/39-45
Methylaluminoxane	F, C, Xn	14/15-17-35	16-23-30-36-43
Methylmethacrylat	F, Xi	11-37/38-43	2-24-37-46
2-Propanol	F, Xi	11-36-67	7-16-24-26
Triisobutylaluminium	F, C	11-14-17-34-48/20	16-26-36/37/39-43-45
Toluene	F, Xn	11-20	16-25-29-33
1,2,4-Trichlorbenzene	Xn, N	22-36/37/38-51/53	26-61
1,1,2,2- Tetracholoethane- <i>d</i> <sub>2</sub>	T <sup>+</sup> , N	26/27-51/53	38-45-61
2,7-Octadienylmethylether	Xi	10	36-37-38
Vinyl Acetate	F	11	[2-]16-23-29-33

## **9.10 Analytical Techniques**

### **9.10.1 NMR Spectroscopy**

Deuterated solvents for NMR measurements were dried over molecular sieves.  $^1\text{H}$  and  $^{13}\text{C}$ NMR spectra were obtained on Bruker Avance 400 Ultrashield spectrometer. Polymer samples were measured at 100.62 MHz. The samples were prepared by dissolving the polymer (10-20mg) in a mixture of (2.5 mL) 1,2,4-trichlorobenzene and (0.5 mL) of 1,1,2,2-tetrachloroethane- $d_2$  and measured at 100°C. All chemical shifts were referred to the solvent of TCE- $d_2$  at 5.94 ppm ( $\delta$ ).

### **9.10.2 Differential Scanning Calorimetry – DSC**

Differential scanning calorimetry measurements were performed on a Mettler Toledo DSC 821e instrument under a nitrogen atmosphere. All samples were prepared in hermetically sealed pans (5-8 mg/sample), and were measured using an empty pan as reference. Calibration was made using indium for the enthalpy standards and n-octane as a standard for peak temperature transition. Samples were melted at 200°C, quenched from 200°C until -200°C, and heated from -200°C to 200°C, at heating rate of 20°C/min. The melting temperature ( $T_m$ ) was taken from the second thermal cycle exclusively.

### **9.10.3 Gel Permeation Chromatography - GPC**

High-temperature gel permeation chromatography (GPC) measurements were performed in 1,2,4-trichlorobenzene at 140°C using a Waters GPCV 2000 instrument with HT 106, 104, and 103 Å columns. The instrument operated with a combined refractive index and viscosity detector unit, which allowed the calculation of appropriate Mark-Houwink constants for each polymer using the Millenium software supplied by Waters. Calibration was applied using polystyrene standards (PSS).

#### **9.10.4 Elemental Analysis**

The samples are placed in an elemental analyzer connected to a mass spectrometer. The sample is then combusted at 1040 degrees Celsius and the gas is pushed through an oxidation core. This produces ions from the gas resulting after combustion. The ions are then analyzed using an IRMS mass spectrometer. Ions are separated based by charge and compared against mass.

#### **9.10.5 Elemental analysis: Determination of oxygen**

The chemical substance is decomposed through a pyrolysis process in a reduced atmosphere in a temperature of 1200 °C. During pyrolysis process, oxygen containing radicals flow inside the pyrolysis tube that contains carbon black and are quantitative converted into carbon monoxide (Boudouard principle). The converted carbon monoxide is detected in a specific CO NDIR photometer. A detection signal obtained from specific CO NDIR-photometer is measured as a peak versus time. This peak is digitalized, integrated and the results are shown in weight %, a result of an integral under the peak curve.

#### **9.10.6 Scanning Electron Microscopy**

The Scanning Electron microscopy was performed using a Philips CM 300 microscope. All samples were sputtered with gold before the measurements.

## 10 References

1. Ziegler, K., *Angew. Chem.* **1952**, 64, 323.
2. Ziegler, K., Holzkamp, E. Breil, H., Martin, H. *Angew.Chem.* **1995**, 67, 541
3. Sinn, H.; Kaminsky, W.; Vollmer, H.J.; Woldt, R., *Angew. Chem.* **1980**, 92(5), 396.
4. Brintzinger, H. H.; Huttner, G.; Wild, R. R. W. P.; Zsolnai, L. *J. Organomet. Chem.* **1982**, 232, 233.
5. Brintzinger, H. H.; Kaminsky, W.; Külper, K.; Wild, F. R. W. P. *Angew. Chem.* **1985**, 97, 507.
6. Spaleck, W.; Antberg, M.; Dolle, V.; Klein, R.; Rohrmann, J.; Winter, A. *New J. Chem.* **1990**, 14, 499.
7. Spaleck, W.; Al, E. *Organometallics* **1994**, 13, 954.
8. Ewen, J. A.; Jones, R. L.; Razavi, A. *J. Am. Chem. Soc.* **1988**, 110, 6255.
9. Aulbach, M.; Küber, F. *Ch. i. u.Z.* **1994**, 28, 197.
10. Brintzinger, H.-H.; Fischer, D.; Mülhaupt, R.; Rieger, B.; Waymouth, R. *Angew. Chem.* **1995**, 107, 1255.
11. Alt, H.G.; Köppl, A., *Chem. Rev.* **2000**, 100(4), 1205.
12. Resconi, L.; Cavallo, L.; Fait, A.; Piemontesi, F., *Chem. Rev.* **2000**, 100(4), 1253.
13. Imanishi, Y.; Naga, N., *Prog. Polym. Sci.* **2001**, 26(8), 1147.
14. Cossee, P., *J. Catal.* **1964**, 3, 80.
15. Arlman, E.J.; Cossee, P., *J. Catal.* **1964**, 3, 99.
16. Busico, V.; Cipullo, R.; Cutillo, F.; Vacatello, M., *Macromolecules* **2002**, 35, 349.
17. Cossee P., *Tetrah. Lett.*, **1960**, 17, 12.
18. Arlmann E.J., *J. Catal.*, **1964**, 3, 89.
19. Sinn, H.; Kaminsky, W., *Adv. Organomet. Chem.* **1980**, 18, 99.
20. Plastics Europe, *WG Market Research & Statistics*
21. Boffa, L. S.; Novak B. M., *Chem. Rev.* **2000**, 100, 1479.
22. T.C. Mike Chung, *Functionalization of Polyolefins*, Academic Press: California, **2002**
23. Nicole, K. Boen and Marc A. Hillmyer, *Chem. Soc. Rev.*, **2005**, 34, 267.
24. Dong J. Y., Hu Y., *Coord. Chem. Rev.*, **2006**, 250, 47
25. Kesti M.R, Coates G.W., R.M. Waymouth, *J. Am. Chem. Soc.*, **1992**, 114, 9679.
26. Aaltonen P., Lofgren B., *Macromolecules*, **1995**, 28, 5357.
27. Wilen C.E., Nasman J.H., *Macromolecules*, **1994**, 27, 4051
28. Rix F.C., Brookhart M., *J. Am. Chem. Soc.*, **1995**, 117, 1137.

29. Mecking S., Johnson L.K., Wang L., Brookhart M., *J. Am. Chem. Soc.*, **1998**, 120, 888.
30. Correia S.G., Marques M.M., Ascenso J.R., Rausch M.D., Chien J.C.W., *J. Polym. Sci. Part A: Polym. Chem.*, **1999**, 37, 2471.
31. Aaltonen, P., G. Fink, B. Lofgren, J. Seppala, *Macromolecules*, **1996**, 29, 5255.
32. Goretzki R., G. Fink, *Macromol. Rapid Commun.*, **1998**, 19, 511.
33. Goretzki R., G. Fink, *Macromol. Chem. Phys.*, **1999**, 200, 881.
34. Aaltonen P., B. Lofgren, *Eur. Polym. J.*, **1997**, 33, 1187.
35. Cohen R. E., *J. Polym. Sci. Part A: Polym. Chem.*, **1986**, 24, 2457
36. Drzewinski M. A., *Macromol. Symp.*, **1995**, 91, 107
37. Schulz, D. N.; Datta, S.; Waymouth, R. M. In *Functional Polymers: Modern Synthetic Methods and Novel Structures*; Patil, A. O., Schulz, D. N., Novak, B. M., Eds.; ACS Symposium Series 704; American Chemical Society: Washington, DC, **1998**, 38.
38. Kaminsky, W. *J. Chem. Soc., Dalton Trans.*, **1998**, 1413.
39. Hagihara, H.; Tsuchihara K.; Takeuchi, K.; Murata, M.; *Journal of Polymer Science: Parte A: Polymer Chemistry*, **2004**, 42, 52.
40. Hagihara, H.; Tsuchihara K.; Sugiyama, J.; Takeuchi, K.; Schiono, T.; *Journal of Polymer Science: Parte A: Polymer Chemistry*, **2004**, 42, 5600.
41. Oberhauser, W.; Bachmann, C.; Stampfl, T.; Haid, R.; Langes, C.; Kopacka, H.; Rieder, A.; Brüggeller, *P. Inorg. Chim. Acta.*, **1999**, 290, 167.
42. Giannini, U.; Brükner, G.; Pellino, E.; Cassata, A. , *J. Polym. Sci.*, Part C, **1968**, 22, 157
43. Hakala, K.; Löfgren, B.; Helaja, T., *Eur. Polym. J.*, **1998**, 34 (8), 1093
44. Yassuda H.; Desurtmont G., Tonaka M., Li Y., Tokimitsu T., Tone S., Yanagase A., *Journal of Polymer Science: Parte A: Polymer Chemistry*, **2000**, 38, 4095.
45. X. Li, Y. Li, Yue. Li, Y. Chen, and N. Hu, *Organometallics* **2004**, 25, 2502.
46. Drent, E. ; Dijk, R. V.; Ginkel, R. V.; Oort, B. V.; Pugh, R. I. *Chem. Commun.* **2002**, 744
47. Wu B. R.W.; Lenz, B. Hazer, *Macromolecules* **1999**, 32, 6856.
48. Yasuda H.; Furo M., H. Yamamoto, *Macromolecules* **1992**, 25, 5115.
49. Folie, B. J., and M. Radosz, "Phase Equilibria in High-pressure Polyethylene Technology," *Ind. Eng. Chem. Res.*, **1995**, 34, 1501.
50. Moreira VX. Utilization of EVA Waste in Nitrile Rubber Compounds. [*Unpublished M.Sc. thesis*] Rio de Janeiro: Instituto de Macromoléculas, Universidade Federal do Rio de Janeiro; **2001**.
51. Dierkes W. Re-use of Rubber Waste – A Recycling Concept. *International Polymer Science and Technology*. **1995**; 22(8): T/17-24.



52. De D, Maiti S, Adhicari B., *Journal of Applied Polymer Science*. **1999**; 73(14):2951.
53. Stael GC, Tavares MIB, de Menezes MC, Gorelova MM, *Journal of Applied Polymer Science*. **2001**; 80(11):2120.
54. Brookhart, M.; White, S.P.; Leatherman, D.M.; Williams, S.B.; *J. Am. Chem. Soc.*, **2005**, 127, 5132.
55. Wunderlich, B., *Thermal Analysis*, Academic Press: New York, **1990**:p 418
56. Meszlenyi, G., Kortvelyessey, G.; *Polymer Testing*, **1999**, 18, 551
57. Zhiqiang S., Ying Z., Yizhuang X., Xiuqin Z., Shannong Z., Dujin W., Jinguang W., Charles C. H. and Duanfu X., *Polymer*, 45, **2004**, 11, 3693
58. Yang, X.; Stern, C. L.; Marks, T. J., *J. Am. Chem. Soc.*, **1991**, 113, 3623.
59. Kaminsky, W.; Kulper, K.; Brintzinger, H. H. *Angew. Chem.*, Int. Ed. Engl. **1985**, 24, 507.
60. Sinn, H.; Kaminsky, W., *Adv. Organomet. Chem.*, **1980**, 18, 99.
61. Bochmann, M. *J. Chem. Soc., Dalton Trans.* **1996**, 255, 270.
62. Brintzinger, H.-H.; Fischer, D.; Mülhaupt, R.; Rieger, B.; Waymouth, R. M. *Angew. Chem.*, Int. Ed. Engl. **1995**, 34, 1143-1170
63. Soga, K.; Terano, M., Eds. *Catalyst Design for Tailor-Made Polyolefins*; Elsevier: Tokyo, **1994**.
64. Möhring, P. C.; Coville, N. J. *J. Organomet. Chem.* **1994**, 479, 1-29.
65. Marks, T. *J. Acc. Chem. Res.* **1992**, 25, 57-65
66. Jordan, R. F. *Adv. Organomet. Chem.* **1991**, 32, 325-387
67. Quirk, R. P., Ed. *Transition Metal Catalyzed Polymerizations*; Cambridge University Press: Cambridge, **1988**.
68. Kaminsky, W., Sinn, H., Eds. *Transition Metals and Organometallics for Catalysts for Olefin Polymerizations*; Springer: New York, **1988**.
69. Deck, P. A.; Marks, T. J. *J. Am. Chem. Soc.* **1995**, 117, 6128-6129.
70. Giardello, M. A.; Eisen, M. S.; Stern, C. L.; Marks, T. J. *J. Am. Chem. Soc.* **1995**, 117, 1214.
71. Jia, L.; Yang, X.; Ishihara, A.; Marks, T. *J. Organometallics* **1995**, 14, 3135.
72. Chien, J. C. W.; Song, W.; Rausch, M. D. *J. Polym. Sci., A: Polym. Chem.* **1994**, 32, 2387.
73. Eisch, J.; Pombrik, S. I.; Zheng, G.-X. *Organometallics* **1993**, 12, 3856.
74. Siedle, A. R.; Lamanna, W. M.; Newmark, R. A.; Stevens, J.; Richardson, D. E.; Ryan, M. *Makromol. Chem., Macromol. Symp.* **1993**, 66, 215.
75. Britovsek G. J.P.; Gibson, V.C.; Spitzmesser, S.K., Tellmann, K.P.; White, A.J.P.; Williams, D.J., *J. Chem. Soc., Dalton Trans.*, **2002**, 1159

76. Colburn, S.E., Bryant, D.K., US Patent 3,560,463, 2-2-**1971** (National Distillers and chemical Co.).
77. Strauss, H. W., US Patent 3,033,840, 5-8-**1962** (DuPont).
78. Sargent, D. E., US Patent 2,467,234, 4-12-**1949** (DuPont).
79. Benoit, G.J. Jr; Abbot, A. D., US Patent 2,748,170, 5-29-**1956** (California Research Corp.).
80. White, W. G.; Walther, R.A., US Patent 3,226,374, 12-28-**1965** (Union Carbide).
81. Gluesenkamp, E.W., US Patent 3,026,290, 3-20-**1962** (Monsanto).
82. Calfee, J.D., US Patent 3,025,267, 3-13-**1962** (Monsanto).
83. Klabunde, U., US Patent 4,698,403, 10-6-**1987** (DuPont).
84. Klabunde, U., US Patent 4,906,754, 3-6-**1990** (DuPont).
85. Greenly, R.Z., Free Radical Copolymerization Reactivity Ratio. In *Polymer Handbook*, 3<sup>rd</sup> ed.; Brandrup, J., Immergut, E.H., Eds.; Wiley-Interscience: New York, **1989**; pp 153-266.
86. Baughman, T.W.; van der Aa, E.; Lehman, S.E.; Wagener, K.B., *Macromolecules*, **2005**, 38, 2550.
87. Odian, G., Principles of polymerization; Wiley: New York, **1991**; p 266.
88. Venkatesh, R., Vergouwen, F., Klumperman B., *J. Polym. Sci., A: Polym. Chem.*, **2004**, 42, 3271.
89. Simanke, G.A.; Mauler, R.S.; Galland, G.B., *J. Polym. Sci., A: Polym. Chem.*, **2002**, 40, 471.
90. Baumhardt, N.R.; Galland, G.B.; Mauler, R.S; Queijada, R., *Polym. Bull* **1998**, 40, 103.
91. Chien, J.C.W.; Wang, B.P., *J. Polym. Sci., A: Polym. Chem.*, **1990**, 28, 15.
92. Chien, J.C.W.; Wang, B.P., *J. Polym. Sci., A: Polym. Chem.*, **1988**, 26, 3089.
93. Herbert, N.; Montag, P.; Fink, G., *Macromol. Chem.*, **1993**, 194, 3167.
94. Alamo, R. G.; Mandelkern, L. *Thermochim Acta* **1994**, 238, 155.
95. Purgett, M. D.; Vogl, O. *J. Polym. Sci., Part A: Polym. Chem.* **1988**, 26, 677.
96. Vogl, O. *J. Macromol. Sci., Chem.* **1985**, 22, 541.
97. Vogl, O. *J. Macromol. Sci., Chem.* **1984**, 21, 1217.
98. Deffieux, A.; Santos, M.R.; Portela, M.F., Pereira, S.G., Nunes, T.G., *Macromol. Chem. Phys.* **2001**, 202, 2195
99. Queijada, R.; Galland, G.B.; Mauler, R. S., *Macromol. Chem Phys* **1996**, 197, 3091.
100. Huang, J.; Rempel, G. L., *Prog. Polym. Sci.* **1995**, 20, 459
101. Ramakrishnan, S.; Berluch, E.; Chung, T.C., *Macromolecules*, **1990**, 23, 378
102. Chung T.C.; Lu, H.L., *J. Polym. Sci., Part A: Polym. Chem.* **1998**, 36, 1017

103. Stiheling, M. U.; Stein, K.M.; Kesti, M.R.; Waymouth R.M., *Macromolecules*, **1998**, 31(7), 2019
104. Pizzoli, M.; Righetti, M.C.; Vitali, M.; Ferrari, P., *Polymer*, **1998**, 39, 1445.
105. Eynde, S.V.; Mathot, V.; Koch, M.H.J.; Reynaers, H., *Polymer*, **2000**, 41, 3437
106. Bowemer, T.N.; Tonelli, A.E., *Polymer*, **1985**, 26, 1195
107. Lee, S.-H.; Lo stracco, M.A.; Hasch, B.M.; McHugh, M.A., *J.Phys. Chem.*, **1994**, 98, 4055
108. Baughman, T.W.; van der Aa, E.; Wagener, K.B., *Macromolecules*, **2006**, 39, 7015.
109. Höcker, H.; Keul, H.; Balk, S.; Frauenhath, H., *Macromol. Rapid. Commun.* **2001**, 22, 1147.

## **Declaration**

I declare to have developed the results presented in this thesis myself, and with the help of no other than the cited references and resources.

This work has not been presented to any inspecting authority in the same or a similar form before.

## **Erklärung**

Der Verfasser erklärt, die vorliegende Arbeit selbständig und ohne fremde Hilfe verfasst zu haben. Andere als die angegebenen Hilfsmittel und Quellen wurden nicht benutzt und die benutzten wörtlich oder inhaltlich entnommen Stellen sind als solche kenntlich gemacht.

Diese Arbeit hat in gleicher oder ähnlicher Form noch keiner Prüfungsbehörde Vorgelegen worden.

Hamburg, im 03.12.2007

---

(Mércia Barbosa Cavalcante Fernandes)

### **Erklärung über frühere Promotionsversuche**

Hiermit erkläre ich, Mércia Barbosa Cavalcante Fernandes, dass vorher keine weiteren Promotionsversuche unternommen worden sind, oder an einer anderen Stelle vorgelegt wurden.

Hamburg, den 03.12.2007

---

(Mércia Barbosa Cavalcante Fernandes)

### **Eidstattliche Versicherung**

Hiermit erkläre ich an Eides Statt, dass die vorliegende Dissertationsschrift selbstständig und allein von mir unter den angegebenen Hilfsmitteln angefertigt wurde.

Hamburg, den 03.12.2007

---

(Mércia Barbosa Cavalcante Fernandes)

## **Posters**

M.Donner, M.Fernandes, W.Kaminsky, Synthese von Copolymeren mit Sterisch Gehinderten und Polaren Monomeren, Hamburger Makromolekulares Symposium 2005, Hamburg, Germany , 10-12, October, **2005**.

## **Publications**

M.Donner, M.Fernandes, W.Kaminsky, Synthesis of Copolymers with Sterically Hindered and Polar Monomers, Macromolecular Symposia, **2006**, 236(1), 193-202.